

Study of Transport Coefficients in
Strongly Interacting Matter
at Finite Temperature

By

SUKANYA MITRA

Enrolment No: PHYS04200904014

Variable Energy Cyclotron Centre, Kolkata

A thesis submitted to

The Board of Studies in Physical Sciences

In partial fulfillment of requirements

For the Degree of

DOCTOR OF PHILOSOPHY

of

HOMI BHABHA NATIONAL INSTITUTE



January, 2015

Homi Bhabha National Institute

Recommendations of the Viva Voce Committee

As members of the Viva Voce Board, we certify that we have read the dissertation prepared by Sukanya Mitra entitled **Study of Transport Coefficients in strongly interacting matter at finite temperature** and recommend that it may be accepted as fulfilling the dissertation requirement for the degree of Doctor of Philosophy.

D. K. Srivastava 17/4/2015 Date:

Chairman- Dr. D. K. Srivastava

Sourav Sarkar Date: 17/04/2015

Supervisor- Dr. Sourav Sarkar

Jane Alam Date: 17/4/2015

Member 1- Dr. Jane Alam

Pradip K. Roy Date: 17/04/2015

Member 2- Prof. Pradip K. Roy

Subrata Pal Date: 17/04/2015

External Examiner- Dr. Subrata Pal

Final approval and acceptance of this thesis is contingent upon the candidates submission of the final copies of the thesis to HBNI.

I/We hereby certify that I/we have read this thesis prepared under my/our direction and recommend that it may be accepted as fulfilling the thesis requirement.

Date: 17/04/2015

Place: VECC, Kolkata

Sourav Sarkar
Guide

STATEMENT BY AUTHOR

This dissertation has been submitted in partial fulfilment of requirements for an advanced degree at Homi Bhabha National Institute (HBNI) and is deposited in the Library to be made available to borrowers under rules of the HBNI.

Brief quotation from this dissertation are allowable without special permission, provided that accurate acknowledgement of source is made. Requests for permission for extended quotation from or reproduction of this manuscript in whole or in part may be granted by the Competent Authority of HBNI when in his or her judgement the proposed use of the material is in the interests of scholarship. In all other instances, however, permission must be obtained from the author.

Sukanya Mitra
Sukanya Mitra

DECLARATION

I, hereby declare that the investigation presented in the thesis has been carried out by me. The work is original and has not been submitted earlier as a whole or in part for a degree/diploma at this or any other Institution/University.

Sukanya Mitra
Sukanya Mitra

Dedicated to my family

ACKNOWLEDGMENTS

In writing this PhD thesis, first and foremost I would like to thank my supervisor Dr. Sourav Sarkar. I consider myself fortunate for pursuing my PhD under his supervision and without his guidance and support this thesis was never possible. The second person to whom I would like to express my gratitude is Dr. Jane Alam for being an excellent collaborator and a wonderful teacher. I would also like to thank Dr. A.K. Chaudhuri for helpful suggestions and useful physics discussions. I am thankful to my seniors Dr. Payal Mohanty, Dr. Sabyasachi Ghosh and Dr. Santosh K Das for being my collaborators and helping me with their advice and suggestions. Furthermore the discussions with Dr. Rupa Chatterjee, Dr. Purnendu Chakraborty, Dr. Somnath De and Dr. Victor Roy have been very helpful and encouraging.

It was a pleasure to work in Variable Energy Cyclotron Centre with my co-researchers. First I should mention my bachmates. All my friends, Amal, Nasim, Surashree, Trambak, Subhash and of course Abhishek have created unforgettable memories in the path of my life. And how can I forget about my charming juniors ! I can not name them all but these people were the fresh air of the Scholar's wing and all of them have been great colleagues to work with.

Finally I would like to convey my heartiest gratitude to my family for being unconditionally supportive without which this thesis would have never been completed. Especially, I thank my husband Mr. Dibya Ranjan Das for always being by my side and encouraging me even in the darkest times, my mother Mrs. Swati Mitra for keeping great faith on me even in the time of my failures and finally my father Mr. Dipankar Mitra who never disappointed that five year old kid with her silly questions even after a tough day and thus revealed the fascinating mysteries of this vast universe to her.

Sukanya Mitra
Sukanya Mitra

LIST OF PUBLICATIONS

JOURNALS:

a. Published

1. Thermal radiation from an evolving viscous quark gluon plasma,
Sukanya Mitra, Payal Mohanty, Sourav Sarkar and Jan-e Alam,
Int. J. Mod. Phys. E **22** (2013) 1350004.
2. Effect of spectral modification of ρ on shear viscosity of a pion gas,
Sukanya Mitra, Sabyasachi Ghosh and Sourav Sarkar,
Phys. Rev. C **85** (2012) 064917 .
3. Effect of running coupling on photon emission from quark gluon plasma,
Mahatsab Mandal, Pradip Roy, Sukanya Mitra and Sourav Sarkar,
Phys. Rev. C **85** (2012) 067901 .
4. Medium effects on the viscosities of a pion gas,
Sukanya Mitra and Sourav Sarkar,
Phys. Rev. D **87** (2013) 9, 094026.
5. Effect of in-medium spectral density of D and D^* mesons on the J/ψ dissociation in hadronic matter,
Sabyasachi Ghosh, Sukanya Mitra and Sourav Sarkar,
Nucl. Phys. A **917** (2013) 71.
6. Electromagnetic Radiations from Heavy Ion Collision,
Payal Mohanty, Sabyasachi Ghosh, and Sukanya Mitra,
Adv. High Energy Phys. **2013** (2013) 176578.

7. Medium effects on the thermal conductivity of a hot pion gas,
Sukanya Mitra and Sourav Sarkar,
Phys. Rev. D 89 (2014) 054013.

b. Accepted

1. Medium effects on the relaxation of dissipative flows in a hot pion gas,
Sukanya Mitra, Utsab Gangopadhyaya and Sourav Sarkar,
accepted in PRD.

c. Communicated

1. Characterizing quark gluon plasma by thermal photons and lepton pairs,
Sukanya Mitra, Payal Mohanty, Sabyasachi Ghosh, Sourav Sarkar and Jan-e Alam,
arXiv:1303.0675(2013).
2. Diffusion of hidden charm mesons in hadronic medium,
Sukanya Mitra, Sabyasachi Ghosh, Santosh K. Das, Sourav Sarkar and Jan-e Alam,
arXiv:1409.4652(2014).

CONFERENCE PROCEEDINGS:

- Thermal radiation from an expanding viscous medium,
Sukanya Mitra, Payal Mohanty, Sourav Sarkar, Jane Alam;
Viscosity of a pion gas,
Sukanya Mitra, Santosh k Das, Sourav Sarkar and Jan-e Alam;
Spectral properties of charmed mesons at finite temperature,
Sabyasachi Ghosh, Sukanya Mitra and Sourav Sarkar,

**Proceedings of the DAE Symposium on Nucl. Phys. 56 (2011) 902-
Visakhapatnam, India, December 26-30, 2011.**

- Shear viscosity of a strongly interacting pion gas,
Sukanya Mitra, Sourav Sarkar and Sabyasachi Ghosh,
Proceedings of the DAE Symposium on Nucl. Phys. 57 (2012) Delhi, India,
December 3-7, 2012.
- Shear viscosity of a strongly interacting pion gas,
Sukanya Mitra, Sourav Sarkar and Sabyasachi Ghosh,
Proceedings of “QGP Meet”, at VECC, Kolkata, India from 3-6 July, 2012.
- Medium effects on the transport coefficients of a hot pion gas,
Sukanya Mitra and Sourav Sarkar,
Proceedings of “Matter at extreme conditions : Then and now” at Bose In-
stitute, Kolkata, India from 15-17 January, 2014.
- The effect of medium on the relaxation of the dissipative flows in an interacting pion gas,
Utsab Gangopadhyaya, Sukanya Mitra and Sourav Sarkar,
Proceedings of the DAE Symposium on Nucl. Phys. 59 (2014) Varanasi,
India, December 08-12, 2014.

Sukanya Mitra
Sukanya Mitra



1. **Name of the Student:** Sukanya Mitra
2. **Name of the Constituent Institution:** Variable Energy Cyclotron Centre
3. **Enrolment No.:** PHYS04200904014
4. **Title of the Thesis:** Study of transport coefficients in strongly interacting matter at finite temperature.
5. **Board of Studies:** Physical Sciences

SYNOPSIS

Motivation for studying transport properties

Transport properties of a thermodynamic system have long been employed as probes to understand the underlying dynamics of the system. For a fluid there are in general two kinds of transport coefficients that are of primary interest : viscosity and thermal conductivity, which are related to the transport of momenta and heat respectively. Since the microscopic mechanism for such energy and momentum transfer is provided by interactions among the constituent particles within the fluid system, investigation of transport properties in turn gives information about the nature of interaction of the system.

In relativistic nucleus-nucleus collisions the created matter has been a subject of much interest because of the large amount of energy involved. The hydrodynamic evolution of this matter involves different dissipative processes which can be quantified by the above mentioned transport

coefficients. They not only provide relevant insights about the fluid dynamics as mentioned above, but also carry information on how far the system is away from an ideal hydrodynamics. Recent results from heavy ion collision experiments show clear indication that the produced matter behaves as a strongly interacting liquid rather than a weakly interacting gas. This is based on the observation of experimentally measured elliptic flow v_2 of hadrons in Au+Au collision at Relativistic Heavy Ion Collider (RHIC), which can be interpreted in terms of viscous hydrodynamics with a very small value of the shear viscosity over entropy density ratio η/s , almost close to that of a perfect fluid. These observations lead to the question of whether there is a fundamental lower limit to the values of shear viscosity as the strength of interaction increases. The possible lower bound, $1/4\pi$ is conjectured by Kovtun, Starinets and Sons [5] from their AdS/CFT calculations. Many other estimations of the transport coefficients have been carried out in QGP [23, 24], as well as in hadronic matter [15, 41, 6, 8]. Since the results provided by viscous hydrodynamics regarding heavy ion collisions depend sensitively on the value of η/s , it is important to use the values of the transport coefficients as accurately as possible in those hydrodynamic models which describe the space-time evolution of the strongly interacting thermal matter created. So far in most of the viscous hydrodynamic models constant, representative values of the transport coefficients [23, 24] have been used to describe the dissipative phenomena within the medium. Using $\eta/s = 1/4\pi$ we have evaluated the direct photon spectra and found a small but finite effect. In view of this we are motivated to estimate the realistic values of the transport coefficients which incorporate the effects of a hot, interacting medium. Inspired by this motivation, in this thesis, the transport coefficients of a hot pion gas have been evaluated. There have been quite a few estimates of the transport coefficients of a pion gas. In Ref. [37, 6] the transport coefficients of a pion gas have been evaluated using the Kubo formalism which relates the transport coefficients to retarded two-point functions. In Ref. [12, 41, 42, 20] the kinetic theory approach has been adopted where the transport coefficients are expressed explicitly in terms of interaction cross-section. In most of the cases of kinetic theory approach either the lowest order chiral perturbation theory has been used [12, 16], or a phenomenological amplitude has been used which is constructed to reproduce the experimental data of $\pi\pi$ interaction cross-section [8]. In [41, 42] a unitarized chiral perturbation theory was used.

In all the above cases the temperature dependence does not occur explicitly in the dynamical cross-sections incorporated in the expressions of transport coefficients. In this thesis an explicitly temperature dependent pion cross-section has been introduced and thereafter the transport coefficients are estimated with the help of the temperature dependent cross-section.

Contents of the thesis

In this thesis the shear and bulk viscosities as well as the thermal conductivity have been studied for a one component hot pion gas out of chemical equilibrium. There are certain approaches available in the literature for evaluating the transport coefficients among which the diagrammatic, two point correlator approach manifested by Kubo formula has been used in quite a few places [37, 6]. The method that has been adopted here is the kinetic theory approach which involves solving the relativistic transport equation. The novelty of this method lies within its approach that corresponds between the non-equilibrium kinetic theory and viscous hydrodynamics. The microscopic cross-section of the constituent particles enters as a dynamical input in the expressions of the macroscopic transport coefficients explicitly. There are a few calculations of transport coefficients which use this kinetic theory technique, also available in the literature [13, 14]. In this thesis advancements are made in the estimation of transport coefficients by introducing an in medium interaction cross-section, which is expected to produce a realistic temperature dependence of the viscosities and thermal conductivity in the context of heavy ion collision.

The basic steps that have been carried out to produce the values of temperature dependent transport coefficients for a hot pion gas are listed as follows.

- Obtain the expressions of transport coefficients from kinetic theory by solving the relativistic transport equation in the Chapman-Enskog approximation.
- Incorporating a temperature dependent $\pi\pi$ cross-section evaluated using thermal field theory with an effective Lagrangian describing $\rho\pi\pi$ and $\sigma\pi\pi$ interactions.

- Inserting a temperature dependent pion chemical potential to take care of the early chemical freeze out of the pion gas.
- Obtain the viscosities and thermal conductivity of a pion gas as a function of temperature.

After evaluation of those transport coefficients they have been applied to determine the time scale over which the energy and momentum are transported utilizing the second order theories of dissipative fluids.

Other transport coefficients, like the drag and diffusion coefficients also have been evaluated for heavy charmed mesons like J/ψ and η_c and hence their propagation in a hadronic medium has been investigated.

Transport coefficients of a hot pion gas

Formalism : Evaluation of transport coefficients

As mentioned earlier the transport coefficients have been evaluated in kinetic theory approach, which involves the solution of the relativistic transport equation. The method, which has been adopted in the present work is the well known Chapman-Enskog method. In general the program of seeking a solution of the transport equation becomes non-trivial due to the non-linearity of the collision term. However if the state of the system is not far from thermal equilibrium, one can assume that a linearized form of the transport equation can provide a reasonably accurate description of the non-equilibrium phenomena which involve dissipative processes like viscosities and thermal conductivity. In Chapman-Enskog method the linearization is performed around a local equilibrium distribution function with parameters which vary in space and time. So in this method the distribution function is expanded in a series, in terms of a parameter as following,

$$f(x, p) = f^0(x, p) + \epsilon f^1(x, p) + \epsilon^2 f^2(x, p) + \dots \quad . \quad (1)$$

Where the expansion parameter $\epsilon = \frac{\lambda}{L}$ is the ratio of two length scales, λ being the length scale associated with the collision term which is evidently the mean free path of the system and L is the length associated with the spatial non-uniformities in the system which is macroscopic dimension over which the thermodynamic quantities describing the system vary appreciably. The series generated by Chapman-Enskog procedure is asymptotic, which means the first Chapman-Enskog approximation, corresponding to the linear terms of the parameter ϵ only, i.e, associated with the linear laws of the transport phenomena, is the most significant. So one can restrict up to the first order of this expansion. Taking L of the order of the dimension of the system we find that this condition is fairly well satisfied and so the first Chapman-Enskog approximation suffices the need to describe the system in a near equilibrium situation. So the out of equilibrium distribution function can be expressed in terms of a deviation function ϕ as follows.

$$f(x, p) = f^{(0)}(x, p)[1 + f^{(0)}(x, p)]\phi(x, p). \quad (2)$$

The form of the transport equation is quite well known where the rate of change of the particle distribution function is quantified by a quantity called collision term or collision integral which takes care of the particle interactions responsible for altering the particle distribution within the system. When the distribution function is expanded in the manner mentioned above the collision term becomes a linear integral operator with a symmetric kernel depending upon the particle interaction. The local equilibrium distribution function for a Bosonic system is expressed in a form of *Jüttner* distribution function, with parameters μ , U^μ and T that again depend on the time-space coordinates. When applying the derivatives on the distribution function the left hand side of the transport equation appears as a sum of terms containing the thermodynamic forces with different tensorial ranks representing a scalar, a vector and a tensor respectively. In order to be a solution of this equation the deviation function ϕ must be a linear combination of these thermodynamic forces. Since the distribution function is a scalar quantity and its deviation should be the same, in order to keep ϕ a scalar quantity the respective coefficients should be of appropriate tensorial rank. The function which is the coefficient of the trace part of velocity gradient term, evidently is a scalar and must be related to the bulk or volume viscosity of the system. The second term which appears as a coefficient of the temperature

gradient term is a vector quantity associated with thermal conductivity of the system and the last one appearing as a tensor coefficient of the traceless part of velocity gradient is related to the shear viscosity of the system.

In this way one obtains three integral equations in terms of the coefficient functions by comparing the two sides of transport equation. The viscosities and the thermal conductivity can be evaluated as a function of the deviation ϕ by the usual prescription of comparing the two different expressions of dissipative energy-momentum stress tensor and heat flow respectively. So we can find the expressions of transport coefficients in terms of the coefficient functions which can be obtained by solving those integral equations mentioned earlier. Then by expanding the coefficients in terms of modified Bessel function of second kind and half integral order one can reach the algebraic expressions for transport coefficients after some tedious algebra [15].

So we observe that in Chapman-Enskog method the distribution function is developed in terms of its five moments - number density, hydrodynamic four-velocity, temperature and the space gradients of last two quantities. The method yields convenient algebraic expressions of transport quantities which explicitly contain the particle interaction through the linearized collision term.

Dynamical input : $\pi\pi$ cross section at finite temperature

As mentioned earlier the transport coefficients consist of the differential scattering cross section which appears explicitly in the denominator of their expressions. This reveals the significant dependence of the transport coefficients upon the interaction cross section of the system which serves as the crucial dynamical input. Previously the scattering amplitude was estimated from the lowest order Lagrangian of chiral perturbation theory [16] and in [6] a unitarized amplitude was employed for a meson gas. Phenomenological amplitudes obtained from fits to phase shift data have been employed in [8]. But all these calculations have been done with a cross-section in vacuum. The novelty of the present work is that we have introduced a $\pi\pi$ scattering cross section evaluated at a non-zero temperature in order to incorporate the effects of a hot pionic medium created in heavy ion collisions. The detailed evaluation of such a quantity is elaborated as follows.

The first task is to obtain the energy-dependent $\pi\pi$ cross section using a phenomenological approach which is close to the experimental value and at the same time is theoretically amenable to the incorporation of medium effects. It is found that the cross section resulting from lowest order chiral perturbation theory fails to match the data beyond 600 MeV of centre of mass energy. To this end we consider the scattering to proceed via ρ exchange since the experimental cross section shows a resonance peaked around $\sim 780\text{MeV}$ which is the mass of ρ meson. The corresponding invariant amplitude is evaluated using effective interactions taken from [11]. To describe the $\pi\pi$ scattering at low energies we also introduced σ exchange diagrams. The cross section so obtained agrees reasonably well with the experimental data.

The next task is to introduce the effect of a medium with non-zero temperature in the cross section. In a thermal medium the ρ propagator appearing in $\pi\pi$ scattering amplitude is expected to get modified which in turn modifies the cross section and as well as the transport coefficients. The effect of medium on ρ propagation is quantified through its self energy. Using the Dyson equation we obtain the in medium propagator in terms of the vacuum propagator and the ρ self energy function. The one loop self energy is evaluated by using the real time formalism of thermal field theory. The ρ self energy is evaluated for $\pi\pi$ loop and loops consisting of a pion and a heavy meson, e.g. ω , a_1 , h_1 etc. Now since these heavy mesons have substantial 3π or $\rho\pi$ decay widths, the contribution from these loops of heavy mesons can be considered as a multipion contribution to the ρ self energy. While the real part of the self energy modifies the mass term in the denominator of the propagator, the imaginary part is related to the decay width of ρ and is hence responsible for the medium modification of ρ -mediated $\pi\pi$ cross section. Actually the imaginary part of self energy is associated with different scattering and decay processes, which control the abundance of ρ meson in the medium. These processes certainly affect the cross section and consequently the transport coefficients as well.

When the medium effects in the $\pi\pi$ scattering cross section are introduced and plotted as a function of centre of mass energy we observe that the peak of the cross section gets suppressed when in medium effects are included. This is because of the fact that in medium the decay width which appears in ρ propagator increases on account of taking all the possible decay and scattering processes and since it appears in the denominator of $\pi\pi$ scattering amplitude it

reduces the cross section. For the $\pi\pi$ loop in the ρ self energy we obtain a moderate suppression where the loops including heavy mesons exhibit a larger suppression in the cross section peak. Thus it can be concluded that indeed non zero medium effects modify the dynamical cross section of the system which affects the transport properties in a significant way.

Temperature dependent pion chemical potential

In heavy ion collisions pions are known to get out of chemical equilibrium early at $T \sim 170$ MeV, resulting in stoppage of the number changing inelastic processes so that only the elastic processes (including the resonances) dominate the kinetics of the gas. At a still lower temperature $T \sim 100$ MeV, kinetic freeze out occurs freezing the momentum transfer. In order to keep the ratio of entropy density to particle number density fixed from chemical to kinetic freeze out a chemical potential starts building up with decrease in temperature. We take the temperature dependent pion chemical potential from Ref. [11] which implements the formalism described in [19] and reproduces the slope of the transverse momentum spectra of identified hadrons observed in experiments. Then this temperature dependent pion chemical potential has been introduced both in the kinematics that is in the phase space part and as well as in the dynamics that is in the interaction cross section of the transport coefficients.

Results

Employing all the treatments discussed above we have generated the set of our results. First let us start with shear viscosity. The temperature dependence of shear viscosity shows an increasing trend which is in accordance with [20, 15]. When the in medium cross sections are introduced we observe this medium suppressed cross section enhances the temperature dependence of transport coefficients which is larger for π -meson loop than $\pi\pi$ loop. Here we observe $\sim 10\%$ change in the value of η at $T=150$ MeV due to medium effects compared to the vacuum when all the loops in the ρ self-energy are considered. The effect reduces with temperature to less than 5% at 100 MeV. Using a temperature dependent pion chemical potential we found the same temperature trend of η with appreciable medium effects and it is noticed that the result

interpolates between the points representing chemical and kinetic freeze out. The temperature dependence of η/s also depicts the same decreasing trend as in [8] and visible medium effects, where the results with temperature dependent pion chemical potential exhibit a decreasing trend compared to the one with $\mu_\pi = 0$.

Next we turn to the results regarding the bulk viscosity. Unlike shear viscosity, the bulk viscosity shows a decreasing trend with increasing temperature. The coefficient of bulk viscosity ζ is also quantitatively much smaller than η , (at a particular temperature almost 10^{-3} times small). Though in this case medium dependence is clearly observed when we compare the results obtained with the vacuum cross section with the ones where the ρ and σ propagations are modified due to $\pi\pi$ and πh (multipion) loops. The temperature dependent μ_π also shows visible effects on the ζ vs. T plot. Finally the ratio ζ/s is represented where also the in medium effects are observed. In both the above cases the entropy density is taken for an interacting pion gas, where corrections up to $O(T^6)$ have been taken into the consideration.

Finally we have plotted the thermal conductivity times temperature as a function of temperature for a finite-temperature medium and using temperature dependent pion chemical potential. Both the in medium modified cross section and $\mu_\pi(T)$ improve its temperature dependence over the vacuum and zero chemical potential values. In all the cases we notice that the effect of medium over the transport coefficients increases with increasing temperature.

Thus we obtain a set of temperature dependent transport coefficients for a hot pionic medium taking the non-zero temperature contribution in their dynamical interaction cross section which shows appreciable improvements over their values evaluated at vacuum.

Transport of thermodynamic flows

In the first order theories of relativistic dissipative fluid dynamics, the entropy four-current contains terms up to linear order in dissipative fluxes of those quantities which are being transported. The resulting equations of motion of the thermodynamic variables do not include the transport related flows and the relation between the thermodynamic fluxes with the thermodynamic forces are expressed as linear laws without any terms containing the time derivative

of those fluxes. These equations of motion of the first order theory are parabolic in structure and lead to the undesirable feature that causality may not be satisfied, i.e. the fluxes may propagate with speeds exceeding that of light. This infinite speed of flows makes it impossible to have access to the relaxation times corresponding to the transport of flows.

To remedy this undesirable causality problem second order theory is introduced, where the entropy four-current includes terms quadratic in dissipative fluxes. The space of the thermodynamic variables is expanded to include the dissipative quantities and so the irreversible flows appear in the equations of motion of the thermodynamic variables of the system. The resulting equations for dissipative fluxes are hyperbolic in structure and they lead to causal propagation of signals. These dissipative quantities are then treated as thermodynamic variables in their own right.

In the present case we have used the Grad's 14 moment method. In this method all the gradients of the flows are taken into consideration in the conservation laws and instead of defining the distribution function from its first five moments, it is now expanded in terms of all its moments. Such an expansion leads to an infinite set of coupled equations for those moments. By truncating the expansion after a relatively small number of terms, one obtains a manageable finite set of equations. Finally from those equations one can determine the time scale over which the energy, momentum or the thermal disturbances are transported due to inter particle collisions. In the present work we obtain three separate equations of motion of the thermodynamic fluxes, namely the bulk viscous pressure equation, heat flow equation and the shear viscous pressure equation which contains explicit time derivatives of the thermodynamic fluxes giving rise to finite, non-zero values of the time scale over which these fluxes decay down to their equilibrium values. The relaxation times corresponding to different thermodynamic flows have been evaluated for a massive pion gas at a non-zero temperature and chemical potential where we can find that the first order transport coefficients for the respective flows serve as an input ingredient. The corresponding results show significant modifications of the temperature dependence of those relaxation times with the in medium cross sections compared to vacuum ones. The temperature dependent pion chemical potential also proved to affect the results in a significant way.

Other transport coefficients

Drag and diffusion coefficients have been estimated for heavy mesons with charm degrees of freedom, like J/ψ and η_c in a mesonic medium of lighter particles consisting of π , k , η , ρ , ω and ϕ . The cross-sections for the necessary interactions are evaluated from an effective Lagrangian taken from [7]. Then the transport quantities of the heavy particles are evaluated both by using those cross sections and by scattering length technique [22]. Finally the drag and diffusion coefficients are plotted as a function of temperature and thus the J/ψ absorption by comoving hadrons have been investigated.

Bibliography

- [1] P. Kovtun, D. T. Son and A. O. Starinets, Phys. Rev. Lett. **94**, 111601 (2005).
- [2] P. B. Arnold, G. D. Moore and L. G. Yaffe, JHEP **0011** (2000) 001; **0305** (2003) 051
- [3] P. B. Arnold, C. Dogan and G. D. Moore, Phys. Rev. D **74** (2006) 085021
- [4] M. Prakash, M. Prakash, R. Venugopalan and G. Welke, Phys. Rept. **227** (1993) 321.
- [5] A. Dobado and S. N. Santalla, Phys. Rev. D **65**, 096011 (2002).
- [6] A. Dobado and F. J. Llanes-Estrada, Phys. Rev. D **69**, 116004 (2004).
- [7] A. Dobado and F. J. Llanes-Estrada, Phys. Rev. D **69**, 116004 (2004).
- [8] D. Fernandez-Fraile and A. Gomez Nicola, Phys. Rev. Lett. **102**, 121601 (2009).
- [9] E.Lu and Guy.D.Moore Phys. Rev. C **83**, 044901 (2011).
- [10] K. Itakura, O. Morimatsu and H. Otomo and J. M. Torres Rinkon, arXiv:hep-ph/0702130 (2007).
- [11] A. Hosoya, M. a. Sakagami and M. Takao, Annals Phys. **154** (1984) 229.
- [12] R. Lang, N. Kaiser and W. Weise, Eur. Phys. J. A **48** (2012) 109.
- [13] S. Gavin, Nucl. Phys. A **435** (1985) 826.
- [14] A. Wiranata and M. Prakash, arXiv:1203.0281 [nucl-th].

- [15] S. R. De Groot, W. A. Van Leeuwen and C. G. Van Weert, *Relativistic Kinetic Theory, Principles And Applications* (Amsterdam, Netherlands, North-holland, 1980).
- [16] E. Nakano, arXiv:hep-ph/0612255.
- [17] T. Hirano and K. Tsuda, Phys. Rev. C **66** (2002) 054905
- [18] H. Bebie, P. Gerber, J. L. Goity and H. Leutwyler, Nucl. Phys. B **378** (1992) 95.
- [19] F. Klingl, N. Kaiser and W. Weise, Z. Phys. A **356** (1996) 193
- [20] D. Davesne, Phys. Rev. C **53**, 3069 (1996).
- [21] K.L. Haglin and C. Gale, Phys. Rev. C 63, 065201 (2001).
- [22] K. Yokokawa, S. Sasaki, T. Hatsuda and A. Hayashigaki Phys. Rev. **D 74**, 034504 (2006).
- [23] A. Muronga Phys. Rev. **C 69**, 034903 (2004).
- [24] M. Luzum and P. Romatschke Phys. Rev. **C 78**, 034915 (2008).

List of publications of Sukanya Mitra

Journals:

a. Published

1. *Sukanya Mitra*, Payal Mohanty, Sourav Sarkar and Jan-e Alam, Thermal radiation from an evolving viscous quark gluon plasma, International Journal of Modern Physics E 22, 1350004(2012).
2. *Sukanya Mitra*, Sabyasachi Ghosh, and Sourav Sarkar, Effect of a spectral modification of the ρ meson on the shear viscosity of a pion gas, Phys. Rev. C 85, 064917 (2012).
3. Mahatsab Mandal, *Sukanya Mitra*, Pradip Roy and Sourav Sarkar, Effect of running coupling on photon emission from quark gluon plasma, Phys. Rev. C 85, 067901 (2012).
4. *Sukanya Mitra* and Sourav Sarkar, Medium effects on the viscosities of a pion gas, Phys. Rev. D 87, 094026 (2013).
5. Sabyasachi Ghosh, *Sukanya Mitra* and Sourav Sarkar, Effect of in-medium spectral density of D and D^* mesons on the J/ψ dissociation in hadronic matter, Nuclear Physics A917(2013)71.
6. Payal Mohanty, Sabyasachi Ghosh, and *Sukanya Mitra*, Electromagnetic Radiations from Heavy Ion Collision, Advances in High Energy Physics, 176578(2013).
7. *Sukanya Mitra* and Sourav Sarkar, Medium effects on the thermal conductivity of a hot pion gas, submitted to Phys. Rev. D.

b. Communicated

1. *Sukanya Mitra*, Payal Mohanty, Sabyasachi Ghosh, Sourav Sarkar and Jan-e Alam, Characterizing quark gluon plasma by thermal photons and lepton pairs, arXiv:1303.0675(2013).

2. *Sukanya Mitra*, Sabyasachi Ghosh, Santosh K. Das, Sourav Sarkar and Jan-e Alam, Diffusion of hidden charm mesons in hadronic medium, arXiv:1409.4652(2014).

Conference proceedings:

- Proceedings of the DAE Symposium on Nucl. Phys. 56 (2011) 902-Vishakhapatnam, India, December 26-30, 2011 and 57 (2012) Delhi, India, December 3-7, 2012.
- *Sukanya Mitra*, Sourav Sarkar and Sabyasachi Ghosh, Shear viscosity of a strongly interacting pion gas, Proceedings of QGP Meet, 2012 held at VECC, Kolkata, India.

Doctoral Committee Report for Sukanya Mitra

On the basis of the work done by Sukanya Mitra, the doctoral committee recommends the submission of thesis to HBNI for Ph. D.

Signature of Student: *Lukanya Mitra*

Date: *5/8/2014*

Doctoral Committee:

S. No.	Name	Designation	Signature	Date
1.	Dr. D.K. Srivastava	Chairman	<i>D.K. Srivastava</i>	<i>5/8/14</i>
2.	Dr. Sourav Sarkar	Guide/ Convener	<i>Sourav Sarkar</i>	<i>5/8/14</i>
3.		Co-guide (if any)		
4.	Dr. Jan-e Alam	Member	<i>Jan-e Alam</i>	<i>5/8/14</i>
5.	Prof. Pradip K. Roy	Member	<i>Pradip K. Roy</i>	<i>05/08/14</i>
6.		Member		

Contents

Synopsis	8
List of Figures	34
1 Introduction	35
1.1 Prelude	35
1.2 General methods to treat many-particle systems	36
1.2.1 Kinetic Theory	36
1.2.2 Hydrodynamics	38
1.3 Irreversible processes and dissipative quantities	38
1.4 Heavy Ion Collision	39
1.4.1 Motivation behind colliding nuclei at high energies	39
1.4.2 Experimental milestones	42
1.4.3 Signatures of QGP	42
1.4.4 Theoretical methods to describe the system created in heavy ion collisions	45
1.4.5 Evidence of dissipation in the matter created in heavy ion collisions . . .	46

1.5	The scope and prospect of the present work	47
2	Elements of fluid dynamics	53
2.1	Thermodynamic quantities	54
2.1.1	Particle number density	54
2.1.2	Energy-momentum tensor	55
2.1.3	Hydrodynamic four-velocity	57
2.1.4	Other thermodynamic quantities	59
2.2	Equilibrium thermodynamic quantities expressed as a sum over infinite series . .	61
2.2.1	Definition of equilibrium distribution function	62
2.2.2	Particle density	64
2.2.3	Energy density	65
2.2.4	Pressure	65
2.2.5	Enthalpy density	66
2.3	Conservation laws	66
2.3.1	Conservation of particle number	68
2.3.2	Conservation of energy-momentum	69
2.4	Equation of motion of thermodynamic quantities	69
2.4.1	Equation of continuity	70
2.4.2	Equation of motion	70
2.4.3	Equation of energy	71
2.4.4	Equation of enthalpy	71

2.4.5	Equation of temperature and chemical potential	72
3	Evaluation of transport coefficients	75
3.1	Origin of transport coefficients	76
3.2	Solution of the relativistic transport equation	78
3.2.1	Relaxation time approximation	79
3.2.2	Chapman-Enskog method	81
3.3	Evaluation of transport coefficients in Chapman-Enskog method	85
3.3.1	Bulk viscosity	91
3.3.2	Thermal conductivity	95
3.3.3	Shear viscosity	97
3.4	Appendix A-Irreducible tensors	99
3.5	Appendix B-Reduction of collision bracket	100
3.6	Appendix C-Reduction of the product of distribution functions	102
4	Evaluation of relaxation times of the dissipative flows	105
4.1	Conservation laws and equations of motions in dissipative fluid dynamics	107
4.2	The need of a second order theory - Limitations of the first order theory	109
4.3	Evaluation of relaxation times - Grad's 14 moment method	111
4.3.1	Solving the transport equation	111
4.3.2	Determination of the coefficients A , B_μ and $C_{\mu\nu}$	113
4.3.3	Equation of motion of dissipative fluxes	116

5	The $\pi\pi$ cross-section in the medium	121
5.1	The $\pi\pi$ cross section in vacuum due to ρ meson exchange	124
5.1.1	Interaction Lagrangian	124
5.1.2	Setting the coupling constant $g_{\rho\pi\pi}$	125
5.1.3	Amplitudes of $\pi\pi$ scattering by exchanging ρ meson	126
5.1.4	Amplitudes of $\pi\pi$ scattering including both ρ and σ mesons exchange . .	134
5.2	The $\pi\pi$ cross section at finite temperature	136
5.3	Inclusion of temperature dependent pion chemical potential	139
6	The effect of medium on the transport coefficients and relaxation of flows in an interacting pion gas	145
6.1	Shear Viscosity	146
6.1.1	Effect of medium on shear viscosity	146
6.1.2	Effect of temperature dependent chemical potential on shear viscosity . .	147
6.1.3	Effect of medium on shear viscosity to entropy density ratio	148
6.2	Bulk Viscosity	151
6.2.1	Effect of medium and temperature dependent chemical potential on bulk viscosity	151
6.2.2	Effect of medium and temperature dependent chemical potential on bulk viscosity to entropy density ratio	152
6.3	Thermal conductivity	153
6.3.1	Effect of medium on thermal conductivity	153
6.3.2	Effect of temperature dependent chemical potential on thermal conductivity	154

6.4	Effect of medium and temperature dependent chemical potential on relaxation times of dissipative flows	155
6.5	Discussions	157
7	Drag and Diffusion of hidden charm mesons in hadronic medium	161
7.1	Introduction	161
7.2	Formalism	162
7.3	Dynamics	163
7.4	Results	168
7.5	Discussions	169
8	Effect of viscosity on the photon spectra	174
8.1	Introduction	174
8.2	Production of thermal photons	176
8.2.1	Thermal photons from QGP	177
8.2.2	Thermal photons from hadronic matter	178
8.3	Viscous correction to the distribution function	178
8.4	Expansion dynamics	179
8.5	Results	181
8.5.1	Photon spectra	182
8.6	Summary and Discussions	186
9	Summary and Outlook	196

List of Figures

1.1	Different stages of heavy ion collision.	42
1.2	Ideal and viscous hydrodynamic models trying to fit the experimental data of elliptic flow of charged hadrons [29].	48
5.1	The $\pi\pi$ phaseshifts (5.4) as a function of energy compared to Roy equation solutions given in Ref. [10]	123
5.2	Cross-section as a function of C.M. energy from LOChPT which fails to represent the experimental data beyond $600MeV$	124
5.3	Different decay modes for the $\rho \rightarrow \pi\pi$ process.	125
5.4	t and u-channel diagrams for $\pi^+\pi^+ \rightarrow \pi^+\pi^+$ scattering	127
5.5	s and u-channel diagrams for $\pi^+\pi^0 \rightarrow \pi^+\pi^0$ scattering	128
5.6	s and t-channel diagrams for $\pi^+\pi^0 \rightarrow \pi^0\pi^+$ scattering	128
5.7	s and t-channel diagrams for $\pi^0\pi^+ \rightarrow \pi^+\pi^0$ scattering	129
5.8	s and u-channel diagrams for $\pi^0\pi^+ \rightarrow \pi^0\pi^+$ scattering	129
5.9	s and t-channel diagrams for $\pi^+\pi^- \rightarrow \pi^+\pi^-$ scattering	130
5.10	s and u-channel diagrams for $\pi^+\pi^- \rightarrow \pi^-\pi^+$ scattering	130
5.11	t and u-channel diagrams for $\pi^+\pi^- \rightarrow \pi^0\pi^0$ scattering	130

5.12	s and u-channel diagrams for $\pi^-\pi^+ \rightarrow \pi^+\pi^-$ scattering	131
5.13	s and t-channel diagrams for $\pi^-\pi^+ \rightarrow \pi^-\pi^+$ scattering	131
5.14	t and u-channel diagrams for $\pi^-\pi^+ \rightarrow \pi^0\pi^0$ scattering	132
5.15	t and u-channel diagrams for $\pi^0\pi^0 \rightarrow \pi^+\pi^-$ scattering	132
5.16	t and u-channel diagrams for $\pi^0\pi^0 \rightarrow \pi^-\pi^+$ scattering	133
5.17	The $\pi\pi$ cross-section evaluated from ρ exchange diagrams shows good agreement with experimental data except at low energies.	134
5.18	The $\pi\pi$ cross-section evaluated from both ρ and σ exchange diagrams agrees with the experimental data quite nicely.	135
5.19	The exact ρ propagator with $\pi - h$ loop diagrams for $h = \pi, \omega, h_1, a_1$ mesons. . .	137
5.20	The $\pi\pi$ cross-section as a function of centre of mass energy. The dashed line indicates the cross-section obtained using eq. (5.37) which agrees well with the experimental values shown by filled circles. The dash-dotted and solid lines depict the in-medium cross-section for $\pi\pi$ and multi-pion loops respectively in the ρ self-energy evaluated at $T=160$ MeV.	140
5.21	The pion chemical potential as a function of temperature [18].	141
5.22	The $\pi\pi$ cross-section as a function of centre of mass energy at $T=160$ MeV and $\mu_\pi = \mu_\pi(T)$	142
6.1	The shear viscosity as a function of temperature in the Chapman-Enskog approximation. The dashed and dot-dashed lines correspond to the use of in-medium cross-sections for $\pi\pi$ and multi-pion loops respectively. The solid line represents the vacuum case.	147
6.2	The shear viscosity as a function of temperature for different values of pion chemical potentials using vacuum cross section.	148

6.3	The shear viscosity in various scenarios as a function of T . The red (upper) and the black (lower) sets of curves correspond to $\mu_\pi = 0$ MeV and $\mu_\pi = \mu_\pi(T)$ respectively. In each set the solid line represents the vacuum cross-section, the dashed line represents the in-medium modification due to pion loop and the dash-dotted line for loops with heavy particles in addition.	149
6.4	The entropy density of an interacting pion gas as a function of T for different values of the pion chemical potential.	150
6.5	η/s as a function of T for different values of μ_π	151
6.6	The bulk viscosity in various scenarios as a function of T . The upper (with circles), middle (with triangles) and lower sets of curves correspond to $\mu_\pi = 85$ MeV, $\mu_\pi = \mu_\pi(T)$ and $\mu_\pi = 0$ respectively. In each set the solid lines represents use of vacuum cross-section, the small dashed lines for in-medium modification due to pion loop and the long dashed lines for loops with heavy particles in addition.	152
6.7	ζ/s as a function of T for different $\pi\pi$ cross-section. The temperature dependent pion chemical potential has been used in all cases.	153
6.8	λT as a function of T for different $\pi\pi$ cross-sections with zero pion chemical potential.	154
6.9	λT as a function of T for different $\pi\pi$ cross-sections and chemical potentials. . .	154
6.10	Relaxation time of bulk viscous pressure as a function of T for different $\pi\pi$ cross-sections with different pion chemical potentials.	155
6.11	Relaxation time of heat flow as a function of T for different $\pi\pi$ cross-sections with different pion chemical potentials.	156
6.12	Relaxation time of shear viscous pressure as a function of T for different $\pi\pi$ cross-sections with different pion chemical potentials.	157

7.1	The s and u channel of J/ψ - V scattering via η_c exchange are respectively depicted in diagrams (A) and (B). Diagrams (C) and (D) are the same for the η_c - V scattering via J/ψ	165
7.2	The drag coefficient (γ) as a function of temperature calculated in the effective Lagrangian approach.	169
7.3	The drag coefficient (γ) as a function of temperature obtained using scattering lengths.	170
7.4	The diffusion coefficient (D) as a function of temperature calculated in the effective Lagrangian approach.	171
7.5	The diffusion coefficient (D) as a function of temperature obtained using scattering lengths.	171
8.1	Variation of temperature with proper time for different phases for various values of the shear viscosities. Inset shows the effect of viscosity on the cooling of the QGP phase (in an amplified scale) for different values of η/s	180
8.2	The p_T dependence of the ratio of the transverse momentum distribution of thermal photons with the equilibrium distribution to the viscous correction.	183
8.3	Transverse momentum distribution of thermal photons from QGP for various values of η/s in the scenario (i).	184
8.4	Transverse momentum distribution of thermal photons from QGP for various values of η/s in the scenario (ii).	186
8.5	Transverse momentum distribution of photons from thermal hadrons for various values of η/s in the scenario (i).	187
8.6	Transverse momentum distribution of photons from thermal hadrons for various values of η/s in the scenario (ii).	188

8.7	Transverse momentum distribution of thermal photons from the entire evolution history of the system for various values of η/s in the scenario (i).	189
8.8	Transverse momentum distribution of thermal photons from the entire evolution history of the system for various values of η/s in the scenario (ii).	190
8.9	Transverse momentum distribution of thermal photons scaled with the effect of radial flow and compared with the direct photon data from PHENIX for 0-20% centrality.	191
8.10	Transverse mass distribution of pions with and without viscous effects.	192

Chapter 1

Introduction

1.1 Prelude

The physical world around us consists of many particle systems. The study of such a system with a large number of degrees of freedom clearly becomes non tractable and the knowledge of each generalized coordinate corresponding to each constituent particle is really not necessary in order to determine the overall properties of the system. In order to learn about the system we need to study its properties which are subject to measurement. We need some particular set of tools to quantify these properties. Now if the system has a well defined boundary that separates it from its surroundings such that there are certain processes only allowed in the interior of the region, it is called a thermodynamic system. The properties mentioned earlier are defined as the thermodynamic parameters or the state variables, which are experimentally measurable macroscopic quantities. These parameters uniquely define the state of a system. The problem then reduces to find a certain prescription to estimate these thermodynamic (macroscopic) quantities in order to describe the many particle thermodynamic system.

1.2 General methods to treat many-particle systems

The dynamics of a given collection of N number of particles can be described in a number of ways. If the de Broglie wavelength associated with each particle is large compared to the interparticle separation, the waveforms corresponding to various particles overlap and a quantum mechanical description is necessary. Then the system is described by the N particle wave functions evolving in time following the *Schrödinger* equation. In the opposite case, if the wave functions of different particles are widely separated, the quantum interference is not important and the individual wave packets evolve according to the *Schrödinger* equation in an isolated fashion, moving like classical particles. In the later case the state of the system is described by the positions and velocities of N particles, and the time evolution is described by the laws of classical mechanics. An accurate description of such systems requires the inclusion of the interparticle potentials in the many particle Schroedinger equations. But handling $\sim 10^{23}$ numbers of equations corresponding to each particle turns out to be an impossible task. So one has to find out some convenient way to describe the properties of a system containing so many number of particles. There exist two general ways to treat a multiparticle system,

- Kinetic theory,
- Hydrodynamics.

1.2.1 Kinetic Theory

Kinetic theory serves as the most unique technique to treat a many particle system starting from the Hamiltonian description of the 10^{23} particles and ending at the equations of fluid dynamics. The first equation of motion we obtain is the evolution of the probability distribution function along any trajectory of the N particle phase space, known as *Liouville's* equation. But this does not make our life simpler since it still includes a function of 10^{23} variables. To proceed, the plan is to limit our ambitions. Instead of focusing on the probability distribution function of all N particles, we define one particle distribution function by singling out each particle within

the system. If we try to obtain the evolution equation of this one particle distribution function we find that the single particle distribution function evolves by a *Lioüville* like equation with a corrected term depending on two particle distribution function. In this manner we obtain a set of coupled equations which tells that any group of N particles evolves in a Hamiltonian fashion, corrected by interactions with one of the particles out side the group. This is called the famous *BBGKY* hierarchy prescribed by Bogoliubov, Born, Green, Kirkwood and Yvon to treat the time evolution of the system. At first glance it does not seem to make life any easier since we still have to deal with N number of coupled equations. However the advantage of working with this scheme is that it gives the opportunity to implement various approximations to decide upto which term the problem is important so that the series can be truncated up to that ignoring the negligible ones. In this way the hierarchy turns out to be something manageable and convenient to use. The simplest, and most useful, of these truncations is the Boltzmann transport equation, where it is assumed that if the time duration of collision is sufficiently smaller than the time between two collisions to occur, the dynamical evolution of the system can be described by the Hamiltonian evolution of single particle distribution function with the perturbations by the collisions. The collision terms include the interaction between the particles and thus the microscopic dynamics is embedded in the evolution equation of single particle distribution function provided by kinetic theory. However even this equation is not trivial to solve because of the collision term which appears as an integral making the transport equation in an integro-differential equation. The non-linearity of the collision term becomes the biggest problem in utilizing the transport equation. There are a number of methods depending on certain approximations to linearize the collision term such that the collision operator becomes a linear integral operator with symmetric kernel which is mathematically more tractable. Once the transport equation is solved the macroscopic thermodynamic quantities describing the system can be defined with solution of single particle distribution function. In this manner the kinetic theory provides an analytical scheme to study a many particle system and obtain the thermodynamic properties that can be measured experimentally. The virtue of this approach is that it connects the macroscopic bulk properties of the system with its microscopic dynamical interaction in a very elegant way. This is the reason that inspite of

the technical difficulties of tackling the collision term it serves as one of the most useful and effective way to describe a many particle system.

1.2.2 Hydrodynamics

The macroscopic quantities or the state variables mentioned earlier are related by one or more functional relationships which are called equations of state for the system. Hydrodynamics provides these relationships among the macroscopic quantities by simple algebraic equations. Actually these state equations such as equation of energy, equation of motion, equation of particle number density etc. follow from some conservation laws. There are mainly two quantities, particle flow and energy-momentum flux, whose conservation laws lead to most of the state equations we need. So hydrodynamics gives the variation of the measurable macroscopic quantities with time and space. So although kinetic theory defines the macroscopic quantities there is no way to obtain their time profile within an evolving system. Hydrodynamics uniquely provides these evolution equations of the state variables for the system under consideration. Since hydrodynamics only deals with bulk properties of the systems and do not care about the single particle functions, the microscopic dynamics of the system is not included in this theory. So in order to describe the system voyaging from kinetic theory to hydrodynamics we are proceeding by loosing informations about the interaction dynamics but constructing newer techniques to estimate those things which are required to study the system in terms of measurable quantities.

1.3 Irreversible processes and dissipative quantities

When a thermodynamic system under consideration experiences no net flow of matter or energy and consequently no change in macroscopic properties, the system is said to be in a state of thermodynamic equilibrium. Any deviation from it where the system is subjected to the net flow of energy or matter, is called non-equilibrium state of the system. When an out of equilibrium system is isolated, it spontaneously evolves towards its own equilibrium. In thermodynamics a change in the thermodynamic states can not be precisely restored to its initial state by

infinitesimal changes in some property of the system without expenditure of energy. So the associated processes always involves dissipation. So a system that is out of equilibrium relaxes to its equilibrium state by increasing entropy which becomes maximum for an equilibrium system. The associated processes are called irreversible processes where the change of entropy is always positive. Evidently non-equilibrium thermodynamics is associated with transport processes since the system tends to restore its equilibrium by transporting matter, energy or momentum.

Transport properties have long been employed as probing tool to understand the characteristics of a thermodynamic system. Since the microscopic mechanism of the energy and momentum transfer involved in transport processes is provided by interactions among the constituent particles within the system, investigation of transport properties in turn gives prediction about the nature of interactions within the system. In all practical systems the hydrodynamic evolution leads to different dissipative processes which can be quantified by some quantity called transport coefficients. These transport coefficients not only provide the relevant insight on the microscopic dynamics of the system under consideration, but also carry information on how far the system appears from ideal hydrodynamics. So investigation of the transport coefficients can be proved very useful to study a particular system. With this motivation we proceed to evaluate the transport quantities for a very special system that will be discussed in the following section.

1.4 Heavy Ion Collision

1.4.1 Motivation behind colliding nuclei at high energies

Nuclear physics is basically a journey towards the interior of matter. After the pioneering discovery of positively charged protons inside the atoms by Rutherford, and charge neutral neutrons by James Chadwick for many years nuclear physicists treated the nucleons as if they were the most fundamental constituents of the nucleus. However in the second half of the

twentieth century, a question was raised that whether the nucleons or more generally hadrons can at all be treated as the most fundamental structure of matter. For this purpose highly energetic collisions of hadrons were suggested as a possible means of “breaking them apart” and then on a series of experimental discoveries firmly established the existence of a subnuclear world constituted by quarks which are bound by gluons. The existence of this substructure is strictly limited to the interior of the particles, leading to the fact that no quarks or gluons can ever be removed from the interior of an elementary particle. It was considered that if a substantial amount of temperature or pressure can be applied to make the particles heated or compressed enough such that they fail to retain their identity on account of large overlap, then one can experimentally produce a large bag of quark-matter or which is conventionally known as “Quark-gluon plasma” (QGP). The transition of the hadrons to this new state of matter denoted by “QGP” can be explained by the property of the Quantum Chromo Dynamics(QCD) called *Asymptotic freedom*.

The possibility of a deconfined phase of QCD was first conjectured by noting that the coupling constant appearing in the thermodynamic potentials approaches to zero at high temperature or density. This was later interpreted that QCD becomes weakly interacting at high temperatures. This is because at very high momentum transfer, the strength of interaction among the partons becomes very weak. The effective coupling constant of the interaction becomes smaller at higher momentum transfer and perturbation theory can be reliably utilized (at least in the extreme case) to obtain quantitative results for observables which have been confirmed by high energy scattering experiments. This behavior is known as the asymptotic freedom. On the other hand in the low momentum domain, the interaction becomes very strong, and perturbation theory ceases to be applicable and nonperturbative mechanisms take over. It is this regime where quark confinement (or clustering of color charged particles to form color neutral objects) and mass generation occur, imposing formidable challenges for their theoretical understanding. Thus, at very high temperatures and densities in the domain of weak coupling between quarks and gluons, the long range interactions are dynamically screened, quarks and gluons are no longer confined to bound hadronic states, and they propagate through a larger volume allowing the possibility of a deconfined state of partons. This leads to the formation of Quark-Gluon Plasma

which can be formed both at high temperatures and at high densities. A direct motivation to understand this high temperature and density region comes from cosmology as well as from astrophysics. The Big Bang theory of cosmology suggests that a few microseconds after the Big Bang, the universe was made up of quark-gluon plasma at a very high temperature of about 200 MeV ($\sim 2 \times 10^{12}K$). Further expansion as well as cooling and probably a phase transition (or may be a cross-over) at some critical temperature (about 170 MeV) produces a hadronic phase from the hot and dense plasma phase. To understand the evolution of the early universe it is necessary to study the properties of QGP at very high temperatures [1]. Another equally important reason to study QGP is to know the properties of matter at extremely high densities, such as in a neutron star. The neutron star is a very heavy and super dense object, which is formed at the end of supernova explosion of a regular star. At the center of neutron stars density is so high that quarks and gluons may not remain confined, leading to a QGP phase at high baryon density.

These facts serve as the motivation of colliding heavy nuclei at relativistic energies. During the collisions, both high baryon density and high temperature may be reached. Thus in a “Heavy Ion Collision”, i.e, in the collision of two relativistically high energy heavy nuclei, a quark-gluon plasma can be formed which will subsequently go through the phase transition and hadronize into particles in the final states. The evolution of the matter created in high energy nucleus-nucleus collision can be pictured in the following way. After the collision a large amount of energy is stored in a small region resulting in a high energy density. The system of quarks and gluons presumably reach a state of thermal equilibrium within a few fm/c and thus the presence of a thermalized medium of quarks and gluons has been assumed. Due to high internal pressure the medium then expands and cools. Finally it undergoes a phase transition and transforms to a hadronic gas phase. Then the hadron gas further expands to reduce energy density and finally reaches the freeze-out, when the mean free path becomes so large that the final state hadrons do not interact with each other anymore. A simulation of the possible stages of evolution of the produced matter in heavy ion collisions are depicted in Fig. (1.1). Thus heavy ion collisions at relativistic energies provide a unique experimental opportunity to probe nuclear matter under extreme conditions.

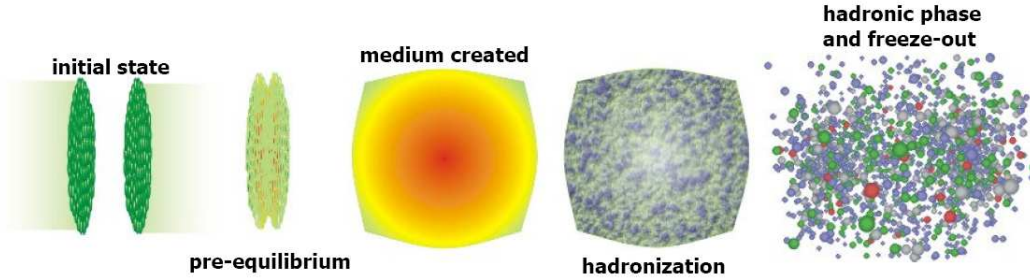


Figure 1.1: Different stages of heavy ion collision.

1.4.2 Experimental milestones

The experimental study of heavy ion collisions was initiated at the BEVALAC at Berkeley. However, the energy deposited in that experiment was not sufficiently high to create a QGP phase. The subsequent attempts of heavy ion experiments were carried out at AGS of BNL (since 80s) and SPS of CERN (since 1994). These were both fixed-target experiments which studied Au+Au and Pb+Pb collisions with $E_{lab} \approx 14$ and 200 AGeV, respectively. The results from those experiments [2] have demonstrated extremely rich physics which could not be explained by simple extrapolation of pp collisions. Through the last decade the experimental program at Relativistic Heavy Ion collider (RHIC) at Brookhaven National Laboratory, USA [3, 4, 5, 6] have provided a significant evidence for the formation of a hot and dense state of matter that had not been observed so clearly in the earlier experiments. Finally the Large Hadron Collider (LHC) at CERN [7], Geneva have produced a fortune of data which have proved to be extremely useful to characterize the properties of the thermodynamic system created out of the matter produced in those collisions. In addition to these, an experimental facility called FAIR at GSI Germany, is proposed to study QGP at very high densities [8].

1.4.3 Signatures of QGP

Over the years many signatures have been proposed to study different aspects of the hot/dense matter created in heavy ion collision. We discuss a few of them in the following sections which have relevance to the work reported in this thesis.

Elliptic flow

In non-central nuclear collisions, or if the colliding nuclei are deformed, the nuclear overlap region is initially spatially deformed. Interactions among the constituents of the matter formed in that zone transfer this spatial deformation onto the momentum space. Since the interactions among the fireball constituents are sensitive to the anisotropic density gradients in the reaction zone, it redirect the momentum flow preferably in the direction of stronger density gradients. The result is a momentum-space anisotropy, with more momentum flowing into the reaction plane than out of it. Such a “momentum-space reflection” of the initial space deformation is a unique signature for strong interactions in the fireball and proves that the fireball matter has undergone significant nontrivial dynamics between creation and freeze out. If this anisotropic momentum distribution with respect to the azimuthal angle of the out going particle is expanded in Fourier series then the polar plot of the first harmonics just appear to shift the fireball with out changing its shape. Hence the coefficient of this term is called the directed flow. However in the polar plot of second harmonics, the fireball appears as an ellipse and so the coefficient of this term is named as elliptic flow. The faster motion of the fireball in the reaction plane than perpendicular to it is due to this elliptic flow and hence the experimental evidence of the elliptic flow serves as a firm signature of the creation of a strongly interacting matter in heavy ion collisions [9, 10]. Moreover since it is observed that all the momentum anisotropy is built up during the first $6fm/c$ [11], it is also a good signature of the fast thermalization and the existence of a partonic medium (QGP). The anisotropic flow in non-central collisions turn out to be very sensitive to viscosity. The hydrodynamic description of elliptic flow requires the inclusion of dissipative effects (will be discussed later in more detail) and hence leads to the study of non-equilibrium phenomena in heavy ion collisions.

Electromagnetic probes

The quark gluon plasma is made up of quarks, anti quarks and gluons. The quarks and anti quarks have electric charge apart from their color charge. So they take part in electromagnetic interactions leading to production of photons and lepton pairs. For example in the lowest order,

a quark can interact with an anti quark in order to produce a photon and a gluon or they can form a virtual photon which subsequently decays into a lepton l^- and an anti lepton l^+ pair (commonly known as dilepton pair). Moreover a quark or an anti quark interacts with a gluon which results in the production of a photon. These photons and dilepton pairs are called electromagnetic probes to investigate the properties of QGP. However they can be produced from the hot hadronic matter also by different electromagnetic interactions among charged hadrons. Since these particles interact with its surroundings only through electromagnetic interactions, in an environment of strong interaction its mean free path becomes really large, so that they pass through the collision region and reach the detector without losing much information. On the other hand the production rate and the momentum distribution of these photons and dileptons depend on the momentum distribution of the initial quarks, anti quarks and gluons in the plasma, which are governed by the thermodynamic conditions of the plasma. Therefore the electromagnetic probes carry the information on the thermodynamic state of the medium at the moment of their production. Moreover since they are produced from all stages of the evolving fireball, they can extract the information from all the stages of the expanding medium through out the evolution. So these dileptons and photons created out of the matter produced in heavy ion collisions are regarded as deep probes of QGP [12, 13, 14, 15, 16].

J/ψ suppression

J/ψ is a bound state of a charm quark c and an anti quark \bar{c} . It is well known that the c and \bar{c} quarks can only be produced in the initial stages from collision of hard partons. In the quark gluon plasma, due to deconfinement of quarks and gluons the string tension between c and \bar{c} pair is zero. The only interaction between them is the Coulomb-type color interaction. If a J/ψ particle is placed in the quark-gluon plasma, the Debye screening will modify the long range Coulomb-type color interaction into the short range Yukawa-type interaction between c and \bar{c} , with the interaction range given by the Debye screening length. The Debye screening length is inversely proportional to the temperature. At high temperatures, the range of this attractive interaction becomes so small that it becomes impossible for the $c\bar{c}$ pair to form a bound state. As a result the J/ψ particle placed in quark-gluon plasma will be dissociated, leading to the

suppression of its production in high energy nucleus nucleus collisions [17]. Subsequently these charm and anti charm quarks combine with light quarks or anti quarks to emerge as open charm mesons such as $D(c\bar{u}, c\bar{d})$, $\bar{D}(\bar{c}u, \bar{c}d)$, $D_s(c\bar{s})$ and $\bar{D}_s(\bar{c}s)$. So if a quark-gluon plasma is formed in the region of J/ψ production, then the effect of plasma will make it unbound leading to the suppression of its production compared to the case where no quark-gluon medium has been formed. Therefore, the suppression of J/ψ production may be used as a signature of quark-gluon plasma.

There are many other signatures like strangeness enhancement or HBT (Hanbury-Brown-Twiss) effect of intensity interferometry which establish the existence of quark-gluon matter. In the next section we will explore different techniques to study such an exotic system.

1.4.4 Theoretical methods to describe the system created in heavy ion collisions

The question now arises how this hot and dense matter created in heavy ion collisions can be treated mathematically so as to investigate its properties. We have two Lorentz-covariant dynamical frameworks at our disposal: (i) covariant transport theory and (ii) relativistic hydrodynamics. They represent opposite limits in their underlying assumptions. The transport theory provides a microscopic description of the system and is suited for the early and late non-equilibrium stages. Transport theories based on parton degrees of freedom can also describe the early thermalization processes. The late hadronic rescattering and freeze-out stage requires a description in terms of a covariant hadron cascade and can be matched to the earlier hydrodynamic evolution of QGP phase [18]. Some of the typical transport based calculations are, A Multi Phase Transport (AMPT) model [19] and Ultra Relativistic Quantum Molecular Dynamic (URQMD) model [20]. All these theoretical descriptions are well developed and can be further advanced.

On the other hand relativistic hydrodynamics is a macroscopic description and assumes approximate local thermal equilibrium. A system in thermodynamic equilibrium can be characterized

by macroscopic observables such as particle number density, hydrodynamic velocity, energy density etc. with no requirement of detailed knowledge of microscopic dynamics. Due to the simplicity of this macroscopic approach it has a long tradition in its application in heavy ion collisions. Starting from Landau [21] and Bjorken [22] a number of hydrodynamic approaches have been used to study the properties of the matter created in heavy ion collisions which proved to be quite successful in predicting the experimental data. Because of their conceptual beauty and simplicity, models based on hydrodynamic principles have been applied to calculate a large number of observables for various colliding systems and over a broad range of colliding energies. One of the most important results from Au+Au collisions at RHIC is the centrality and transverse momentum (p_T) dependence of the elliptic flow coefficient at mid rapidity [24]. For central to midperipheral collisions and for $p_T \lesssim 1.5 GeV/c$ the data were found to be in very good agreement with the hydrodynamic predictions [23].

1.4.5 Evidence of dissipation in the matter created in heavy ion collisions

Earlier most of the predictions about the properties of the hot and dense matter created in heavy ion collisions were made with ideal hydrodynamics without considering any dissipative effects in it. Realizing that the created matter undergoes irreversible phenomena in its course of evolution a few attempts were made to quantify the dissipation. In [25] the dissipative phenomena for a quark gluon system have been discussed. The transport properties and the corresponding relaxations have been discussed in [26, 27] for a QGP system. The transport coefficients in ultra-relativistic heavy ion collisions have been estimated both for QGP and hadron matter in [28]. These theoretical estimations of transport coefficients needed to be supported by the experimental data from heavy ion collisions and first the RHIC data indeed demonstrated the evidence of transport quantities in the matter created out of the collisions. Though earlier attempts were made with ideal hydrodynamics considering the system as a weakly interacting one which seems to offer first handedly a sensible description of the data, however a closer inspection to some of the bulk observables such as multiplicity, radial or elliptic flow reveals

that the ideal hydrodynamics do not suffice the explanation and demands the inclusion of a dissipative hydrodynamics to describe the space-time evolution of the system. In Ref. [29] the elliptic flow (v_2) data of charged hadrons in 200 GeV per nucleon Au+Au collision at RHIC was explained with a viscous hydrodynamic model with small but finite value of shear viscosity to entropy density ratio (η/s), indicating that the created matter behaves much like a strongly interacting liquid than a weakly interacting gas. In Fig. 1.2 it can be viewed that the ideal hydrodynamics clearly overpredicts the data both from Phobos and Star where the viscous hydrodynamics describes the experimental data reasonably. Then on it is realized that the created matter undergoes dissipative processes on its way to space time evolution and hence requires a non-ideal theory to describe its kinematics. A series of works has been carried out since then [30, 31] to obtain the cooling laws for a dissipative evolving system created in heavy ion collisions. So far the dissipative effects on the electromagnetic as well as hadron spectra have been tested widely [32, 33, 34, 35, 36]. All these estimations require the transport coefficients as the measure of the dissipation to incorporate in the non-ideal hydrodynamic models. That is why the transport coefficients are needed to be evaluated with great precision. The motivation of this thesis is to estimate the magnitude of the transport coefficients and their corresponding temperature dependence for a system of hot interacting pion gas at finite temperature.

1.5 The scope and prospect of the present work

In this work the temperature dependence of both the first order transport coefficients, such as viscosities and thermal conductivity as well as the second order ones which are the relaxation times of flows have been evaluated for an interacting pion gas at finite temperature. There have been quite a few estimates of the transport coefficients of a pion gas. In Ref. [37, 38, 39] the transport coefficients of a pion gas have been evaluated using the Kubo formalism which relates the transport coefficients to retarded two-point functions. In Ref. [40, 41, 42, 43] the kinetic theory approach has been adopted where the transport coefficients are expressed explicitly in terms of interaction cross-section. In most of the cases of kinetic theory approach either the lowest order chiral perturbation theory has been used [40, 44], or a phenomenological ampli-

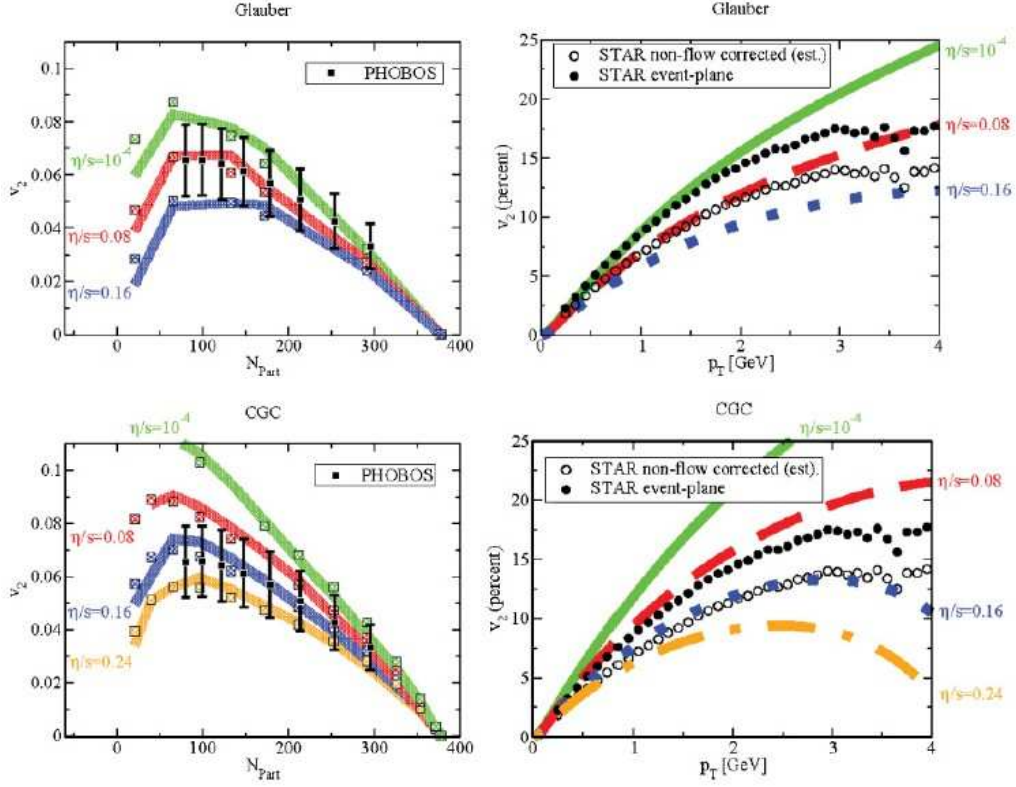


Figure 1.2: Ideal and viscous hydrodynamic models trying to fit the experimental data of elliptic flow of charged hadrons [29].

tude has been used which is constructed to reproduce the experimental data of $\pi\pi$ interaction cross-section [45]. In [41, 42] a unitarized cross section has been used from the inverse amplitude method of chiral perturbation theory. In all the above cases the temperature dependence does not occur explicitly in the dynamical cross-sections incorporated in the expressions of transport coefficients. In this thesis an explicit temperature dependent pion cross-section has been introduced and thereafter the transport coefficients are estimated with the help of the temperature dependent interaction cross-section.

The chapters of the thesis are arranged as follows. In Chapter-2 the fluid properties have been discussed for a non-ideal system. The expression of the thermodynamic quantities have been explicitly given in this chapter. In Chapter-3 the Chapman-Enskog method from kinetic the-

ory has been discussed in detail from which the expressions of first order transport coefficients such as shear and bulk viscosities and thermal conductivity have been explicitly estimated. In Chapter-4 another formalism of kinetic theory, namely Grad's 14 moment method has been employed to obtain the relaxation time of dissipative flows. After obtaining the expressions of transport coefficients, in Chapter-5 a medium modified $\pi\pi$ interaction cross section has been evaluated at finite temperature. Finally in Chapter-6 the effect of this medium dependent pion cross section on the temperature dependence of transport coefficients has been discussed. In Chapter-7 other transport coefficients namely the drag and diffusion coefficients have been evaluated for heavy mesons with charmed degrees of freedom like J/ψ and η_c . In Chapter-8 the effect of viscosity on the electromagnetic spectra from QGP as well as hadronic matter is investigated. We end this thesis with Chapter-9 which contains discussions and possible outlook of the work presented here.

Bibliography

- [1] U. Heinz, CERN Yellow Report CERN-2004-001, arXiv: 0407360 [hep-ph].
- [2] Proceeding of Quark Matter'93, Sweden, edited by E. Stenlund et al. [Nucl. Phys. bf A566, 1c (1994)].
- [3] I. Arsene *et al.* (BRAHMS Collaboration), Nucl. Phys. A **757**, 1 (2005).
- [4] B. B. Back *et al.* (PHOBOS Collaboration), Nucl. Phys. A **757**, 28 (2005).
- [5] J. Adams *et al.* (STAR Collaboration), Nucl. Phys. A **757**, 102 (2005).
- [6] K. Adcox *et al.* (PHENIX Collaboration), Nucl. Phys. A **757**, 184,(2005).
- [7] B. Muller, J. Schukraft and B. Wyslouch, Annu. Rev. Nucl. Part. Sci. 62 (2012) 361, arXiv:1202.3233 [hep-ex].
- [8] P. Senger, J. Phys. G 30, S1087 (2004).
- [9] V. Greco, M. Mitrovski and G. Torrieri, Phys. Rev. C **86** (2012) 044905 [arXiv:1201.4800 [nucl-th]].
- [10] K. Aamodt *et al.* [ALICE Collaboration], Phys. Rev. Lett. **105** (2010) 252302 [arXiv:1011.3914 [nucl-ex]].
- [11] Ulrich Heinz, Early Collective Expansion: Relativistic Hydrodynamics and the Transport Properties of QCD Matter, Elementary Particles, Nuclei and Atoms Volume 23, 2010, pp 240-292.

- [12] K. Kajantie, J. I. Kapusta, L. D. McLerran and A. Mekjian, Phys. Rev. D **34** (1986) 2746.
- [13] G. Domokos and J. I. Goldman, Phys. Rev. D **23** (1981) 203.
- [14] J. I. Kapusta, P. Lichard and D. Seibert, Nucl. Phys. A **544** (1992) 485C.
- [15] J. Alam, B. Sinha and S. Raha, Phys. Rept. **273**, 243 (1996).
- [16] S. Sarkar, J. e. Alam, P. Roy, A. K. Dutt-Mazumder, B. Dutta-Roy and B. Sinha, Nucl. Phys. A **634**, 206 (1998) [nucl-th/9712007].
- [17] T. Matsui and H. Satz, Phys. Lett. B178, 416 (1986).
- [18] H. Song, S. A. Bass and U. Heinz, Phys. Rev. C 83, 024912 (2011) [arXiv:1012.0555 [nucl-th]].
- [19] Z. W. Lin, C. M. Ko, B. A. Li, B. Zhang and S. Pal, Phys. Rev. C 72, 064901 (2005) [arXiv:nucl-th/0411110].
- [20] M. Bleicher et al., J. Phys. G 25, 1859 (1999) [arXiv:hep-ph/9909407].
- [21] L.D. Landau, Izv. akd. Nauk SSSR 17,51 (1953).
- [22] J. D. Bjorken, Phys. Rev. D 27, 140 (1983).
- [23] P. F. Kolb, J. Sollfrank and U. W. Heinz, Phys. Rev. C **62** (2000) 054909 [hep-ph/0006129].
- [24] K. H. Ackermann *et al.* [STAR Collaboration], Phys. Rev. Lett. **86** (2001) 402 [nucl-ex/0009011].
- [25] P. Danielewicz and M. Gyulassy, Phys. Rev. D **31** (1985) 53.
- [26] H. Heiselberg and C. J. Pethick, Phys. Rev. D **48** (1993) 2916.
- [27] H. Heiselberg, Phys. Rev. D **49** (1994) 4739 [hep-ph/9401309].
- [28] S. Gavin, Nucl. Phys. A **435**, 826 (1985).
- [29] M. Luzum and P. Romatschke, Phys. Rev. C **78**, 034915 (2008).

- [30] A. Muronga, Phys. Rev. **Lett** **88**, 6 (2002).
- [31] P. Romatchke, IJMPE**19**,1-53, (2010).
- [32] S. Sarkar, P. Roy, J. Alam, S. raha, B. Sinha, J. Phys. G:Nucl. part. Phys. **23** (1997) 469.
- [33] Derek Teaney, Phys. Rev. C **68**, 034913 (2003).
- [34] K. Dusling and S. Lin, Nucl. Phys. A **809** (2008) 246-258.
- [35] K. Dusling, Nucl. Phys. A **839** (2010) 70-77.
- [36] Jitesh R. Bhatt, H. Mishra and V. Shreekanth, Journal of High Energy Physics **11** (2010) 106.
- [37] A. Hosoya, M. A. Sakagami and M. Takao, Annals Phys. **154** (1984) 229.
- [38] R. Lang, N. Kaiser and W. Weise, Eur. Phys. J. A **48** (2012) 109.
- [39] S. Sarkar, Adv. High Energy Phys. **2013** (2013) 627137 [arXiv:1308.1771 [nucl-th]].
- [40] E. Lu and Guy D. Moore Phys. Rev. C **83**, 044901 (2011).
- [41] A. Dobado and S. N. Santalla, Phys. Rev. D **65**, 096011 (2002).
- [42] A. Dobado and F. J. Llanes-Estrada, Phys. Rev. D **69**, 116004 (2004).
- [43] D. Davesne, Phys. Rev. C **53** (1996) 3069.
- [44] E. Nakano, arXiv:hep-ph/0612255.
- [45] K. Itakura, O. Morimatsu and H. Otomo and J. M. Torres Rinkon, arXiv:hep-ph/0702130 (2007).

Chapter 2

Elements of fluid dynamics

The properties of a fluid which can be considered as a many particle system evidently depend on the interactions of the constituent particles and any external forces exerted on the system. Since the phenomena considered in fluid dynamics are macroscopic, the fluid is regarded as a continuous medium. This requires that any small volume element in the fluid is supposed to be so large that it can contain a very great number of molecules. So a characteristic small fluid element corresponds to the dimension which is very small compared to the system size under consideration, but large compared to the intermolecular distances. In general different processes in a fluid are described by the means of a tool called kinetic theory of fluids. In this theory the fluid dynamical properties are realized by means of a statistical description in terms of a quantity called distribution function of the constituent particles in their phase space. It is in general, a function of generalized co-ordinates q and the corresponding generalized momenta p and for a non-steady state also of time t and indicated by the notation $f(t, q, p)$. This function may be interpreted as the average number of particles with a certain momentum at each space-time point. Consequently the distribution function bears the concept of temperature and as well as of a thermal equilibrium. This requires defining the local thermal equilibrium associated with the volume element of the fluid system mentioned above. If the dimension of the volume element dV is not large compare to the average intermolecular distance \bar{r} , the particle number density which is the momentum integration of the distribution function within

that volume element, is not a macroscopic quantity. The fluctuations of the number of particles present in the volume dV are comparable with its mean value. The number density N becomes a macroscopic quantity only when it is defined with respect to a volume element dV which contains many particles. This is only possible if the dimension of the volume element d satisfies $\bar{r} \ll d \ll L$, where L is the distance over which the distribution function changes considerably. So if such a fluid element is defined obeying the above conditions, within that volume element a local thermal equilibrium can be defined which results in specifying the macroscopic quantities such as temperature, number density, pressure etc [1, 2].

To describe a system of particles at its local equilibrium we need to specify these macroscopic quantities. On the macroscopic level the state of a many particle system is described by the particle density, the energy density and its hydrodynamic velocity. As argued above for a non-uniform system such quantities are functions of time and space co-ordinates. In the next section we will discuss the definition of these macroscopic thermodynamic quantities in the language of relativistic kinetic theory.

2.1 Thermodynamic quantities

2.1.1 Particle number density

Let us start with the local particle number density discussed in earlier section. For a non-uniform system this particle number density $n(\vec{x}, t)$ is function of the space co-ordinates \vec{x} and the time co-ordinate t . This quantity actually denotes the average number of particles per unit volume such that $n(\vec{x}, t)dV$ gives the average number of particles in the spatial volume element dV . So the total number of particles in some volume V of space becomes $\int_V n dV$. Since the number of particles flowing in unit time through an element $d\vec{f}$ of the surface bounding this volume is $n\vec{v} \cdot d\vec{f}$, so the total number of particles flowing out of this volume through the closed surface is, $\oint n\vec{v} \cdot d\vec{f}$ where \vec{v} is the velocity of fluid particles. Since this amounts to the decrease in number of particles within that volume per unit time which is $-\frac{\partial}{\partial t} \int n dV$, for an arbitrary

volume this facts lead to the famous continuity equation of fluid, $\frac{\partial n}{\partial t} + \vec{\nabla} \cdot \vec{j} = 0$. Here we have defined a new quantity called particle flow $\vec{j}(x, t) = n\vec{v}$. So for a relativistic system of particles, the particle density and particle flow, constitute a 4-vector field, which is indicated by [3],

$$N^\mu(x) = (n(\vec{x}, t), \vec{j}(\vec{x}, t)), \quad (2.1)$$

called particle 4-flow.

The index μ runs from 0,1,2,3 while $x = x^\mu = (t, \vec{x})$. Now we have mentioned earlier that the particle number density $n(x)$ can be expressed in terms of the particle distribution function integrated over all momenta at a particular point of space,

$$n(x) = \int \frac{d^3p}{(2\pi)^3} f(x, p). \quad (2.2)$$

In the same spirit we can define particle current as,

$$\vec{j}(x) = \int \frac{d^3p}{(2\pi)^3} \vec{v}_p f(x, p). \quad (2.3)$$

Where we have used the abbreviation $\vec{v}_p = \frac{\vec{p}}{p^0}$ as the velocity of the relativistic particles with momentum \vec{p} . As a consequence of the above two equations the particle-4 flow can be expressed as,

$$N^\mu(x) = \int \frac{d^3p}{(2\pi)^3 p^0} p^\mu f(x, p). \quad (2.4)$$

The last equation gives one very useful insight regarding the distribution function. Since the quantity $\frac{d^3p}{p^0}$ is a Lorentz scalar and both $N^\mu(x)$ and p^μ transforms like a four-vector so the distribution function $f(x, p)$ must be a scalar quantity. This fact holds acceptable with the interpretation of $f(x, p)$ as a probability density of the particles within the system.

2.1.2 Energy-momentum tensor

Let us consider a system of particles labeled by n with position co-ordinates $\vec{x}_n(t)$ and energy-momentum four-vector $p_n^\alpha(t)$, the density of p_n^α is defined as [4],

$$T^{\alpha 0}(\vec{x}, t) = \sum_n p_n^\alpha(t) \delta^3(\vec{x} - \vec{x}_n(t)). \quad (2.5)$$

The corresponding current is defined as,

$$T^{\alpha i}(\vec{x}, t) = \sum_n p_n^\alpha(t) \frac{dx_n^i(t)}{dt} \delta^3(\vec{x} - \vec{x}_n(t)). \quad (2.6)$$

These two definitions can be united in a single formula,

$$T^{\alpha\beta}(x) = \sum_n p_n^\alpha(t) \frac{dx_n^\beta(t)}{dt} \delta^3(\vec{x} - \vec{x}_n(t)). \quad (2.7)$$

From equation (2.7) for a continuous system, the average density and the flows of energy and momentum can be written in an integral form over the particle distribution function which is given by the following equations.

The 00-component is

$$T^{00}(x) = \int \frac{d^3p}{(2\pi)^3} p^0 f(x, p). \quad (2.8)$$

Since energy per particle is p^0 , this quantity is indicated as the macroscopic energy density ϵ . The energy flow or energy flux along the i th axis is given by

$$T^{0i}(x) = \int \frac{d^3p}{(2\pi)^3} p^0 v_p^i f(x, p). \quad (2.9)$$

Here v_p^i is the cartesian component of the particle velocity along i th axis.

Next we define the density of i th component of momentum by,

$$T^{i0}(x) = \int \frac{d^3p}{(2\pi)^3} p^i f(x, p). \quad (2.10)$$

This is evidently the average value of particle momentum \vec{p} . Finally

$$T^{ij}(x) = \int \frac{d^3p}{(2\pi)^3} p^i v_p^j f(x, p) \quad (2.11)$$

is the expression of momentum flow or flux along the direction of j th axis of the i th component of momentum. So in the covariant form the energy-momentum stress tensor can be written as,

$$T^{\mu\nu} = \int \frac{d^3p}{(2\pi)^3 p^0} p^\mu p^\nu f_0(x, p). \quad (2.12)$$

In the local rest frame of the fluid, the energy momentum tensor takes the following form characteristic of the spherical symmetry,

$$\tilde{T}^{ij} = P\delta^{ij}, \quad \tilde{T}^{i0} = \tilde{T}^{0i} = 0, \quad \tilde{T}^{00} = \epsilon. \quad (2.13)$$

Now in any general frame the energy momentum tensor can be expressed in terms of hydrodynamic four-velocity and the metric tensor of the system in the following manner,

$$T^{\mu\nu} = Au^\mu u^\nu + Bg^{\mu\nu}. \quad (2.14)$$

A and B are appropriate coefficients that should express (2.14) in terms of (2.13) in the local rest frame of the fluid. Following the above prescription, in the lab frame the energy momentum tensor takes the following form with ϵ as energy density and P as pressure,

$$T^{\mu\nu} = (\epsilon + P)u^\mu u^\nu - Pg^{\mu\nu}. \quad (2.15)$$

Here we have used the metric $g^{\mu\nu} = (1, -1, -1, -1)$ and the same convention will be followed through out the thesis.

2.1.3 Hydrodynamic four-velocity

To describe the motion of a fluid, which is considered as a continuous media, the most important notion is the hydrodynamic four-velocity $u^\mu(x)$, which is a vector field. It is defined as a time-like vector with unit length at each space-time point

$$u^\mu(x)u_\mu(x) = 1. \quad (2.16)$$

Let us now define a projection operator $\Delta^{\mu\nu}(x)$ with the help of this hydrodynamic four-velocity $u^\mu(x)$ and the metric tensor $g^{\mu\nu}$ such as it is orthogonal to u^μ ,

$$\Delta^{\mu\nu}(x)u_\nu(x) = 0. \quad (2.17)$$

The most convenient form of constructing such a projection operator which is symmetric and orthogonal to velocity is given below,

$$\Delta^{\mu\nu}(x) = g^{\mu\nu} - u^\mu(x)u^\nu(x). \quad (2.18)$$

Since the hydrodynamic velocity is time-like, one can consider a proper Lorentz frame at each space-time point. This frame is identified as local rest frame and it is distinguished from observer's frame ($x = (t, \vec{x})$) by considering that this frame is moving with the fluid at each space time point. In the local rest frame, abbreviated by the index LR , the hydrodynamic velocity has the following components

$$u_{LR}^\mu = (1, 0, 0, 0). \quad (2.19)$$

In this local rest frame the projection operator mentioned above takes the form, $\Delta_{LR}^{\mu\nu} = \text{diag}(0, -1, -1, -1)$.

To specify hydrodynamic velocity we will discuss here two definitions which is popularly used in literatures.

(i) **Eckart's definition**-In this definition the hydrodynamic velocity is defined in terms of the particle four-flow N^μ as [5],

$$u^\mu = \frac{N^\mu}{\sqrt{N^\nu N_\nu}}. \quad (2.20)$$

It is normalized in agreement with (2.16). In this definition we can see that the hydrodynamic velocity is parallel to the particle flow. In the view of this normalization the alternative definition of u^μ reads,

$$u^\mu = \frac{N^\mu}{N^\nu u_\nu}. \quad (2.21)$$

These definitions invariably follow the orthogonal property of particle number density with the projection operator in Eckart approach,

$$\Delta_{\mu\nu}(x)N^\mu(x) = 0. \quad (2.22)$$

This orthogonality relation directly follows that in local rest frame the spatial components of particle four flow $N^\mu(x)$ vanishes.

$$N_{LR}^i = 0 \quad i = 1, 2, 3. \quad (2.23)$$

Thus the hydrodynamic velocity defined in (2.20) is the mean particle velocity.

(ii) **Landau and Lifshitz's definition** - According to this definition the hydrodynamic four velocity is defined as [2] ,

$$u^\mu = \frac{T^{\mu\nu}u_\nu}{\sqrt{u_\rho T^{\rho\sigma} T_{\sigma\tau} u^\tau}} . \quad (2.24)$$

This definition of the hydrodynamic velocity is defined in terms of energy-momentum tensor. The normalization condition of velocity (2.16) gives another alternative definition,

$$u^\mu = \frac{T^{\mu\nu}u_\nu}{u_\rho T^{\rho\sigma} u_\sigma}, \quad (2.25)$$

which again with the help of projector operator follows the following condition,

$$\Delta^{\mu\nu} T_{\nu\sigma} u^\sigma = 0. \quad (2.26)$$

This follows that in the local rest frame associated with Landau-Lifshitz velocity the momentum density and the energy flow vanishes.

$$T_{LR}^{i0} = T_{LR}^{0i} = 0, \quad i = 1, 2, 3. \quad (2.27)$$

Thus the hydrodynamic velocity defined in (2.24) is related to the momentum density or what amounts to the same, the flow of energy for the system of particles.

2.1.4 Other thermodynamic quantities

Based on the quantities discussed above we have define a few fundamental quantities needed to describe the macroscopic properties of the system.

From the definition of particle four flow (2.4), one can define the particle number density, which is a function of time-space coordinates x , as a scalar quantity

$$n = N^\mu u_\mu. \quad (2.28)$$

In the local rest frame of the fluid, characterized by (2.19) the definition of the above quantity takes the following form

$$n = N_{LR}^0. \quad (2.29)$$

This equation clearly shows that the particle number density $n(x)$ is indeed the density of particles with respect to this frame.

Similarly we can define the energy density of the system as en where e is the average energy per particle,

$$en = u_\mu T^{\mu\nu} u_\nu. \quad (2.30)$$

In the local rest frame this reduces to $en = T_{LR}^{00}$, which shows in local rest frame en is indeed the energy density.

Let us now define the heat flow function by the following equation.

$$I_q^\mu = (u_\nu T^{\nu\sigma} - hN^\sigma)\Delta_\sigma^\mu \quad (2.31)$$

The enthalpy or heat function per particle is $h = e + Pn^{-1}$, where P is the hydrostatic pressure. We can see that the heat flow so defined is also orthogonal to $u^\mu(x)$. The definition (2.31) is such that in local rest frame the heat flow has spatial components only,

$$I_{q(LR)}^0 = 0, \quad I_{q(LR)}^i = T_{(LR)}^{0i} - hN_{(LR)}^i, \quad i = 1, 2, 3. \quad (2.32)$$

We will now define another quantity called pressure tensor as,

$$P^{\mu\nu} = \Delta_\sigma^\mu T^{\sigma\tau} \Delta_\tau^\nu. \quad (2.33)$$

It is a symmetric quantity if the energy-momentum tensor $T^{\mu\nu}$ is symmetric as discussed here. In the local rest frame it is purely spatial,

$$P_{LR}^{00} = 0, \quad P_{LR}^{0i} = P_{LR}^{i0} = 0, \quad P_{LR}^{ij} = T_{LR}^{ij}, \quad i, j = 1, 2, 3. \quad (2.34)$$

It turns out that the pressure tensor contains a reversible and an irreversible part according to the splitting

$$P^{\mu\nu} = -P\Delta^{\mu\nu} + \Pi^{\mu\nu}. \quad (2.35)$$

The quantity $\Pi^{\mu\nu}$ is called the viscous pressure tensor. With the help of the above relations the energy-momentum stress tensor $T^{\mu\nu}$ also can be similarly decomposed into reversible and irreversible contributions.

$$T^{\mu\nu} = T^{(0)\mu\nu} + T^{(1)\mu\nu}, \quad (2.36)$$

where the reversible part directly follows from (2.15),

$$T^{(0)\mu\nu} = enu^\mu u^\nu - P\Delta^{\mu\nu}, \quad (2.37)$$

and the irreversible part,

$$T^{(1)\mu\nu} = [(I_q^\mu + h\Delta^{\mu\sigma} N_\sigma)u^\nu + (I_q^\nu + h\Delta^{\nu\sigma} N_\sigma)u^\mu] + \Pi^{\mu\nu}. \quad (2.38)$$

It can be shown now that these general definitions of heat flow and energy-momentum tensor can be influenced by the choice of hydrodynamic velocity. If we first consider the Eckart's approach of (2.20) the heat flow and the dissipative part of energy-momentum tensor takes the respective values,

$$I_q^\mu = u_\nu T^{\nu\sigma} \Delta_\sigma^\mu, \quad (2.39)$$

and

$$T^{(1)\mu\nu} = [(I_q^\mu)u^\nu + (I_q^\nu)u^\mu] + \Pi^{\mu\nu}. \quad (2.40)$$

On the other hand the Landau-Lifshitz condition (2.24) leads to two different sets of equations for them such as,

$$I_q^\mu = -hN^\sigma \Delta_\sigma^\mu \quad (2.41)$$

and

$$T^{(1)\mu\nu} = \Pi^{\mu\nu}. \quad (2.42)$$

2.2 Equilibrium thermodynamic quantities expressed as a sum over infinite series

The thermodynamic quantities defined in the previous section play important roles in describing the collective dynamics of the fluid. Different observables regarding the characteristics of the fluid are expressed in terms of these thermodynamic quantities. In relativistic kinetic theory the macroscopic quantities are all defined with the help of scalar distribution function mentioned above. In previous section we have seen that most of them can be expressed in integral form over the equilibrium distribution function of the constituent particles. For the purpose mentioned

above it is convenient to express these quantities in a simple algebraic form. Here we have expressed them in a series sum over the modified Bessel function of second kind. But before that we need to define the required form of the equilibrium distribution function.

2.2.1 Definition of equilibrium distribution function

Let us consider the collision between two particles, each having the initial distribution function $f(x, p)$ and $f_1(x, p_1)$, which after the collision results into the final distribution function, $f'(x, p')$ and $f'_1(x, p'_1)$ respectively. At equilibrium, from the principle of detailed balance one should have the following condition to satisfy,

$$f_0(x, p)f_{01}(x, p_1) = f'_0(x, p')f'_{01}(x, p'_1). \quad (2.43)$$

The subscript 0 here indicates the value of distribution function at equilibrium. The H -theorem for entropy production expresses the fact that as a result of the irreversible process taking place inside the system the entropy increases. The entropy production vanishes if and only if the distribution functions obey the above functional relation for equilibrium distribution function since it is the necessary condition for equilibrium. Now alongside with this above condition, we need an equation satisfied by the particle distribution function which describes its space-time behavior within the system. The solution will provide the shape of the equilibrium distribution function.

The basic equation that describes the changes of distribution function along its phase path is the Boltzmann transport equation. For a relativistic system the equation is given as,

$$p^\mu \partial_\mu f = C[f] . \quad (2.44)$$

The quantity $C[f]$ is referred as the collision term. This term actually involves the inter particle collisions which is responsible for the change of distribution function. More about this will be discussed in the later chapters. For the time being we will require the transport equation to find a solution which in turn will give a suitable form of the equilibrium distribution function. Now for a equilibrium system the collision term on the right hand side of equation (2.44) becomes

zero. Again we have argued earlier that the necessary condition for equilibrium is steady state of entropy production. This condition, together with the requirement that the equilibrium distribution function must be a solution of the transport equation, uniquely determines its form. The equilibrium distribution function contains the density, the temperature and the hydrodynamic four-velocity of the system as parameters.

Now taking logarithm of equation (2.43) we find f_0 to satisfy the following equation.

$$\log f_0(x, p) + \log f_{01}(x, p_1) = \log f'_0(x, p') + \log f'_{01}(x, p'_1) \quad (2.45)$$

From the above equation we conclude that $\log f_0$ is a summational invariant. The most general summational invariant is a linear combination of a constant and the four-momentum p^μ , where the coefficients are functions of the four space-time co-ordinates. So we have the desired form for $\log f_0$ is,

$$\log f_0(x, p) = a(x) + b_\mu(x)p^\mu . \quad (2.46)$$

Here $a(x)$ and $b_\mu(x)$ are space-time dependent arbitrary parameters. The transport equation implies that the parameters $a(x)$ and $b_\mu(x)$ must obey the following equation,

$$p^\mu \partial_\mu a(x) + p^\mu p^\nu \partial_\mu b_\nu(x) = 0. \quad (2.47)$$

From which we conclude,

$$\begin{aligned} \partial_\mu a(x) &= 0 \\ \partial_\mu b_\nu(x) + \partial_\nu b_\mu(x) &= 0. \end{aligned} \quad (2.48)$$

From the above two equations it is anticipated that, $a^\mu = \mu(x)/T$ and $b^\mu = -u^\mu(x)/T$.

Following such arguments the Boltzmann distribution function for an equilibrium system reads,

$$\{f_0(p)\}_{MB} = \exp\left(\frac{\mu - p^\mu u_\mu}{T}\right). \quad (2.49)$$

Here we have used the Bose-Einstein distribution function for a Bosonic system such as,

$$f_0(p) = \frac{1}{\exp\left\{\frac{p^\mu u_\mu(x) - \mu(x)}{T(x)}\right\} - 1} . \quad (2.50)$$

2.2.2 Particle density

Having specified the distribution function, the expression of particle number density as given from equation (2.28), can be explicitly written as,

$$n = \int \frac{d^3p}{(2\pi)^3 p^0} (p^\mu u_\mu) \frac{1}{\exp\left\{\frac{p^\mu u_\mu}{T} - \frac{\mu}{T}\right\} - 1}. \quad (2.51)$$

This integral is clearly a scalar quantity. Now we intend to evaluate this quantity in the local rest frame where the fluid velocity components are $u^\mu = (1, 0, 0, 0)$. For this purpose we have introduced two dimensionless quantities namely τ and z defined as follows,

$$z = \frac{m}{T}, \quad \tau = \frac{p^\mu u_\mu}{T} = \frac{1}{T} \{|\vec{p}|^2 + m^2\}^{1/2}. \quad (2.52)$$

This clearly shows that the integration element can be replaced by these dimensionless quantities and the polar angles in the following way,

$$\frac{d^3p}{p^0} = T^2 (\tau^2 - z^2)^{1/2} d\tau d\Omega. \quad (2.53)$$

Where $d\Omega = d(\cos\theta)d\phi$ is the differential solid angle. The integral can now be expressed in terms of modified Bessel function of second kind which has the following definition.

$$K_n(z) = \frac{2^n n!}{(2n)!} \frac{1}{z^n} \int_z^\infty d\tau (\tau^2 - z^2)^{n-\frac{1}{2}} e^{-\tau} \quad (2.54)$$

Now using the expansion identity $\frac{1}{z^{-1}e^x - 1} = \sum_{k=1}^\infty (ze^{-x})^k$ and integrating by parts we obtain,

$$n = \frac{1}{2\pi^2} T m^2 \sum_{k=1}^\infty \frac{1}{k} \exp\left\{\frac{\mu k}{T}\right\} k_2(kz). \quad (2.55)$$

Now we define another function S_n^α which is actually a series over the modified Bessel function of second kind and particle fugacity associated with the chemical potential,

$$S_n^\alpha = \sum_{k=1}^\infty \exp\left\{\frac{k\mu}{T}\right\} \frac{1}{k^\alpha} k_n(kz). \quad (2.56)$$

Utilizing this function the particle number density and the mass density of the fluid come out to be respectively,

$$n = \frac{1}{2\pi^2} m^2 T S_2^1, \quad (2.57)$$

$$\rho = \frac{1}{2\pi^2} m^3 T S_2^1. \quad (2.58)$$

2.2.3 Energy density

The definition of energy density we have introduced earlier in (2.30) is given by,

$$\begin{aligned} en &= u_\mu T^{\mu\nu} u_\nu \\ &= \int \frac{d^3p}{(2\pi)^3 p^0} (p^\mu u_\mu)^2 f_0(x, p), \end{aligned} \quad (2.59)$$

which with the help of the dimensionless quantities τ and z and the polar co-ordinates turns out to be,

$$ne = \frac{1}{2\pi^2} T^4 \int_z^\infty \tau^2 (\tau^2 - z^2)^{\frac{1}{2}} \frac{1}{e^{-\frac{\mu}{T}} e^\tau - 1} d\tau. \quad (2.60)$$

Integrating by parts and using the definitions of Bessel function and S_n^α it comes out as,

$$ne = \frac{1}{2\pi^2} m^4 \left\{ \frac{S_3^1}{z} - \frac{S_2^2}{z^2} \right\}. \quad (2.61)$$

So from the above relation the energy per particle is defined as,

$$e = m \frac{S_3^1}{S_2^1} - T \frac{S_2^2}{S_2^1}. \quad (2.62)$$

2.2.4 Pressure

The equilibrium pressure is defined as,

$$\begin{aligned}
P &= -\frac{1}{3}T^{\mu\nu}\Delta_{\mu\nu} \\
&= -\frac{1}{3}\int\frac{d^3p}{(2\pi)^3p^0}p^\mu p^\nu(g_{\mu\nu}-u_\mu u_\nu)f_0(x,p) \\
&= -\frac{1}{3}\int\frac{d^3p}{(2\pi)^3p^0}\{p^2-(p^\mu u_\mu)^2\}f_0(x,p) \quad .
\end{aligned} \tag{2.63}$$

Following the same prescription as before we obtain the thermodynamic pressure as follows,

$$P = nT\frac{S_2^2}{S_2^1}. \tag{2.64}$$

2.2.5 Enthalpy density

The enthalpy per particle is defined as,

$$h = e + \frac{P}{n}. \tag{2.65}$$

Evidently it can be expressed in terms of the function S_n^α following the same procedure as before,

$$h = m\frac{S_3^1}{S_2^1}. \tag{2.66}$$

The enthalpy density per unit volume is then simply given by,

$$H = nh = \rho\frac{S_3^1}{S_2^1}, \tag{2.67}$$

where $\rho = nm$ is the mass density of the system.

2.3 Conservation laws

In the previous section we have mentioned that a fluid system can be described by the equation of motion satisfied by the distribution function along the phase path of the particle ensem-

ble. The equation of motion satisfied by the distribution functions is the relativistic transport equation, derived by Ludwig Boltzmann in 1872.

$$p_k^\mu \partial_\mu f_k(x, p_k) = \sum_{l=1}^N C_{kl}(x, p_k). \quad (2.68)$$

This integro-differential equation describes the motion of the k^{th} particle among an ensemble of N number of particles due to their mutual interactions. The quantity $C[f]$, the collision term as mentioned before, can be interpreted as the rate of change of distribution function by virtue of collisions.

Now from the consequence of the microscopic conservation laws obeyed by various reactions, it can be proved that the collision term possesses the following property,

$$\sum_{k,l=1}^N \int \frac{d^3 p_k}{(2\pi)^3 p_k^0} \psi_k(x, p_k) C_{kl}(x, p_k) = 0, \quad (2.69)$$

when the quantity $\psi(x, p)$ is a linear combination of a constant and the four-vector p^μ .

$$\psi_k(x, p) = a_k(x) + b_\mu(x) p_k^\mu \quad (2.70)$$

The space-time function $a_k(x)$ and $b_\mu(x)$ are arbitrary, except for the fact that the function $a_k(x)$ is constrained by the following addition conservation, $a_k(x) + a_l(x) = a_i(x) + a_j(x)$ for a binary collision $k + l \rightarrow i + j$. This constraint along with the four-momentum conservation $p_k^\mu + p_l^\mu(x) = p_i^\mu(x) + p_j^\mu(x)$, the lemma (2.69) can be proved easily. Now it can be predicted intuitively that for purely elastic collisions the constraint reduces to an identity leading to the following equation,

$$\int \frac{d^3 p_k}{(2\pi)^3 p_k^0} C_{kl}(x, p_l) = 0. \quad (2.71)$$

This follows from the fact that since elastic collisions do not alter the number of particles or their total energy, the collisional part of change in the distribution function can not affect the

macroscopic quantities in each volume element of the fluid as well. The collisional parts of change in total number, energy and momentum of the particles in each such volume elements is given by zero integrals.

In the following section it will be shown that lemma (2.69) satisfied by collision term $C[f]$ eventually leads to the conservation of thermodynamic quantities describing the relativistic fluid system. In other words the conservation laws of macroscopic variables are considered as a consequence of the microscopic conservation laws obeyed in various reactions by the constituent particles.

2.3.1 Conservation of particle number

Let us start with the general expression of the summation invariant in lemma (2.69). If we set $b^\mu(x)$ equals to zero and the first function $a_k(x)$ is the same single function $a(x)$ for all the participant particles, then since $a(x)$ is an arbitrary function from definition, then lemma (2.69) simply reduces to,

$$\sum_{k,l=1}^N \int \frac{d^3 p_k}{(2\pi)^3 p_k^0} C_{kl}(x, p_k) = 0. \quad (2.72)$$

Now if the collision term $C[f]$ is replaced by the left hand side of transport equation (2.68) we obtain,

$$\sum_{k,l=1}^N \int \frac{d^3 p_k}{(2\pi)^3 p_k^0} p_k^\mu \partial_\mu f_k(x, p_k) = 0. \quad (2.73)$$

Now following the definition of particle four flow N^μ from equation (2.4), one simply reaches the following conservation law.

$$\partial_\mu N_k^\mu(x) = 0 \quad (2.74)$$

So equation (2.74) tells us that the number of particles of each component is conserved separately.

2.3.2 Conservation of energy-momentum

If in lemma (2.69) the constant $a_k(x)$ is set to zero, then since b_μ is arbitrary we obtain the collision term to satisfy the following equation,

$$\sum_{k,l=1}^N \int \frac{d^3 p_k}{(2\pi)^3 p_k^0} p_k^\mu C_{kl}(x, p_k) = 0. \quad (2.75)$$

Again replacing the collision term $C[f]$ with the help of transport equation we get,

$$\sum_{k,l=1}^N \int \frac{d^3 p_k}{(2\pi)^3 p_k^0} p_k^\mu p_k^\nu \partial_\nu f_k(x, p_k) = 0. \quad (2.76)$$

With the help of the definition of energy-momentum stress-tensor from equation (2.12) it results in the following conservation law of energy-momentum stress-tensor.

$$\partial_\nu T^{\mu\nu} = 0. \quad (2.77)$$

For $\mu = 0$ in equation (2.77), the law expresses conservation of energy and for $\mu = 1, 2, 3$ it reveals the conservation of momentum.

2.4 Equation of motion of thermodynamic quantities

The above conservation laws give rise to equations of motion of different thermodynamic quantities. For this purpose the space-time derivative ∂^μ is decomposed with the aid of hydrodynamic four-velocity into a time like and a space like part. The identity is written as,

$$\partial^\mu = u^\mu D + \nabla^\mu, \quad (2.78)$$

where we have introduced the following notations,

$$D = u^\mu \partial_\mu \quad \nabla^\mu = \Delta^{\mu\nu} \partial_\nu. \quad (2.79)$$

D is the convective time-derivative. In local rest frame it is just the partial time derivative $\partial/\partial t$. The ∇^μ is the purely spatial part. In local rest frame it is nothing but $-\partial/\partial x^i$. Moreover this quantity is orthogonal to u^μ , i.e. $u^\mu \nabla_\mu = 0$. The equation of motion of thermodynamic quantities can be expressed now in terms of these time and space like derivatives.

2.4.1 Equation of continuity

The total particle four-flow N^μ can be split into a part carried by the hydrodynamic velocity u^μ and a remaining part V^μ according to,

$$N^\mu = nu^\mu + V^\mu. \quad (2.80)$$

This function V^μ is a transport quantity defined as, $V^\mu = \Delta^{\mu\nu} N_\nu$ and orthogonal to hydrodynamic velocity, i.e, $V^\mu u_\mu = 0$. Now with the help of the particle conservation law (2.74) and using the identity $u^\mu Du_\mu = 0$, we get the equation of motion for the particle number density n as,

$$Dn = -n\nabla^\mu u_\mu - \nabla^\mu V_\mu + V_\mu Du^\mu. \quad (2.81)$$

Now this quantity V_μ is related to the transport or the flows of the fluid system which is actually given by the heat flow and energy momentum flux and found to be of first order of gradients of thermodynamic variables. We restrict ourselves only upto the zeroth order of gradients by ignoring such “flow quantities” in the equations of motion. In that way the continuity equation turns out to be,

$$Dn = -n\nabla_\mu u^\mu. \quad (2.82)$$

This is the equation of motion of the particle number density for a nearly perfect fluid.

2.4.2 Equation of motion

From the conservation law of energy and momentum we can get the equation of motion. Contracting equation (2.77) with the projection operator one gets,

$$\Delta_\nu^\mu \partial_\sigma T^{\nu\sigma} = 0. \quad (2.83)$$

Now using the definition of $T^{\mu\nu}$ from equation (2.15), we obtain the equation of motion for the hydrodynamic velocity u^μ as follows,

$$Du^\mu = \frac{1}{nh} \nabla^\mu P. \quad (2.84)$$

This equation clearly depicts the relation between the hydrodynamic acceleration and the pressure gradient in a linear law.

2.4.3 Equation of energy

Again contracting equation (2.77) with the hydrodynamic velocity we obtain,

$$u_\mu \partial_\nu T^{\mu\nu} = 0. \quad (2.85)$$

Again taking the definition of $T^{\mu\nu}$ from equation (2.15) we obtain two sets of equations for energy density and energy per particle as follows,

$$\begin{aligned} D\epsilon &= -hn\partial_\mu u^\mu \\ De &= -\frac{P}{n}\partial_\mu u^\mu. \end{aligned} \quad (2.86)$$

The quantity $\epsilon = ne$ is the energy density per unit volume.

2.4.4 Equation of enthalpy

Starting from equation (2.84) and decomposing the space gradient we get,

$$\Delta_{\mu\rho}\partial^\rho P = nhDu_\mu. \quad (2.87)$$

Now using the relativistic Gibbs-Duhem relationship,

$$\partial_\nu P = nT\partial_\nu\left(\frac{\mu}{T}\right) + nhT^{-1}\partial_\nu T, \quad (2.88)$$

we obtain,

$$nT\partial_\mu\left(\frac{\mu}{T}\right) + nhT^{-1}\partial_\mu - u_\mu DP = nhDu^\mu. \quad (2.89)$$

Contracting the above equation by u^μ from left we get the equation of motion of enthalpy per particle,

$$Dh = TD\left(\frac{\mu}{T}\right) + hT^{-1}DT. \quad (2.90)$$

2.4.5 Equation of temperature and chemical potential

Let us Expand De and Dh by taking derivatives with respect to temperature T and chemical potential over temperature μ/T .

$$\begin{aligned} De &= \left. \frac{\partial e}{\partial T} \right|_{\mu/T} DT + \left. \frac{\partial e}{\partial(\mu/T)} \right|_T D\left(\frac{\mu}{T}\right) \\ Dh &= \left. \frac{\partial h}{\partial T} \right|_{\mu/T} DT + \left. \frac{\partial h}{\partial(\mu/T)} \right|_T D\left(\frac{\mu}{T}\right) \end{aligned} \quad (2.91)$$

Now insertion of these two expansions on the left hand side of equation (2.86) and (2.90), results in a coupled set of equations as depicted below,

$$\begin{aligned} \left[\frac{\partial e}{\partial(\frac{\mu}{T})} \right]_T D\left(\frac{\mu}{T}\right) + \left[\frac{\partial e}{\partial T} \right]_{\frac{\mu}{T}} dT &= -\left(\frac{P}{n}\right) \partial_\mu u^\mu, \\ \left[T - \left\{ \frac{\partial h}{\partial(\frac{\mu}{T})} \right\}_T \right] D\left(\frac{\mu}{T}\right) + [hT^{-1} - \left\{ \frac{\partial h}{\partial T} \right\}_{\frac{\mu}{T}}] DT &= 0. \end{aligned}$$

These are easily solved to arrive at

$$\begin{aligned} DT &= \frac{(P/n) \left[T - \left. \frac{\partial h}{\partial(\mu/T)} \right|_T \right] \partial_\mu u^\mu}{\left. \frac{\partial e}{\partial(\mu/T)} \right|_T \left[hT^{-1} - \left. \frac{\partial h}{\partial T} \right|_{\mu/T} \right] - \left. \frac{\partial e}{\partial T} \right|_{\mu/T} \left[T - \left. \frac{\partial h}{\partial(\mu/T)} \right|_T \right]}, \\ D\left(\frac{\mu}{T}\right) &= \frac{-(P/n) \left[hT^{-1} - \left. \frac{\partial h}{\partial T} \right|_{\mu/T} \right] \partial_\mu u^\mu}{\left. \frac{\partial e}{\partial(\mu/T)} \right|_T \left[hT^{-1} - \left. \frac{\partial h}{\partial T} \right|_{\mu/T} \right] - \left. \frac{\partial e}{\partial T} \right|_{\mu/T} \left[T - \left. \frac{\partial h}{\partial(\mu/T)} \right|_T \right]}. \end{aligned} \quad (2.92)$$

We next evaluate the partial derivatives of e and h with respect T and (μ/T) using the relations in section [2.2]. Finally we get

$$\begin{aligned} \left. \frac{\partial h}{\partial T} \right|_{\mu/T} &= z \left[5 \frac{S_3^1}{S_2^1} + z \frac{S_2^0}{S_2^1} - z \frac{S_3^1 S_3^0}{(S_2^1)^2} \right] \\ \left. \frac{\partial e}{\partial T} \right|_{\mu/T} &= 4z \frac{S_3^1}{S_2^1} + z \frac{S_2^2 S_3^0}{(S_2^1)^2} - \frac{S_2^2}{S_2^1} + z^2 \left[\frac{S_2^0}{S_2^1} - \frac{S_3^1 S_3^0}{(S_2^1)^2} \right] \\ \left. \frac{\partial h}{\partial(\mu/T)} \right|_T &= Tz \left[\frac{S_3^0}{S_2^1} - \frac{S_3^1 S_2^0}{(S_2^1)^2} \right] \\ \left. \frac{\partial e}{\partial(\mu/T)} \right|_T &= -T \left[1 - \frac{S_2^2 S_2^0}{(S_2^1)^2} \right] + Tz \left[\frac{S_3^0}{S_2^1} - \frac{S_3^1 S_2^0}{(S_2^1)^2} \right]. \end{aligned} \quad (2.93)$$

Putting these in (2.92) we get

$$\begin{aligned} T^{-1}DT &= (1 - \gamma')\partial_\mu u^\mu , \\ TD\left(\frac{\mu}{T}\right) &= [(\gamma'' - 1)h - \gamma'''T]\partial_\mu u^\mu , \end{aligned} \quad (2.94)$$

where

$$\gamma' = \frac{(S_2^0/S_2^1)^2 - (S_3^0/S_2^1)^2 + 4z^{-1}S_2^0S_3^1/(S_2^1)^2 + z^{-1}S_3^0/S_2^1}{(S_2^0/S_2^1)^2 - (S_3^0/S_2^1)^2 + 3z^{-1}S_2^0S_3^1/(S_2^1)^2 + 2z^{-1}S_3^0/S_2^1 - z^{-2}} \quad (2.95)$$

$$\gamma'' = 1 + \frac{z^{-2}}{(S_2^0/S_2^1)^2 - (S_3^0/S_2^1)^2 + 3z^{-1}S_2^0S_3^1/(S_2^1)^2 + 2z^{-1}S_3^0/S_2^1 - z^{-2}} \quad (2.96)$$

$$\gamma''' = \frac{S_2^0/S_2^1 + 5z^{-1}S_3^1/S_2^1 - S_3^0S_3^1/(S_2^1)^2}{(S_2^0/S_2^1)^2 - (S_3^0/S_2^1)^2 + 3z^{-1}S_2^0S_3^1/(S_2^1)^2 + 2z^{-1}S_3^0/S_2^1 - z^{-2}} . \quad (2.97)$$

These are the conservation laws and equations of motion of the thermodynamic quantities we have at our exposure. In the following chapters we will utilize them as the thermodynamic identities to evaluate the transport coefficients for a dissipative fluid.

Bibliography

- [1] E.M. Lifshitz, L.P. Pitaevskii, Physical Kinetics (Elsevier, Amsterdam,1981).
- [2] L.D. Landau and E.M. Lifshitz, Fluid Mechanics (Elsevier, Amsterdam,1987).
- [3] S.R. de Groot, W.A. van Leeuwen and Ch.G. van Weert, Relativistic kinetic theory (North-Holland, Amsterdam, 1980).
- [4] Steven Weinberg, Gravitation and Cosmology: Principles and Applications of the General Theory of Relativity, (Wiley-VCH, 1972).
- [5] C. Eckart, Phys. Rev. 58, 919 (1940).

Chapter 3

Evaluation of transport coefficients

In general the notion “transport phenomena” is attributed to the exchange or transport of some physical quantity. The exchanged quantities can be mass, energy or momentum within the system which is being studied. The transport of all these quantities are irreversible in nature, stemming from the random continuous motion of the constituent particles within the system. Transport properties have been long employed as probing tools to understand the characteristics of a thermodynamic system. Since the macroscopic mechanism of the energy and momentum transfer involved in transport processes, is provided by interactions among the particles, investigation of transport properties in turn gives information about the nature of the interaction of the system under consideration. The hydrodynamic evolution of the matter created in relativistic heavy ion collisions involves different dissipative processes which can be quantified by transport coefficients. These quantities not only provide relevant insight about the fluid dynamics, but also carries the information about how far away the system is from ideal hydrodynamics. These facts serve a good motivation to evaluate the transport coefficients in the context of high energy nuclear collisions.

3.1 Origin of transport coefficients

The description of irreversible phenomena taking place in non equilibrium systems is characterized by two kinds of concepts : the thermodynamic forces and thermodynamic flows. The first one creates spatial non-uniformities of the macroscopic thermodynamic state variables where the later tends to smooth out those non-uniformities. As a result a closed system relaxes to its equilibrium state in course of time. Evidently the relaxation of the out of equilibrium system to its equilibrium state is irreversible, i.e. it involves dissipation. So it can be argued that these non-uniformities are wiped out to restore the equilibrium, at the expense of transport of some quantities such as matter or energy-momentum. So the flow of these quantities can be termed as the transport processes. Phenomenologically, one finds to a good approximation that these fluxes are linearly related to the thermodynamic forces. So effectively transport coefficients provide a measure of the amount of energy or momentum or heat needed to transfer, in order to eliminate the spatial inhomogeneities created by the thermodynamic forces for a non-equilibrium system. So mathematically one can write,

$$\textit{Thermodynamic flows} = C \times \textit{thermodynamic forces}, \quad (3.1)$$

Where the constant of proportionality C refers to the transport coefficients.

As a consequence the irreversible part of the energy momentum tensor and the heat flow can be expressed in a linear law, directly proportional to the corresponding thermodynamic forces which is respectively the velocity gradient and temperature gradient. From the second law of thermodynamics, it is known that the restoration of equilibrium is achieved by the processes which involve increasing entropy. From these criteria the irreversible flows are expressed by the following equations [1, 2].

$$\begin{aligned} \Pi^{\mu\nu} &= 2\eta\langle\partial^\mu u^\nu\rangle + \zeta\Delta^{\mu\nu}\partial \cdot u \\ I^\mu &= \lambda(\partial_\sigma T - T D u_\sigma)\Delta^{\mu\sigma}, \end{aligned} \quad (3.2)$$

where the constant of proportionalities η, ζ and λ are referred to as the transport coefficients. The η and ζ are coefficients of shear and bulk viscosity respectively and λ is the thermal conductivity.

Now at the microscopic level the transport of matter or energy is basically carried out by collisions among the constituent particles due to their mutual interactions. So at microscopic level we find an alternative definition of the thermodynamic flows in terms of an integral over the non-equilibrium or collisional part of the distribution function of particles and an irreducible tensor of the quantity which is being transported. Mathematically this can be written as,

$$\begin{aligned} \textit{Thermodynamic flows} = \int & (\textit{phasespacefactor}) \times (\textit{irreducible tensor of the} \\ & \textit{quantity being transported}) \times (\textit{non-equilibrium part} \\ & \textit{of distribution function}). \end{aligned} \quad (3.3)$$

The definition and the properties of irreducible tensor will be discussed in Appendix-A. This alternative expression of thermodynamic flows stems from the definition of distribution function which is the average number of particles within the momentum range p and $p + dp$ and within the volume element dV . So the flow can be interpreted as the flux of that particular quantity carried out by the collisional part of the particle numbers, integrated over total momentum range. Following this prescription the viscous part of the energy momentum stress tensor and the irreversible heat flow can be given by the following integral equations,

$$\Pi^{\mu\nu} = \int \frac{d^3p}{(2\pi)^3 p^0} \Delta_\sigma^\mu \Delta_\tau^\nu p^\sigma p^\tau \delta f, \quad (3.4)$$

$$\Delta I^\mu = \int \frac{d^3p}{(2\pi)^3 p^0} (p \cdot u - h) p^\sigma \Delta_\sigma^\mu \delta f. \quad (3.5)$$

When the two expressions of thermodynamic flows from equation (3.1) and (3.3) are compared we find that the transport coefficients come out to be as functions of the collisional part of the distribution function, that is the non-equilibrium contribution to the distribution function. So this quantity is needed to be obtained by solving the equation of motion of the distribution function which is the Boltzmann transport equation from the kinetic theory of fluids. So in the

following sections we will find a solution of the relativistic transport equation and obtain the transport coefficients therefrom.

3.2 Solution of the relativistic transport equation

The relativistic transport equation for an out of equilibrium system is given by,

$$p^\mu \partial_\mu f(x, p) = C[f]. \quad (3.6)$$

This equation expresses the rate of change of particle distribution function in terms of the collision integral,

$$C[f] = \int d\Gamma_{p_1} d\Gamma_{p'} d\Gamma_{p'_1} [f(x, p') f(x, p'_1) \{1 + f(x, p)\} \{1 + f(x, p_1)\} - f(x, p) f(x, p_1) \{1 + f(x, p')\} \{1 + f(x, p'_1)\}] W. \quad (3.7)$$

This is the collision term for a binary elastic collision $p + p_1 \rightarrow p' + p'_1$. The phase space factors are given by, $d\Gamma_q = \frac{d^3q}{(2\pi)^3 E_q}$. The collision term makes the transport equation a integro differential equation which is not trivial to solve. The factors indicate the Bose enhancement of the final state particles in a Bosonic system, which introduces the quantum statistical effects in the transport equation. The quantity W is the interaction rate given by,

$$W = \frac{s}{2} \frac{d\sigma}{d\Omega} (2\pi)^6 \delta^4(p + p_1 - p' - p'_1), \quad (3.8)$$

where the $1/2$ factor comes from the indistinguishability of the initial state particles. This term takes care of particle interactions responsible for altering the particle distribution within the system and explicitly contains the scattering cross-section through which the dynamical input of the system enters into the transport equation. Kinetic theory thus gives a basis to the phenomenological scheme mentioned earlier and expresses the transport coefficients in terms of microscopic interactions between constituent particles. Thus kinetic theory forms a bridge

between the microscopic dynamics of particle interaction and its macroscopic effects on the thermodynamic system. There are a few methods of solving the transport equation for an out of equilibrium system. Here we will mention two such methods in the following sections.

3.2.1 Relaxation time approximation

In general the program of seeking solution of transport equation becomes non-trivial due to the non-linearity of the collision term discussed above. However if the state of the system is not too far from the equilibrium, one may assume that a linearized form of the transport equation provides a reasonably accurate description of the non-linear phenomena. The simplest method of linearizing the transport equation is replacing the collision term by the rate of change of the distribution function over a quantity called relaxation time τ , such that the transport equation becomes,

$$\frac{df}{dt} = -\frac{\delta f_p}{\tau} = -\frac{(f - f^{(0)})}{\tau}. \quad (3.9)$$

Here $f^{(0)}$ is the local equilibrium distribution function and τ is the time over which the out of equilibrium distribution function relaxes to its equilibrium value. The negative sign indicates that the system always tends towards its equilibrium state. From equation (3.9) the deviation of the particle distribution function at near equilibrium situation comes out to be,

$$\delta f_p = -\tau \left\{ \frac{\partial f^{(0)}}{\partial t} + \vec{v}_p \cdot \vec{\nabla} f^{(0)} \right\}, \quad (3.10)$$

where \vec{v}_p is the velocity of p th particle. The equilibrium distribution function for a Bosonic system is,

$$f^{(0)} = \frac{1}{\exp\left[\frac{1}{T} \left\{ -\mu + \frac{E_p - \vec{p} \cdot \vec{v}}{\sqrt{1-v^2}} \right\}\right] - 1}. \quad (3.11)$$

Here E_p and \vec{p} are the energy and momenta of p th particle. T , μ and \vec{v} are the temperature, chemical potential and the hydrodynamic three velocity of the thermal bath concerning the

system. With the help of (3.11), equation (3.10) becomes

$$\delta f_p = -\tau \left[\frac{\{f^{(0)}(1+f^{(0)})\}}{T} \left\{ \frac{E_p - c_p T}{T} \vec{v}_p \cdot \vec{\nabla} T + \frac{1}{E_p} p^\alpha p^\beta (v_{\alpha\beta} - \frac{1}{3} \delta_{\alpha\beta} \vec{\nabla} \cdot \vec{v}) + \frac{1}{3E_p} ((1-3c_s^2)E_p^2 - m_p^2) \vec{\nabla} \cdot \vec{v} \right\} \right]. \quad (3.12)$$

The notations we have used are as follows, c_v and c_p are the specific heat at constant volume and at constant pressure respectively, c_s is the velocity of sound within the medium and m_p is the particle mass. The notation $v_{\alpha\beta}$ is defined as $v_{\alpha\beta} = \frac{1}{2} \left\{ \frac{\partial v_\alpha}{\partial x_\beta} + \frac{\partial v_\beta}{\partial x_\alpha} \right\}$.

Now in order to extract the coefficients of shear and bulk viscosities we will compare two expressions of the spatial components of dissipative part of energy-momentum stress tensor given below. The first one follows from the positive entropy production of the second law of thermodynamics

$$\Delta T^{ij} = -2\eta \left\{ \frac{1}{2} \partial^i u^j + \frac{1}{2} \partial^j u^i - \frac{1}{3} \vec{\nabla} \cdot \vec{v} \delta^{ij} \right\} - \zeta \vec{\nabla} \cdot \vec{v} \delta^{ij}, \quad (3.13)$$

and the second one follows from the integral representations of dissipative fluxes

$$\Delta T^{ij} = \int \frac{d^3 p}{(2\pi)^3 p^0} p^i p^j \delta f. \quad (3.14)$$

Comparing the (3.13) and (3.14) we obtain the expression of shear viscosity and bulk viscosity as follows,

$$\eta = \frac{1}{15T} \int \frac{d^3 p}{(2\pi)^3} \tau \frac{\vec{p}^4}{E_p^2} \{f^{(0)}(1+f^{(0)})\}, \quad (3.15)$$

$$\zeta = \frac{1}{9T} \int \frac{d^3 p}{(2\pi)^3} \tau \frac{1}{E_p^2} \{(1-3c_s^2)E_p^2 - m_p^2\}^2 \{f^{(0)}(1+f^{(0)})\}. \quad (3.16)$$

Similarly for the case of thermal conductivity from the analogous two expressions of heat flow vector we obtain ,

$$\lambda = \frac{1}{3T^2} \int \frac{d^3 p}{(2\pi)^3} \tau \frac{\vec{p}^2}{E_p^2} (E_p - h)^2 \{f^{(0)}(1+f^{(0)})\}, \quad (3.17)$$

where h is the enthalpy per particle.

The relaxation times τ is the inverse of the collision frequency ω for a particular dynamical process such as,

$$\tau = \frac{1}{\omega(E_p)} . \quad (3.18)$$

For a binary elastic collision $p + k \rightarrow p' + k'$ the collision frequency is given by [3],

$$\omega(E_p) = \frac{1}{2} \int \frac{d^3k}{(2\pi)^3} \int \frac{d^3p'}{(2\pi)^3} \int \frac{d^3k'}{(2\pi)^3} f_k(E_k) (2\pi)^4 \frac{\delta^4(p + k - p' - k')}{2E_p 2E_k 2E_{p'} 2E_{k'}} \langle |M|^2 \rangle , \quad (3.19)$$

where M is the interaction amplitude and the half factor comes from the initial state indistinguishability for identical particles. After doing simplifications the collision frequency becomes,

$$\omega(E_p) = \int \frac{\vec{k}^2 d\vec{k}}{4\pi E_p E_k} \lambda^{1/2}(s, m_p^2, m_k^2) \int d(\cos\theta_k) d(\cos\theta_{CM}) f(E_k) \left\{ \frac{1}{2} \frac{d\sigma}{d\Omega} \right\} . \quad (3.20)$$

Here $\frac{d\sigma}{d\Omega}$ is the differential scattering cross section of the respective interaction. θ_{CM} is the scattering angle in the centre of mass frame and θ_k is the angle between the two colliding particles. Equations (3.15), (3.16) and (3.17) gives the expressions of transport coefficients which with the help of (3.18) and (3.20), appear to be inversely proportional to the interaction cross section of the scattering processes.

3.2.2 Chapman-Enskog method

In the relaxation time approximation method for linearizing the transport equation the actual integral form of the collision term is not considered. A more precise evaluation of the transport quantities is based upon the perturbation techniques, where the distribution function is expanded in a series in terms of a parameter. Before introducing a quantity which can be used as the expansion parameter let us investigate the transport equation. If the derivative on the left hand side of equation (3.6) is decomposed into a time-like and a space-like part, then the resulting equation we obtain is,

$$p^\mu u_\mu Df + p^\mu \nabla_\mu f = C[f, f]. \quad (3.21)$$

The length scale associated with the collision term on the right hand side of the transport equation is the mean free path (λ) of the hydrodynamic system. The length scale associated with the terms on the left hand side of transport equation is the characteristic dimension for the spatial non-uniformities within the system, i.e, it is the typical length L over which the macroscopic thermodynamic quantities within the system can vary appreciably. The dimensionless ratio λ/L is called the Knudsen number and let us denote it by $\epsilon = \lambda/L$. The order of magnitude of the ratio of a typical term on the right hand side of transport equation to a typical term on the left hand side is the Knudsen number ϵ and due to this fact one can introduce ϵ (which must be small), as a dimensionless parameter in front of the left hand side of the transport equation depicted below to balance the magnitude of length scale of both sides of transport equation.

$$\epsilon\{p^\mu U_\mu Df + p^\mu \nabla_\mu f\} = C[f, f]. \quad (3.22)$$

This dimensionless quantity ϵ can be treated now as the expansion parameter of the distribution function mentioned earlier and the expansion should be such that if the n th term in the power series is expressed as $\sigma_n(\epsilon)$ then, $\lim_{\epsilon \rightarrow 0} \sigma_{n+1}(\epsilon)/\sigma_n(\epsilon) = 0$. This means the series should be an asymptotic one rather than convergent, so that the leading terms of the series will be contributing the most for a vanishing value of the expansion parameter ϵ . There exist many different perturbation methods corresponding to different functional choice of ϵ . In the Chapman-Enskog approximation for solving the transport equation which will be discussed here, the expansion is restricted to power series in ϵ .

$$f = \sum_{n=0}^{\infty} \epsilon^n f^{(n)} \quad (3.23)$$

In the Chapman-Enskog method the transport equation is linearized and this linearization is performed around a local equilibrium distribution function with parameters that vary in space and time. The collision operator then becomes a linear integral operator with symmetric kernel depending upon the particle interaction. The mathematical properties of the linear collision operator are more tractable but at the same time some rigorous results can be obtained using this method of functional analysis.

The series expansions in powers of ϵ fail to give uniformly valid solution for specific initial and boundary value problems. However in Chapman-Enskog procedure the problem can be avoided since in this method we do not expand the solutions but the equations instead. To understand the scenario lets start from the general form of Euler equation,

$$\frac{\partial \rho^\alpha}{\partial t} = S^\alpha, \quad (3.24)$$

where ρ^α are the basic macroscopic quantities (density, hydrodynamic velocity, temperature or energy density) and S^α is some source term. The basic idea of Chapman-Enskog method is to expand S^α while leaving ρ^α unchanged. To expand this equation in power series instead of its solutions let us write it in the following form,

$$\frac{\partial \rho^\beta}{\partial t} = D_\beta(\rho^\alpha). \quad (3.25)$$

Here D_β is a non-linear operator acting upon the space dependence of the ρ^α . Expanding S^α clearly means expanding D_β as follows,

$$D_\beta = \sum_{n=0}^{\infty} \epsilon^n D_\beta^{(n)}. \quad (3.26)$$

The crucial step in the Chapman-Enskog procedure is now the observation that the distribution function depends upon the space and time variables only through a functional dependence on the ρ^α . In other words we have,

$$\frac{\partial f}{\partial t} = \sum_{k=0}^{\infty} \frac{\partial f}{\partial(\nabla^k \rho^\alpha)} \frac{\partial(\nabla^k \rho^\alpha)}{\partial t} \quad (3.27)$$

where ∇^k formally denotes the k -th order space derivatives. Since equation (3.25) gives

$$\frac{\partial}{\partial t} \nabla^k \rho^\beta = \nabla^k D_\beta(\rho^\alpha), \quad (3.28)$$

the expansion of D_β implies an expansion of the operator giving the time evolution of f as well.

We can write this formally as follows:

$$\frac{\partial f}{\partial t} = \sum_{n=0}^{\infty} \epsilon^n \frac{\partial^{(n)} f}{\partial t}, \quad (3.29)$$

where $\partial^{(n)} f / \partial t$ denotes the contribution to $\partial f / \partial t$ coming from $D_\beta^{(n)}$ through equation (3.26).

So in covariant notation the time derivative over distribution function is expanded as follows,

$$Df = (Df)^0 + \epsilon(Df)^1 + \epsilon^2(Df)^2 + \dots, \quad (3.30)$$

where the term $(Df)^n$ simply denotes $\partial^{(n)} f / \partial t$. The above equation along with equation (3.23) helps to expand transport equation in terms of the non-uniformity parameter ϵ . Substituting them into the transport equation (3.22) and equating the coefficients of equal power in ϵ , we obtain the hierarchy of equations,

$$0 = C[f^{(0)}, f^{(0)}] \quad (3.31)$$

$$p^\mu u_\mu (Df)^{r-1} + p^\mu \nabla_\mu f^{r-1} = \sum_{s=0}^r C[f^s, f^{r-s}], \quad r \geq 1. \quad (3.32)$$

Equation (3.31) reveals nothing but the Boltzmann transport equation for a fluid in equilibrium where the collision term involving equilibrium distribution function reduces to zero. Equation (3.32) provides a hierarchy of equations where in the left hand side of the transport equation the derivatives appear on the lower order of distribution function, and the next order appear on the right hand side only under the collision term. If the r th order of distribution function is expressed as $f^{(r)} = f^{(0)}(1 + f^{(0)}\phi^{(r)})$, then employing the principle of detailed balance $f^{(0)}(x, p)f^{(0)}(x, p_1) = f^{(0)}(x, p')f^{(0)}(x, p'_1)$ we obtain,

$$C[f^{(0)}, f^{(r)}] + C[f^{(r)}, f^{(0)}] = -\mathcal{L}[\phi^{(r)}]. \quad (3.33)$$

The unknown function $\phi^{(r)}$, which depends upon particle 4-momenta and fluid space-time coordinates, is needed to be determined. Here we can see that the non-linear collision term becomes linearized under the function ϕ and the linearized collision operator is defined as,

$$\begin{aligned} \mathcal{L}[\phi] = & f^{(0)}(x, p) \int d\Gamma_{p_1} d\Gamma_{p'} d\Gamma_{p'_1} f^{(0)}(x, p_1) \{1 + f^{(0)}(x, p')\} \{1 + f^{(0)}(x, p'_1)\} \\ & [\phi(x, p) + \phi(x, p_1) - \phi(x, p') - \phi(x, p'_1)] W(p, p_1 | p', p'_1). \end{aligned} \quad (3.34)$$

Here W is the interaction cross sections for the corresponding dynamical processes. In this way the Chapman-Enskog hierarchy becomes,

$$p^\mu U_\mu (Df)^{r-1} + p^\mu \nabla_\mu f^{r-1} - \sum_{s=1}^{r-1} C[f^s, f^{r-s}] = -\mathcal{L}[\phi^r]. \quad (3.35)$$

From the foregoing discussion it follows that the first Chapman-Enskog approximation is determined by equation (3.35) for $r=1$

$$p^\mu U_\mu (Df)^0 + p^\mu \nabla_\mu f^{(0)} = -\mathcal{L}[\phi^{(1)}], \quad (3.36)$$

with

$$f_0(x, p) = \frac{1}{\exp\left[\frac{p^\mu u_\mu}{T} - \frac{\mu}{T}\right] - 1}, \quad (3.37)$$

and

$$(Df)^0 = \frac{\partial f^{(0)}}{\partial(\frac{\mu}{T})} \left(D\left(\frac{\mu}{T}\right)\right) + \frac{\partial f^{(0)}}{\partial T} (DT) + \frac{\partial f^{(0)}}{\partial u^\mu} (Du^\mu). \quad (3.38)$$

In equation (3.36) the quantity $\phi^{(1)}$ is the measure of the deviation of the distribution function in the first approximation of Chapman-Enskog method from its equilibrium value and from here on we are restricting our estimations for $\phi^{(1)}$ only.

From the above hierarchy of equations it is very nicely understood that the Chapman-Enskog technique is an iterative method. With the help of the known lower order distribution function we are able to determine the next order by successive approximation.

3.3 Evaluation of transport coefficients in Chapman-Enskog method

In equation (3.36) the quantity $\phi^{(1)}$ is the measure of the deviation of the distribution function in the first approximation of Chapman-Enskog method from its equilibrium value and since from here on we will proceed with the first Chapman-Enskog approximation, we will simply denote this quantity by ϕ . So in the first approximation of Chapman-Enskog technique the deviation of distribution function from its lowest order local equilibrium value is given by,

$$\delta f = f^{(0)}(1 + f^{(0)})\phi(x, p). \quad (3.39)$$

Equation (3.36) is the key equation for solving the relativistic transport equation in the first Chapman-Enskog approximation which gives the evolution of the phase-space distribution of

the constituent particles. To proceed further the space time derivative on the left hand side of the transport equation is decomposed into a space-like and a time like part as follows,

$$\partial^\mu = u^\mu D + \nabla^\mu. \quad (3.40)$$

Where $D = u^\mu \partial_\mu$ is the convective time derivative and $\nabla^\mu = \Delta^{\mu\nu} \partial_\nu$ is the spatial gradient defined with the help of the projection operator $\Delta^{\mu\nu} = g^{\mu\nu} - u^\mu u^\nu$.

The form of $f^{(0)}(x, p)$ as given in (3.37) is now used on the left side of (3.36) and after operating the time and the spatial gradients on it we find that the transport equation takes the following form,

$$\left\{ \frac{(p_\mu u^\mu)^2}{T^2} DT + p^\mu u_\mu D\left(\frac{\mu}{T}\right) - \frac{p^\mu u_\mu}{T} p^\nu D u_\nu \right\} + p_\mu \left\{ \frac{p^\nu u_\nu}{T^2} (\nabla^\mu T) + \nabla^\mu \left(\frac{\mu}{T}\right) - \frac{p^\nu}{T} \nabla^\mu u_\nu \right\} = - \frac{\mathcal{L}[\phi]}{f^{(0)}(1 + f^{(0)})} \quad (3.41)$$

Eliminating the time derivative terms in the above equation with the help of equilibrium thermodynamic laws discussed in chapter-2 and replacing the spatial gradient of μ/T by relativistic Gibbs-Duhem equation it leads to the following linear equation satisfied by the deviation function ϕ .

$$[Q \partial_\nu u^\nu + p_\mu \Delta^{\mu\nu} (p \cdot u - h) (T^{-1} \partial_\nu T - D u_\nu) - \langle p_\mu p_\nu \rangle \langle \partial^\mu u^\nu \rangle] f^{(0)} (1 + f^{(0)}) = -T \mathcal{L}[\phi] \quad (3.42)$$

We have used the notation $\langle t^{\mu\nu} \rangle \equiv [\frac{1}{2} (\Delta^{\mu\alpha} \Delta^{\nu\beta} + \Delta^{\nu\alpha} \Delta^{\mu\beta}) - \frac{1}{3} \Delta^{\mu\nu} \Delta^{\alpha\beta}] t_{\alpha\beta}$ indicating a space-like symmetric and traceless form of the tensor $t^{\mu\nu}$, which is actually an irreducible tensor of rank-2.

In this equation

$$Q = -\frac{1}{3} m_\pi^2 + (p \cdot u)^2 \left\{ \frac{4}{3} - \gamma' \right\} + p \cdot u \{ (\gamma'' - 1) h - \gamma''' T \}. \quad (3.43)$$

So it is now observed that in the left hand side of the transport equation, different thermodynamic forces appear with different tensorial rank representing a scalar, a vector and a tensor respectively. So now the transport equation has become a linear equation where the collision term has been converted to a linear integral operator $\mathcal{L}[\phi]$. Since this integral operator only

involves integration over the momenta of scattered particle, in order to be a solution of (3.42) the deviation function ϕ must be a linear combination of the thermodynamic forces with appropriate coefficients. Now since the distribution function as well as its derivative is a scalar quantity, so in order to keep ϕ a scalar the respective coefficients should be of appropriate tensorial rank. Keeping these criteria in mind the most general solution we obtain for ϕ is,

$$\phi = A\partial \cdot u + B_\mu \Delta^{\mu\nu} (T^{-1}\partial_\nu T - Du_\nu) - C_{\mu\nu} \langle \partial^\mu u^\nu \rangle. \quad (3.44)$$

The coefficient A must be scalar and since it is the coefficient of the velocity divergence term, it must be related to volume viscosity or bulk viscosity of the system. B_μ is a vector and being the coefficient of the temperature gradient term it must be related to the thermal conductivity of the system. Finally the quantity $C_{\mu\nu}$ which is the coefficient of the traceless part of velocity gradient is a tensor and related to the shear viscosity. Substituting (3.44) in (3.42) and comparing coefficients of the independent thermodynamic forces on both sides, yields the set of equations satisfied by the coefficient functions.

$$\mathcal{L}[A] = -Qf^{(0)}(p)\{1 + f^{(0)}(p)\}/T \quad (3.45)$$

$$\mathcal{L}[B_\mu] = -\Delta_{\mu\sigma} p^\sigma (p \cdot u - h) f^{(0)}(p) \{1 + f^{(0)}(p)\}/T \quad (3.46)$$

$$\mathcal{L}[C_{\mu\nu}] = -\langle p_\mu p_\nu \rangle f^{(0)}(p) \{1 + f^{(0)}(p)\}/T \quad (3.47)$$

Here, $C_{\mu\nu} = C \langle p_\mu p_\nu \rangle$ and $B_\mu = B \Delta_{\mu\nu} p^\mu$. These integral equations are needed to be solved to get the coefficients A , B_μ and $C_{\mu\nu}$.

The next task is to link these quantities to the transport coefficients. For this purpose we replace δf by equation (3.39) into the integral representations of the thermodynamic fluxes displayed in (3.4) and (3.5).

The viscous pressure tensor is now modified to take the following form,

$$\Pi^{\mu\nu} = \int \frac{d^3 p}{(2\pi)^3 p^0} \Delta_\sigma^\mu \Delta_\tau^\nu p^\sigma p^\tau f^{(0)}(1 + f^{(0)}) \phi. \quad (3.48)$$

It is convenient to split $\Pi^{\mu\nu}$ into a traceless part and a remainder such as,

$$\Pi^{\mu\nu} = \overset{\circ}{\Pi}^{\mu\nu} + \Pi\Delta^{\mu\nu}. \quad (3.49)$$

The viscous pressure Π is defined as one third of the trace of the viscous pressure tensor,

$$\Pi = \frac{1}{3} \int \frac{d^3p}{(2\pi)^3 p^0} \Delta_{\mu\nu} p^\mu p^\nu f^{(0)}(1 + f^{(0)})\phi. \quad (3.50)$$

So the trace less part of viscous trace tensor comes out to be,

$$\begin{aligned} \overset{\circ}{\Pi}^{\mu\nu} &= \Pi^{\mu\nu} - \Pi\Delta^{\mu\nu} \\ &= \int \frac{d^3p}{(2\pi)^3 p^0} \left\{ \Delta_\sigma^\mu \Delta_\tau^\nu - \frac{1}{3} \Delta_{\sigma\tau} \Delta^{\mu\nu} \right\} p^\sigma p^\tau f^{(0)}(1 + f^{(0)})\phi \\ &= \int \frac{d^3p}{(2\pi)^3 p^0} \langle p^\mu p^\nu \rangle f_0(1 + f_0)\phi. \end{aligned} \quad (3.51)$$

Again from equation (3.2) we obtain the following linear law,

$$\overset{\circ}{\Pi}^{\mu\nu} = 2\eta \langle \partial^\mu u^\nu \rangle. \quad (3.52)$$

Comparing (3.51) and (3.52) we obtain the expression of shear viscosity,

$$\eta = -\frac{1}{10} \int \frac{d^3p}{(2\pi)^3 p^0} f^{(0)}(1 + f^{(0)}) C \langle p^\alpha p^\beta \rangle \langle p_\alpha p_\beta \rangle. \quad (3.53)$$

The case for bulk viscosity is a little different. Let us start with the integral equation (3.45) for A . We can see that equation (3.45) does not have a unique solution. For the present case of binary elastic collisions among same species of particles, starting from one solution $A(E)$ we can generate an infinite number of solutions by making the replacement, $A \rightarrow A(E) + a + bE$, where a and b are arbitrary constants associated with particle number conservation and energy conservation. For a system with zero net quantum number (such as electric charge or baryon number) the quantity a can be set to zero, where the constant b acts like inverse of temperature and yet to be determined [3].

We can start with the Landau-Lifshitz condition $u_\mu u_\nu \Delta T^{\mu\nu} = 0$, which actually comes from the solubility condition $\int \frac{d^3p}{(2\pi)^3 p^0} (p_\mu u^\mu)^2 f^{(0)}(1 + f^{(0)})\phi = 0$, [1]. So this equation actually sets a constraint over the coefficient A in the following way,

$$u_\mu u_\nu \int \frac{d^3p}{(2\pi)^3 p^0} p^\mu p^\nu f^{(0)}(p) \{1 + f^{(0)}(p)\} \phi = 0. \quad (3.54)$$

If in the above equation the replacement $A \rightarrow A(E) + a + bE$, is performed then after few steps of algebra the coefficient b comes to be,

$$b = -\frac{1}{T^2 c_v} \int \frac{d^3p}{(2\pi)^3} E f^{(0)}(1 + f^{(0)}) A(E). \quad (3.55)$$

If the same replacement is done in (3.50) then the viscous pressure obtains the following form,

$$\begin{aligned} \Pi &= -(\partial \cdot u) \frac{1}{3} \int \frac{d^3p}{(2\pi)^3 p^0} \{-m^2 + E^2(1 - 3c_s^2)\} f^{(0)}(p) \{1 + f^{(0)}(p)\} A(E), \\ &= -(\partial \cdot u) \int \frac{d^3p}{(2\pi)^3 p^0} \{Q\} \{A\} f^{(0)}(p) \{1 + f^{(0)}(p)\}. \end{aligned} \quad (3.56)$$

It can be proved that $Q = \frac{1}{3}\{-m^2 + E^2(1 - 3c_s^2)\}$ in a trivial way where E and m are the energy and mass corresponding to each particle. Here we have defined the following thermodynamic quantities such as,

$$\begin{aligned} c_v &= \frac{1}{T^2} \int \frac{d^3p}{(2\pi)^3} \{E^2\} f^{(0)}(p) \{1 + f^{(0)}(p)\}, \\ s &= \frac{1}{3T^2} \int \frac{d^3p}{(2\pi)^3} \{|\vec{p}|^2\} f^{(0)}(p) \{1 + f^{(0)}(p)\}, \\ c_s^2 &= \frac{\partial P}{\partial \epsilon}, \end{aligned} \quad (3.57)$$

where c_v , s and c_s^2 are respectively specific heat per unit volume, entropy density and velocity of sound within the system. Similar to the shear viscosity case, from (3.2) we obtain,

$$\Pi = \zeta(\partial \cdot u). \quad (3.58)$$

Comparing (3.56) and (3.58) we obtain the expression for bulk viscosity as the following,

$$\zeta = - \int \frac{d^3p}{(2\pi)^3 p^0} Q A f^{(0)}(1 + f^{(0)}). \quad (3.59)$$

In the case of thermal conductivity the integral form of dissipative heat flow,

$$\begin{aligned} \Delta I^\mu &= \int \frac{d^3p}{(2\pi)^3 p^0} (p \cdot u - h) p^\sigma \Delta_\sigma^\mu f^{(0)} \{1 + f^{(0)}\} \phi \\ &= \int \frac{d^3p}{(2\pi)^3 p^0} (p \cdot u - h) p^\sigma \Delta_\sigma^\mu B_\mu \Delta^{\mu\alpha} \{T^{-1} \partial_\alpha T - D u_\alpha\} f^{(0)}(1 + f^{(0)}) \end{aligned} \quad (3.60)$$

Comparing (3.2) and (3.60) we obtain the expression for thermal conductivity,

$$\lambda = \frac{1}{3T} \int \frac{d^3p}{(2\pi)^3 p^0} B_\mu \Delta_\nu^\mu p^\nu (p \cdot u - h) f^{(0)} (1 + f^{(0)}). \quad (3.61)$$

So we have integral representations of shear viscosity, bulk viscosity and thermal conductivity depicted by equation (3.53), (3.59) and (3.61), which are now explicit functions of the unknown coefficients A , B_μ and $C_{\mu\nu}$. These unknown coefficients are again needed to be evaluated from their respective integral equations (3.45), (3.46) and (3.47), which involve the linearized collision term in order to produce convenient algebraic expressions of transport coefficients. The detailed method of obtaining these is discussed in the next section. Here we note one important thing, that the coefficient functions A , B_μ and $C_{\mu\nu}$ are so constructed such that they represent irreducible tensors of rank 0, 1 and 2 respectively. This is done because the expressions of transport coefficients appear to be scalar product of a irreducible tensor of the transported quantity and the coefficient functions. Due to the isotropy and the relativistic invariance of the collision term it can be found out that thermodynamic flow and forces of different rank do not couple while those of equal rank do couple via scalar coefficients. The inner product of two irreducible tensors of different rank gives zero. This is the Curie's principle in the framework of the relativistic kinetic theory. The transport coefficients in equations (3.53), (3.59) and (3.61) come out to be a phase space integration over the product of two irreducible tensors which are completely contracted and finally leads to scalar values of the transport coefficients.

Our next task is to obtain the coefficients A , B_μ and $C_{\mu\nu}$ from their respective integral equations. For this purpose we adopt a technique called variational method, where the coefficients are expanded in terms of orthogonal Laguerre polynomial of half-integral order with the argument $\tau = \frac{p^\mu u_\mu - m}{T}$. For each transport coefficients the respective processes are elaborated in the subsequent subsections.

3.3.1 Bulk viscosity

Let us start from equation (3.45). We multiply both sides of (3.45) with Laguerre polynomial of order $1/2$ and degree $n = 0, 1, 2, \dots$ and then integrate over the phase space factor $d\Gamma_p = \int \frac{d^3p}{(2\pi)^3 p_0}$. We obtain the following equation,

$$[A(\tau), L_n^{1/2}(\tau)] = \frac{\alpha_n}{n}. \quad (3.62)$$

where

$$\alpha_n = -\frac{1}{nT} \int d\Gamma_p f^{(0)}(p) \{1 + f^{(0)}(p)\} Q L_n^{1/2}(\tau), \quad (3.63)$$

and the abbreviation

$$[F, G] = \frac{1}{4n^2} \int d\Gamma_p d\Gamma_{p_1} d\Gamma_{p'} d\Gamma_{p'_1} f^{(0)}(p) f^{(0)}(p_1) \{1 + f^{(0)}(p')\} \{1 + f^{(0)}(p'_1)\} \delta(F) \delta(G) W, \quad (3.64)$$

with

$$\begin{aligned} \delta(F) &= F(p) + F(p_1) - F(p') - F(p'_1) \\ \delta(G) &= G(p) + G(p_1) - G(p') - G(p'_1). \end{aligned} \quad (3.65)$$

The quantity expressed in (3.64) is called the bracket quantity in transport theory, which explicitly contains the dynamical cross-section for the respective processes through the rate of interaction W .

Now we proceed to expand A as mentioned before in terms of orthogonal Laguerre polynomial as depicted below,

$$A(\tau) = \sum_{m=0}^{\infty} a_m L_m^{1/2}(\tau) \quad (3.66)$$

Putting this expansion back in the bracket term in (3.62) we obtain the following summation series,

$$\sum_{m=0}^{\infty} a_m a_{mn} = \frac{\alpha_n}{n}, \quad (3.67)$$

where $a_{mn} = [L_m^{1/2}(\tau), L_n^{1/2}(\tau)]$, $(m, n = 0, 1, 2, \dots)$ is called the collision bracket involving only two Laguerre polynomial.

Now from the solubility condition $\int \frac{d^3p}{(2\pi)^3 p^0} f^{(0)}(1 + f^{(0)})Q\psi = 0$, where ψ is the summation invariant 1 or p^μ one obtains,

$$a_{0n} = a_{n0} = 0 \quad (3.68)$$

$$a_{1n} = a_{n1} = 0 \quad (n = 0, 1, 2, 3 \dots \dots) \quad (3.69)$$

$$\alpha_0 = \alpha_1 = 0. \quad (3.70)$$

An approximate solution for the first r coefficients of a_m of the set of equations given in (3.67) is obtained by limiting the infinite number of equations to a finite number r ,

$$\sum_{m=2}^{r+1} a_m^{(r)} a_{mn} = \frac{\alpha_n}{n} \quad (n = 2, 3 \dots \dots r). \quad (3.71)$$

Now putting the expansion of A from (3.66) into (3.59) we can obtain,

$$\begin{aligned} \zeta &= - \sum_{m=0}^{\infty} a_m \int \frac{d^3p}{(2\pi)^3 p_0} f^{(0)}(1 + f^{(0)})L_m^{1/2}(\tau)Q \\ &= nT \sum_{m=2}^{\infty} a_m \alpha_m. \end{aligned} \quad (3.72)$$

So in the first approximation the bulk viscosity is,

$$[\zeta]_1 = nT a_2^{(1)} \alpha_2 = T \frac{\alpha^2}{a_{22}}. \quad (3.73)$$

Where we have,

$$\alpha_2 = -\frac{1}{nT} \int d\Gamma_p f^{(0)}(p) \{1 + f^{(0)}(p)\} Q L_2^{1/2}(\tau), \quad (3.74)$$

and

$$a_{22} = [L_2^{1/2}(\tau), L_2^{1/2}(\tau)]. \quad (3.75)$$

Evaluation of α_2

Utilizing the property of Laguerre polynomial

$$L_n^\alpha(x+y) = \sum_{k=0}^n L_{n-k}^{\alpha+k}(x) \frac{(-y)^k}{k!}, \quad (3.76)$$

we obtain,

$$\alpha_n = -\frac{1}{nT} \sum_{k=2}^n (-1)^k \frac{z^k}{k!} L_{n-k}^{1/2+k}(-z) u_{\nu_1 \dots \nu_k} Q^{\nu_1 \dots \nu_k}, \quad (3.77)$$

where, $u_{\nu_1 \dots \nu_k} = u_{\nu_1} \dots u_{\nu_k}$ and the quantity Q is defined as $Q^{\nu_1 \dots \nu_k} = \frac{1}{m^k} \int \frac{d^3 p}{(2\pi)^3 p^0} f^{(0)}(1 + f^{(0)}) p^{\nu_1 \dots \nu_k} Q$. So from (3.77) we can get the expressions of α_2 which is given by,

$$\alpha_2 = -\frac{1}{nT} L_0^{5/2}(-z) \frac{1}{2!} z^2 u_{\mu\nu} Q^{\mu\nu}. \quad (3.78)$$

Now we define the moments of the distribution function by the following expression,

$$F_{\nu_1 \dots \nu_n} = \int \frac{d^3 p}{(2\pi)^3 p^0} f^{(0)}(1 + f^{(0)}) p_{\nu_1} \dots p_{\nu_n}, \quad (3.79)$$

which can be written down in form of the algebraic equation,

$$F_{\nu_1 \dots \nu_n} = \frac{\rho(m)^n}{mT S_2^1} \sum_{l=0}^{\lfloor \frac{n}{2} \rfloor} a_{nl} (\Delta u)_{nl}, \quad (3.80)$$

where,

$$a_{nl} = \sum_{k=1}^{\infty} k \sum_{s=0}^{\lfloor \frac{n}{2} - l \rfloor} (-1)^s (2l + 2s - 1)!! \{^{(l+s)} C_s\} \{^{(n)} C_{(2l+2s)}\} \frac{k_{n-l-s+1}(kz)}{(kz)^{l+s+1}} \exp\left\{\frac{k\mu}{T}\right\}, \quad (3.81)$$

and,

$$(\Delta u)_{nl} = \Delta_{(\alpha_1 \alpha_2 \dots \alpha_{(2l-1)\alpha_{2l}} u_{\alpha_{(2l+1)} u_{\alpha_{(2l+2)} \dots u_{\alpha_n})}, \quad (3.82)$$

with $t_{(\alpha_1 \dots \alpha_n)} = \frac{1}{n!} \sum_P t_{P(\alpha_1 \dots \alpha_n)}$, where the summation is extended over all permutations P of the indices.

Using the above formulas after some algebraic calculations we are able obtain the value of α_2 as follows,

$$\alpha_2 = \frac{z^3}{2} \left[\frac{1}{3} \left(\frac{S_3^0}{S_2^1} - z^{-1} \right) + \left(\frac{S_2^0}{S_2^1} + \frac{3 S_3^1}{z S_2^1} \right) \left\{ (1 - \gamma'') \frac{S_3^1}{S_2^1} + \gamma''' z^{-1} \right\} - \left(\frac{4}{3} - \gamma' \right) \left\{ \frac{S_3^0}{S_2^1} + \frac{15 S_3^2}{z^2 S_2^1} + \frac{2}{z} \right\} \right] \quad (3.83)$$

Evaluation of a_{22}

From equation (3.75) the expression of a_{22} is given by,

$$\begin{aligned} a_{22} &= [L_2^{1/2}(\tau), L_2^{1/2}(\tau)] \\ &= \frac{1}{4n^2} \int d\Gamma_p d\Gamma_{p'} d\Gamma_{p_1} d\Gamma_{p'_1} f^{(0)} f_1^{(0)} (1 + f^{(0)}) (1 + f_1^{(0)}) W \delta\{L_2^{\frac{1}{2}}(\tau)\} \delta\{L_2^{\frac{1}{2}}(\tau)\} \end{aligned} \quad (3.84)$$

To perform this 12-dimensional integral we make proper choice of geometry by introducing relative four-momenta before and after collision

$$g_\alpha \equiv \frac{1}{2}(p_{1\alpha} - p_\alpha), \quad g'_\alpha \equiv \frac{1}{2}(p'_{1\alpha} - p'_\alpha), \quad (3.85)$$

and total momentum of two particles,

$$P_\alpha \equiv (p_{1\alpha} + p_\alpha) = (p'_{1\alpha} + p'_\alpha) \equiv P'_\alpha, \quad (3.86)$$

which reduces a_{22} as,

$$a_{22} = \frac{z^2}{4} I_3, \quad (3.87)$$

with the definition of the integrals $I_\alpha(z)$,

$$\begin{aligned} I_\alpha(z) &= \frac{8z^4}{[S_2^1(z)]^2} e^{(-2\mu\pi/T)} \int_0^\infty d\psi \cosh^3 \psi \sinh^7 \psi \int_0^\pi d\Theta \sin \Theta \left\{ \frac{1}{2} \frac{d\sigma}{d\Omega}(\psi, \Theta) \right\} \int_0^{2\pi} d\phi \\ &\times \int_0^\infty d\chi \sinh^{(2\alpha)} \chi \int_0^\pi d\theta \sin \theta \frac{e^{2z \cosh \psi \cosh \chi}}{(e^E - 1)(e^F - 1)(e^G - 1)(e^H - 1)} M_\alpha(\theta, \Theta), \end{aligned} \quad (3.88)$$

in which the functions $M_\alpha(\theta, \Theta)$ represent

$$\begin{aligned} M_1(\theta, \Theta) &= 1 - \cos^2 \Theta, \\ M_2(\theta, \Theta) &= \cos^2 \theta + \cos^2 \theta' - 2 \cos \theta \cos \theta' \cos \Theta, \\ M_3(\theta, \Theta) &= [\cos^2 \theta - \cos^2 \theta']^2. \end{aligned} \quad (3.89)$$

The definitions of the integration variables used and the details of the reduction of the collision brackets are given in Appendix-B. The product of the distribution functions with the Bose enhancement in the final state particles in terms of the exponents of E, F, G and H is evaluated in Appendix-C.

3.3.2 Thermal conductivity

In the case of thermal conductivity we will start from (3.46). By multiplying both sides of (3.46) with Laguerre polynomial of order $3/2$ and degree $n = 0, 1, 2, \dots$ and then integrate over the phase space factor $d\Gamma_p$ we obtain the following equation,

$$[Bp^\alpha, L_n^{3/2}(\tau)\Delta_{\alpha\mu}p^\mu] = \frac{T}{n}\beta_n. \quad (3.90)$$

where,

$$\beta_n = -\frac{1}{nT^2} \int d\Gamma_p f^{(0)}(p) \{1 + f^{(0)}(p)\} L_n^{3/2}(\tau) (p \cdot u - h) \Delta_{\mu\nu} p^\mu p^\nu, \quad (3.91)$$

and the bracket quantity has their usual meaning.

Expanding B as before in terms of orthogonal Laguerre polynomial as shown below,

$$B(\tau) = \sum_{m=0}^{\infty} b_m L_m^{3/2}(\tau), \quad (3.92)$$

and putting back in the bracket term in (3.90) we obtain the following summation series,

$$\sum_{m=0}^{\infty} b_m b_{mn} = \frac{\beta_n}{\rho}, \quad (3.93)$$

where $b_{mn} = \frac{1}{mT} [L_m^{3/2}(\tau)p^\mu, L_n^{3/2}(\tau)\Delta_{\mu\nu}p^\nu]$ is the bracket quantity discussed earlier. Arguing for the same solubility condition it comes out to be that, $b_{0n} = b_{n0} = 0$ for $n = 0, 1, 2, 3, \dots$ and simultaneously $\beta_0 = 0$. Now an approximate solution of the first r coefficients of b_m of the set of equations given in (3.93) is obtained by limiting the infinite number of equations to a finite number r ,

$$\sum_{m=1}^r b_m^{(r)} b_{mn} = \frac{\beta_n}{\rho}, \quad (n = 1, 2, 3, \dots, r). \quad (3.94)$$

Now putting the expansion of B from (3.92) into (3.61) we can obtain,

$$\begin{aligned}\lambda &= -\frac{1}{3} \sum_{m=1}^{\infty} b_m \int \frac{d^3p}{(2\pi)^3 p_0} f^{(0)}(1 + f^{(0)}) L_m^{3/2}(\tau) \Delta_{\mu\nu} p^\mu p^\nu T^{-1} (p \cdot u - h) \\ &= \frac{1}{3} nT \sum_{m=1}^{\infty} b_m \beta_m.\end{aligned}\quad (3.95)$$

So in the first approximation the thermal conductivity is,

$$[\lambda]_1 = -\frac{1}{3} nT b_1^{(1)} \beta_1 = -\frac{T}{3m} \frac{\beta_1^2}{b_{11}}.\quad (3.96)$$

Where we have,

$$\beta_1 = -\frac{1}{nT^2} \int d\Gamma_p f^{(0)}(p) \{1 + f^{(0)}(p)\} L_1^{3/2}(\tau) (p \cdot u - h) \Delta_{\mu\nu} p^\mu p^\nu, \quad (3.97)$$

and

$$b_{11} = \frac{1}{mT} \Delta_{\mu\nu} [L_1^{3/2}(\tau) p^\mu, L_1^{3/2}(\tau) p^\nu]. \quad (3.98)$$

Evaluation of β_1

Taking the definition of β_n from (3.91) and using the property of Laguerre polynomial from (3.76) we obtain,

$$\beta_n = -\frac{1}{nT^2} \sum_{k=1}^n \frac{(-1)^k}{k!} z^k L_{n-k}^{\frac{3}{2}+k}(-z) u_{\nu_1 \dots \nu_k} G^{\nu_1 \dots \nu_k}, \quad (3.99)$$

where $G^{\nu_1 \dots \nu_k} = (m)^{-k} \int \frac{d^3p}{(2\pi)^3 p_0} f^{(0)}(1 + f^{(0)}) p^{\nu_1} \dots p^{\nu_k} G$ with $G = (p \cdot u - h) \Delta_{\mu\nu} p^\mu p^\nu$. Following this prescription β_1 comes out to be,

$$\beta_1 = \left(\frac{1}{nT^2}\right) z u_\mu G^\mu, \quad (3.100)$$

where from the previous definition it turns out that $G^\mu = (m)^{-1} \Delta_{\alpha\beta} \{u_\nu F^{\mu\nu\alpha\beta} - h F^{\mu\alpha\beta}\}$. Finally after doing the moment calculation we get,

$$\beta_1 = 3z^2 \left[1 + 5z^{-1} \frac{S_3^2}{S_2^1} - \left(\frac{S_3^1}{S_2^1}\right)^2\right]. \quad (3.101)$$

Evaluation of b_{11}

From equation (3.98) the expression of b_{11} is given by,

$$\begin{aligned}
b_{11} &= \frac{1}{mT} \Delta_{\alpha\beta} [L_1^{3/2}(\tau) p^\alpha, L_1^{3/2}(\tau) p^\beta] \\
&= \frac{1}{4n^2 mT} \int d\Gamma_p d\Gamma_{p'} d\Gamma_{p_1} d\Gamma_{p'_1} f^{(0)} f_1^{(0)} (1 + f'^{(0)}) (1 + f_1'^{(0)}) W(pp_1|p'p'_1) \\
&\times \Delta_{\alpha\beta} \delta\{L_1^{\frac{3}{2}}(\tau) p^\alpha\} \delta\{L_1^{\frac{3}{2}}(\tau) p^\beta\}.
\end{aligned} \tag{3.102}$$

Using the same choice of geometry as before finally we obtain,

$$b_{11} = -z \{I_2(z) + I_3(z)\}, \tag{3.103}$$

where the integrals are having their usual meaning as before given in (3.88).

3.3.3 Shear viscosity

For the case of shear viscosity we will start from equation (3.47). We multiply both sides of (3.47) with Laguerre polynomial of order 5/2 and degree $n = 0, 1, 2, \dots$ and then integrate over the phase space factor $d\Gamma_p$. Finally we obtain the following equation,

$$[C \langle p_\mu p_\nu \rangle, L_n^{5/2}(\tau) \langle p^\mu p^\nu \rangle] = \frac{mT}{n} \gamma_n. \tag{3.104}$$

where,

$$\gamma_n = -\frac{1}{\rho T^2} \int d\Gamma_p f^{(0)}(p) \{1 + f^{(0)}(p)\} L_n^{5/2}(\tau) \langle p_\mu p_\nu \rangle \langle p^\mu p^\nu \rangle. \tag{3.105}$$

Expanding C as before in terms of orthogonal Laguerre polynomial as shown below,

$$C(\tau) = \sum_{m=0}^{\infty} c_m L_m^{5/2}(\tau), \tag{3.106}$$

and putting back in the bracket term in (3.104) we obtain the following summation series,

$$\sum_{m=0}^{\infty} c_m c_{mn} = \frac{1}{\rho T} \gamma_n, \tag{3.107}$$

where $c_{mn} = \frac{1}{(mT)^2} [L_m^{5/2}(\tau) \langle p_\mu p_\nu \rangle, L_n^{5/2}(\tau) \langle p^\mu p^\nu \rangle]$ is the bracket quantity discussed earlier. Now an approximate solution of the first r coefficients of c_m of the set of equations given in (3.107) is obtained by limiting the infinite number of equations to a finite number r ,

$$\sum_{m=0}^{(r-1)} c_m^{(r)} c_{mn} = \frac{1}{\rho T} \gamma_n, \quad (n = 0, 1, 2, \dots, (r-1)). \quad (3.108)$$

Now putting the expansion of C from (3.106) into (3.53) we can obtain,

$$\begin{aligned} \eta &= -\frac{1}{10} \sum_{m=0}^{\infty} c_m \int \frac{d^3 p}{(2\pi)^3 p_0} f^{(0)}(1 + f^{(0)}) L_m^{5/2} \langle p_\mu p_\nu \rangle \langle p^\mu p^\nu \rangle \\ &= \frac{\rho T^2}{10} \sum_{m=0}^{\infty} c_m \gamma_m. \end{aligned} \quad (3.109)$$

So in the first approximation the shear viscosity is,

$$[\eta]_1 = \frac{\rho T^2}{10} c_0^{(1)} \gamma_0 = \frac{T}{10} \frac{\gamma_0^2}{c_{00}}. \quad (3.110)$$

Where we have,

$$\gamma_0 = -\frac{1}{\rho T^2} \int d\Gamma_p f^{(0)}(p) \{1 + f^{(0)}(p)\} L_0^{5/2}(\tau) \langle p_\mu p_\nu \rangle \langle p^\mu p^\nu \rangle, \quad (3.111)$$

and

$$c_{00} = \frac{1}{(mT)^2} [L_0^{5/2}(\tau) \langle p_\mu p_\nu \rangle, L_0^{5/2}(\tau) \langle p^\mu p^\nu \rangle]. \quad (3.112)$$

Evaluation of γ_0

Taking the definition of γ_n from (3.105) and using the property of Laguerre polynomial from (3.76) we obtain,

$$\gamma_n = -\frac{1}{\rho T^2} \sum_{k=0}^n \frac{(-1)^k}{k!} z^k L_{n-k}^{\frac{5}{2}+k}(-z) \Delta_{\alpha\beta\gamma\delta} u_{\nu_1 \dots \nu_k} F^{\alpha\beta\gamma\delta \nu_1 \dots \nu_k}. \quad (3.113)$$

So for γ_0 we obtain the following expressions,

$$\gamma_0 = -\frac{1}{\rho T^2} L_0^{\frac{5}{2}}(-z) \Delta_{\alpha\beta\gamma\delta} F^{\alpha\beta\gamma\delta}. \quad (3.114)$$

After doing all the contractions we obtain the value of γ_0 as,

$$\gamma_0 = -10 \frac{S_3^2}{S_2^1}. \quad (3.115)$$

Evaluation of c_{00}

From equation (3.112) the expression of c_{00} is given by,

$$\begin{aligned} c_{00} &= \frac{1}{(mT)^2} [L_0^{5/2}(\tau) \langle p_\mu p_\nu \rangle, L_0^{5/2}(\tau) \langle p^\mu p^\nu \rangle] \\ &= \frac{1}{4\rho^2 T^2} \int d\Gamma_p d\Gamma_{p'} d\Gamma_{p_1} d\Gamma_{p'_1} f^{(0)} f_1^{(0)} (1 + f'^{(0)}) (1 + f_1'^{(0)}) W(pp_1|p'p'_1) \\ &\times \delta\{L_0^{\frac{5}{2}}(\tau) \langle p_\mu p_\nu \rangle\} \delta\{L_0^{\frac{5}{2}}(\tau) \langle p^\mu p^\nu \rangle\}. \end{aligned} \quad (3.116)$$

Using the property of Laguerre polynomial from (3.76) and reducing the collision brackets using the proper geometrical choice discussed in Appendix-B we obtain,

$$c_{00} = 2I_1(z) + 2I_2(z) + \frac{2}{3}I_3(z). \quad (3.117)$$

The integrals have their usual meaning as before given in (3.88).

3.4 Appendix A-Irreducible tensors

The irreducible tensors of rank one and two is described below respectively,

$$\langle t^\mu \rangle = \Delta^{\mu\nu} t_\nu, \quad (3.118)$$

$$\langle t^{\mu\nu} \rangle = \left[\frac{1}{2} (\Delta^{\mu\alpha} \Delta^{\nu\beta} + \Delta^{\nu\alpha} \Delta^{\mu\beta}) - \frac{1}{3} \Delta^{\mu\nu} \Delta^{\alpha\beta} \right] t_{\alpha\beta}. \quad (3.119)$$

These tensors are irreducible with respect to the transformations of the little group associated with the hydrodynamic four-velocity $u^\mu(x)$, i.e. the group consisting of those Lorentz transformations Λ which leave the time-like vector u^μ invariant

$$\Lambda_{\nu}^{\mu} u^{\nu} = u^{\mu} . \quad (3.120)$$

The advantage of using irreducible tensors in kinetic theory is that it arise naturally in problems involving spherical symmetry and form a complete tensor set with minimum number of members.

3.5 Appendix B-Reduction of collision bracket

In order to reduce the collision brackets occurring in the expression of transport coefficients we define two sets of four-momenta for the binary elastic collision $p+p_1 \rightarrow p'+p'_1$ we are discussing about.

The total four-momenta is defined as,

$$P_{\mu} = p_{\mu} + p_{1\mu} = p'_{\mu} + p'_{1\mu} = P'_{\mu}, \quad (3.121)$$

and the relative four-momenta is defined as,

$$\begin{aligned} g_{\mu} &= \frac{1}{2}(p_{1\mu} - p_{\mu}) , \\ g'_{\mu} &= \frac{1}{2}(p'_{1\mu} - p'_{\mu}) . \end{aligned} \quad (3.122)$$

The four momenta corresponding to each set are mutually orthogonal to each other such that,

$$g_{\mu} P^{\mu} = g'_{\mu} P'^{\mu} = 0 . \quad (3.123)$$

Now in the local rest frame of the fluid the four vector P^{μ} is written in terms of polar coordinates as follows,

$$P^{\mu} = P(\cosh\chi, \sinh\chi\bar{e}), \quad \text{with} \quad \bar{e} = (\sin\bar{\theta}\cos\bar{\phi}, \sin\bar{\theta}\sin\bar{\phi}, \cos\bar{\theta}) . \quad (3.124)$$

The set of three spatial axes with respect to which the angles $\bar{\theta}$ and $\bar{\phi}$ are measured are defined to be fixed in the local rest frame of the fluid.

After defining P_μ the relative four vectors g_μ and g'_μ are defined with the help of another set of three vectors in the previous local rest frame in terms of the same polar angles $\bar{\theta}$ and $\bar{\phi}$,

$$\begin{aligned} \vec{e}_1 &= (\cos\bar{\theta}\cos\bar{\phi}, \cos\bar{\theta}\sin\bar{\phi}, -\sin\bar{\theta}) \\ \vec{e}_2 &= (-\sin\bar{\phi}, \cos\bar{\phi}, 0) \\ \vec{e}_3 &= (\cosh\chi\bar{e}) , \end{aligned} \quad (3.125)$$

which are orthogonal to each other and the three momenta \vec{P} also. So these three vectors form an orthogonal triad. In this frame the direction of \vec{g} with respect to (3.125) is fixed by polar angles θ and ϕ in the following way,

$$\vec{g} = g\{\vec{e}_1\sin\theta\cos\phi + \vec{e}_2\sin\theta\sin\phi + \vec{e}_3\cos\theta\}. \quad (3.126)$$

It is convenient to introduce instead of g a variable ψ such that,

$$g = m\sinh\psi. \quad (3.127)$$

From this definition it can be easily proved that,

$$P = 2m\cosh\psi. \quad (3.128)$$

In order to specify \vec{g}' we define another set of three vectors in the centre of mass frame of the collision as follows,

$$\begin{aligned} \hat{E}_1 &= \hat{e}_1\cos\theta\cos\phi + \hat{e}_2\cos\theta\sin\phi - \hat{e}_3\sin\theta \\ \hat{E}_2 &= -\hat{e}_1\sin\phi + \hat{e}_2\cos\phi \\ \hat{E}_3 &= \frac{\vec{g}}{g} . \end{aligned} \quad (3.129)$$

These three vectors also form an orthogonal triad with the polar axis parallel to \vec{g} . The direction of \vec{g}' in this set is determined by the polar angles Θ and Φ as follows

$$\frac{\vec{g}'}{g} = \hat{E}_1\sin\Theta\cos\Phi + \hat{E}_2\sin\Theta\sin\Phi + \hat{E}_3\cos\Theta. \quad (3.130)$$

With this prescription it comes out that

$$\frac{\vec{g} \cdot \vec{g}'}{g^2} = \cos\Theta, \quad (3.131)$$

defining Θ as the scattering angle in the centre of mass system of collision. Now with the help of these polar coordinates introduced so far six variables of \vec{p} and \vec{p}_1 can be expressed with the help of other six variables, namely P^μ, θ and ϕ in the following way,

$$\frac{d^3p}{p^0} \frac{d^3p_1}{p_1^0} = 8m^4 (\sinh\chi \cosh\psi \sinh\psi)^2 \sin\theta \sin\bar{\theta} d\theta d\bar{\theta} d\phi d\bar{\phi} d\psi d\chi. \quad (3.132)$$

Analogously it can be proved,

$$\frac{d^3p'}{p'^0} \frac{d^3p_1}{p_1^0} = \frac{1}{2} \tanh\psi d^4P' \sin\Theta d\Theta d\Phi. \quad (3.133)$$

Putting all these together we obtain the expression of collision bracket as,

$$\int FW(pp_1|p'p'_1) \frac{d^3p}{(2\pi)^3 p^0} \frac{d^3p_1}{(2\pi)^3 p_1^0} \frac{d^3p'}{(2\pi)^3 p'^0} \frac{d^3p'_1}{(2\pi)^3 p_1'^0} = \frac{2m^6}{\pi^4} \int F \frac{d\sigma}{d\Omega}(\psi, \Theta) \sinh^2\chi (\sinh\psi \cosh\psi)^3 \sin\theta \sin\Theta d\chi d\psi d\theta d\Theta d\Phi, \quad (3.134)$$

where $F = f^{(0)} f_1^{(0)} (1 + f'^{(0)}) (1 + f_1'^{(0)}) \{G(p) + G(p_1) - G(p') - G(p'_1)\} \{H(p) + H(p_1) - H(p') - H(p'_1)\}$.

3.6 Appendix C-Reduction of the product of distribution functions

Utilizing the above coordinate systems defined in Appendix-B we can reduce the product of distribution functions as follows,

$$f^{(0)} f_1^{(0)} (1 + f'^{(0)}) (1 + f_1'^{(0)}) = \frac{e^{-\frac{2\mu}{T}} e^{2z \cosh\psi \cosh\chi}}{(e^E - 1)(e^F - 1)(e^G - 1)(e^H - 1)}, \quad (3.135)$$

with

$$\begin{aligned}
E &= z(\cosh \psi \cosh \chi - \sinh \psi \sinh \chi \cos \theta) - \frac{\mu}{T}, \\
F &= z(\cosh \psi \cosh \chi - \sinh \psi \sinh \chi \cos \theta') - \frac{\mu}{T}, \\
G &= E + 2z \sinh \psi \sinh \chi \cos \theta, \\
H &= F + 2z \sinh \psi \sinh \chi \cos \theta'.
\end{aligned} \tag{3.136}$$

The relative angle θ' is defined by, $\cos \theta' = \cos \theta \cos \Theta - \sin \theta \sin \Theta \cos \Phi$.

Bibliography

- [1] W. A. Van Leeuwen, P. H. Polak and S. R. De Groot, “On Relativistic Kinetic Gas Theory-IX: Transport coefficients for systems of particles with arbitrary interaction”, *Physica* **66**, 455 (1973).
- [2] S. Weinberg, “Entropy generation and the survival of protogalaxies in an expanding universe,” *Astrophys. J.* **168** (1971) 175.
- [3] P. Chakraborty and J. I. Kapusta, “Quasi-Particle Theory of Shear and Bulk Viscosities of Hadronic Matter,” *Phys. Rev. C* **83** (2011) 014906.

Chapter 4

Evaluation of relaxation times of the dissipative flows

It is well established from the experimental data available from the high energy nucleus nucleus collisions that the created matter behaves more like a strongly interacting liquid than a weakly interacting gas. Then on it is realized that the created matter undergoes dissipative processes on its way to space time evolution and hence requires a non-ideal theory to describe its kinematics. The first order theories of dissipative fluid dynamics are derived by Eckart [1] and by Landau and Lifshitz [2] by introducing different definitions of the hydrodynamic four-velocity as discussed in Chapter-2. The theories are based on the assumption that the entropy four-current contains terms up to the linear order in dissipative fluxes and hence they are referred to as the first order theories of dissipative fluids. Consequently these theories produce linear relationship between thermodynamic fluxes and forces where the first order transport coefficients such as bulk viscosity, thermal conductivity and shear viscosity appear as the proportionality constants. But the first order theory results in parabolic equations of motion of the thermodynamic state variables leading to severe causality violation problem. This crisis requires the introduction of a second order theory which provides hyperbolic equations of motion resulting in finite time scale for the thermodynamic flows to dissipate. The second order theory is based on the assumption that the entropy four-current includes quadratic terms in the dissipative

fluxes and the space of the thermodynamic quantities is expanded to include the dissipative quantities for the system under consideration. Thus in this case the dissipative quantities are treated as thermodynamic variables in their own right. Moreover the equations of motion of the thermodynamic macroscopic variables along with the dissipative quantities in the second order theory determine the hydrodynamic evolution of the system. The relaxation times of the corresponding flows play an important role to determine the rate of evolution of the system with time and consequently yield the cooling rate of the system. Those hyperbolic equations can be estimated from second law of thermodynamics as well as from kinetic theory where the relaxation times of different flows appear to bear important contribution to the evolution of the hydrodynamic quantities. Consequently they play an important role to set the temperature profile, i.e, the cooling law of the system. Hence it is important to evaluate these quantities as accurately as possible so that they usefully determine the nature of evolution of the thermodynamic quantities when the system under consideration expands and cools down. Kinetic theory provides us the tool to evaluate the relaxation times explicitly in which the first order transport coefficients go as an input. In this chapter the relaxation times corresponding to viscous and thermal flows for an interacting pion gas system have been evaluated. Previously in [4] the cooling law has been depicted for a relativistic QGP as well as hadronic system, where the relaxation times have been constructed from constant values of transport coefficients as inputs. In [5] those quantities have been evaluated using conformal quantum field theory for strongly coupled system. There are few other estimations of the temperature dependence of relaxation times available in the literature. In [6] those quantities have been evaluated with constant cross sections. In [7, 8] the temperature dependence of the relaxation times has been estimated with a parameterized cross section which was independent of temperature. The temperature dependence in these cases only enters through the explicit temperature containing terms along with the phase space parts. In our estimation we have taken a medium dependent interaction cross section evaluated at finite temperature to provide a more realistic estimation of the relaxation times of dissipative flows. In next few sections we will provide the necessary tools to determine the relaxation times of viscous and thermal flows of an interacting pion gas at finite temperature taking care of the early chemical freeze out.

4.1 Conservation laws and equations of motions in dissipative fluid dynamics

To describe a fluid system with the help of dissipative thermodynamics first we need to introduce some macroscopic quantities, which specify the dynamical properties of the system under consideration. We start with the particle 4-flow $N_\mu(x) = nu_\mu$, where n is the particle number density and u^μ is hydrodynamic 4-velocity, for which we use Eckart's definition. Next we define the energy-momentum stress tensor $T^{\mu\nu}$ for a dissipative fluid which consists of an ideal and a dissipative part respectively in the following way,

$$T^{\mu\nu} = T^{(0)\mu\nu} + T^{(1)\mu\nu}, \quad \text{with } T^{(0)\mu\nu} = enu^\mu u^\nu - P\Delta^{\mu\nu} \quad \text{and } T^{(1)\mu\nu} = (I_q^\mu u^\nu + I_q^\nu u^\mu) + \Pi^{\mu\nu}. \quad (4.1)$$

Here I_q^μ is the irreversible heat flow and $\Pi^{\mu\nu}$ is viscous pressure tensor. Following the summation invariant technique in the transport equation we obtain the conservation of particle 4-flow and conservation of energy-momentum respectively by the following equations.

$$\partial_\mu N^\mu(x) = 0 \quad (4.2)$$

$$\partial_\mu T^{\mu\nu} = 0 \quad (4.3)$$

From (4.2) we can obtain the equation of motion for particle number density which is known as continuity equation,

$$Dn = -n\partial \cdot u. \quad (4.4)$$

Contracting equation (4.3) respectively with the hydrodynamic velocity u^μ and the projection operator $\Delta^{\mu\nu} = g^{\mu\nu} - u^\mu u^\nu$ we get the equation of energy,

$$nDe = -P\partial \cdot u - \nabla_\nu I_q^\nu, \quad (4.5)$$

and equation of motion,

$$hnDu^\mu = \nabla^\mu P - \Delta_\nu^\mu \nabla_\sigma \Pi^{\nu\sigma} - \Delta_\nu^\mu DI_q^\nu. \quad (4.6)$$

In all the above cases it has been assumed that the gradients of the primary macroscopic variables may be treated as small quantities with respect to the dissipative fluxes. Using

equation of energy (4.5) and implementing the relativistic Gibbs-Duhem relationship $\partial^\sigma P = nT\partial^\sigma\{\frac{\mu}{T}\} + nhT^{-1}\partial^\sigma T$, we obtain the equation of enthalpy,

$$Dh = TD\{\frac{\mu}{T}\} + hT^{-1}DT - \frac{1}{n}\nabla_\nu I_q^\nu. \quad (4.7)$$

With the help of equation of energy (4.5) and equation of enthalpy (4.7) we finally obtain the equation of temperature and chemical potential,

$$T^{-1}DT = (1 - \gamma')[\partial \cdot u + \frac{\delta}{P}\nabla_\nu I_q^\nu], \quad (4.8)$$

$$TD\{\frac{\mu}{T}\} = \{(\gamma'' - 1)h - \gamma'''T\}[\partial \cdot u + \frac{\delta}{P}\nabla_\nu I_q^\nu] - \frac{\delta'}{n}\nabla_\nu I_q^\nu. \quad (4.9)$$

The quantities have been used in the above expressions are given as,

$$\gamma' = \frac{(S_2^0/S_2^1)^2 - (S_3^0/S_2^1)^2 + 4z^{-1}S_2^0S_3^1/(S_2^1)^2 + z^{-1}S_3^0/S_2^1}{(S_2^0/S_2^1)^2 - (S_3^0/S_2^1)^2 + 3z^{-1}S_2^0S_3^1/(S_2^1)^2 + 2z^{-1}S_3^0/S_2^1 - z^{-2}} \quad (4.10)$$

$$\gamma'' = 1 + \frac{z^{-2}}{(S_2^0/S_2^1)^2 - (S_3^0/S_2^1)^2 + 3z^{-1}S_2^0S_3^1/(S_2^1)^2 + 2z^{-1}S_3^0/S_2^1 - z^{-2}} \quad (4.11)$$

$$\gamma''' = \frac{S_2^0/S_2^1 + 5z^{-1}S_3^1/S_2^1 - S_3^0S_3^1/(S_2^1)^2}{(S_2^0/S_2^1)^2 - (S_3^0/S_2^1)^2 + 3z^{-1}S_2^0S_3^1/(S_2^1)^2 + 2z^{-1}S_3^0/S_2^1 - z^{-2}} \quad (4.12)$$

$$\delta = \frac{S_2^2S_2^0/(S_2^1)^2}{1 - z\{S_3^0S_2^1 - S_3^1S_2^0\}/(S_2^1)^2} \quad (4.13)$$

$$\delta' = \frac{-1}{1 - z\{S_3^0S_2^1 - S_3^1S_2^0\}/(S_2^1)^2} \quad (4.14)$$

with $z = m_\pi/T$ and $h = m_\pi S_3^1/S_2^1$. The terms S_n^α are defined in Chapter-2.

From the above set of equations it is observed that the contribution of transport quantities (thermodynamic fluxes) may not affect the thermodynamic macroscopic quantities much, but the rate of transport of those dissipative quantities affects the conservation laws in a significant way. In a first order theory the dissipative terms are neglected considering them small in a near equilibrium situation. In second order theory all the dissipative quantities are included in the equations of motion and conservation laws. Hence in second order theory those dissipative fluxes are treated as thermodynamic variables in their own right as mentioned earlier.

4.2 The need of a second order theory - Limitations of the first order theory

A first order theory is one in which the rate of change of entropy 4-current, s^α is linearly dependent on dissipative fluxes in the following way.

$$T\partial_\mu s^\mu = I_q^\mu \left\{ \frac{1}{T} \nabla^\mu T - Du^\mu \right\} + \Pi^{\mu\nu} \langle \nabla_\mu u_\nu \rangle + \Pi \nabla_\mu u^\mu. \quad (4.15)$$

So in first order theory the relationship between the thermodynamic flux and the corresponding thermodynamic forces are expressed as linear laws depicted by the following two equations, where the viscous pressure tensor and the heat flow are linearly dependent on the velocity and temperature gradients respectively.

$$\Pi^{\mu\nu} = 2\eta \langle \partial^\mu u^\nu \rangle + \zeta \Delta^{\mu\nu} \partial_\sigma u^\sigma \quad (4.16)$$

$$I^{\mu\nu} = \lambda (\partial_\sigma T - T Du_\sigma) \Delta^{\mu\sigma}. \quad (4.17)$$

The proportionality constants η , ζ and λ serve as the shear and bulk viscous coefficients and the thermal conductivity respectively.

If we proceed to solve for the hydrodynamic velocity u^μ from equation (4.6) with the help of equation (4.16), then only considering the shear flow we will eventually obtain the following equation satisfied by u^μ ,

$$Du^\mu + \frac{2\eta}{hn} [\nabla_\sigma \nabla^\mu u^\sigma + \nabla_\sigma \nabla^\sigma u^\mu - \frac{2}{3} \nabla^\mu \nabla^\sigma u_\sigma] = \frac{\nabla^\mu P}{hn}. \quad (4.18)$$

Equation (4.18) is a parabolic partial differential equation which is similar to the 1-dimensional heat flow equation, $\frac{\partial T}{\partial t} = k \nabla^2 T$. So the equation of motion depicted in (4.18) is clearly a parabolic equation. Its non-causal behavior can be easily visualized by taking a look that how the signal propagates in an infinite one-dimensional medium. Assuming that the velocity is

zero for $t < 0$, and putting a source at $x = x_0$ at $t = 0$, the three velocity of the system takes the following profile for $t > 0$,

$$v \propto \frac{1}{\sqrt{t}} \exp\left[-\frac{(x - x_0)^2}{t}\right]. \quad (4.19)$$

This implies that for $t = 0$, $v(x) = \delta(x - x_0)$ and for $t > 0$, $v(x)$ has a non-zero finite value for all values of x . So it can be said that the presence of a source at x_0 is instantaneously felt everywhere, no matter how far away the spatial coordinate be from x_0 . It means that the momentum transfer starts taking place simultaneously everywhere with the appearance of the velocity gradient and vanishes instantaneously with the disappearance of the velocity gradient. Similar case may arise if equation (4.17) is inserted into (4.9) to obtain the profile of temperature which similarly turns out to be felt everywhere instantaneously with the ignition of heat flow. This implies that the thermodynamic energy-momentum as well as the heat flux propagates within the medium with infinite speed, giving rise to vanishing relaxation times to restore back its equilibrium situation. This undesirable feature certainly violates causality demanding a second order theory where explicit time derivative occurs over the flows in the equation of motion along with the linear term to make it a hyperbolic theory which describes propagation of thermodynamic fluxes with finite speed. In the next section we will derive those causal equations of motion of the thermodynamic fluxes along with their explicit values of relaxation times in kinetic theory approach. The technical tool we have opted for this purpose is the Grad's 14 moment method.

4.3 Evaluation of relaxation times - Grad's 14 moment method

4.3.1 Solving the transport equation

We start with the evolution of the phase space distribution of the pion which is governed by the relativistic transport equation given by,

$$p^\mu \partial_\mu f(x, p) = C[f]. \quad (4.20)$$

Here the term $C[f]$ is the same collision integral mentioned in Chapter-3 for the binary elastic collisions $p + k \rightarrow p' + k'$.

The basic idea of the moment method is to obtain an approximate solution of the transport equation (4.20) by expanding the distribution function $f(x, p)$ in momentum space around its local equilibrium value when the deviation from it is small. In such a situation the out of equilibrium distribution function can be expressed with the help of a deviation function ϕ in the following manner,

$$f(x, p) = f^{(0)}(x, p)[1 + \phi(x, p)], \quad (4.21)$$

where the equilibrium distribution function is given by

$$f^{(0)}(x, p) = \left[e^{\frac{p^\mu u_\mu(x) - \mu_\pi(x)}{T(x)}} - 1 \right]^{-1}, \quad (4.22)$$

with $T(x)$, $u_\mu(x)$ and $\mu_\pi(x)$ representing the local temperature, flow velocity and chemical potential respectively. Note that the metric $diag(1, -1, -1, -1)$ is used. Also, we take $u_\mu u^\mu = 1$ where $u_\mu = (1, \vec{0})$ in the local rest frame.

Now we proceed to solve the transport equation (4.20) with the help of the out of equilibrium distribution function (4.21). Unlike the first order case we should not neglect the term containing derivative over ϕ , because though in a near equilibrium situation the deviation function ϕ is a small quantify, its deviation over time and space may not be that small to ignore and should be incorporated in a second order theory. Following this argument and considering that

ϕ is sufficiently small than f_0 the transport equation (4.20) turns out to be,

$$p_\mu \partial^\mu f^{(0)} + f^{(0)}(1 + f^{(0)})p_\mu \partial^\mu \phi = -\mathcal{L}[\phi], \quad (4.23)$$

where the linearized collision term is given by,

$$\begin{aligned} \mathcal{L}[\phi] = & f^{(0)}(x, p) \int d\Gamma_k d\Gamma_{p'} d\Gamma_{k'} f^{(0)}(x, k) \{1 + f^{(0)}(x, p')\} \{1 + f^{(0)}(x, k')\} \\ & [\phi(x, p) + \phi(x, k) - \phi(x, p') - \phi(x, k')] W, \end{aligned} \quad (4.24)$$

where $d\Gamma_q$ is the phase-space factors defined in Chapter-3. In order to solve equation (4.23) we will require some thermodynamic identities in form of equations of motion. Using the equations of motions discussed in section-4.1, we observe that the first term on the left hand side of (4.23) turns out to be,

$$\begin{aligned} \Pi^\mu \partial_\mu f^{(0)} = & f^{(0)}(1 + f^{(0)}) \left[(\tau - \hat{h}) \Pi_\alpha \frac{\nabla^\alpha T}{T} + \frac{1}{Tn} \Pi_\alpha \nabla^\alpha P - \langle \Pi_\mu \Pi_\nu \rangle \langle \nabla^\mu u^\nu \rangle - \tau \Pi_\mu D u^\mu + \hat{Q} \partial \cdot u \right. \\ & \left. + \tau [\{\tau(1 - \gamma') + (\gamma'' - 1)\hat{h} - \gamma'''\} \frac{\delta}{P} \nabla_\alpha I_q^\alpha - \frac{\delta'}{nT} \nabla_\alpha I_q^\alpha] \right] \end{aligned} \quad (4.25)$$

with $\Pi^\mu = \frac{p^\mu}{T}$ and $\hat{Q} = \frac{1}{T^2} Q$, where, $Q = -\frac{1}{3} m_\pi^2 + (p \cdot u)^2 \{\frac{4}{3} - \gamma'\} + (p \cdot u) \{(\gamma'' - 1)h - \gamma'''T\}$.

We have also defined reduced enthalpy per particle as, $\hat{h} = h/T$.

For the rest of the two terms we need to define the deviation function ϕ and its derivatives. Since the distribution function is a scalar depending on the particle momentum p^μ and the space-time coordinate x^μ , the deviation function should be the same and it may be expressed as a sum of scalar products of tensors formed from p^μ and tensors functions of x^μ . Following the argument ϕ is constructed on the basis of irreducible tensors in the following way,

$$\phi(x, p) = A(x, \tau) - B_\mu(x, \tau) \langle \Pi^\mu \rangle + C_{\mu\nu}(x, \tau) \langle \Pi^\mu \Pi^\nu \rangle. \quad (4.26)$$

The notation $\langle \rangle$ denotes the irreducible tensors defined as $\langle \Pi^\mu \rangle \equiv \Delta^{\mu\nu} \Pi_\nu$ and $\langle \Pi^\mu \Pi^\nu \rangle \equiv [\frac{1}{2}(\Delta^{\mu\alpha} \Delta^{\nu\beta} + \Delta^{\nu\alpha} \Delta^{\mu\beta}) - \frac{1}{3} \Delta^{\mu\nu} \Delta^{\alpha\beta}] \Pi_{\alpha\beta}$. So now we can say that instead of only first five moments of the first order theory (number density, energy density and hydrodynamic velocity) now the distribution function is developed from 14 moments where the additional 9 moments are contributing from the dissipative quantities I^μ and $\Pi^{\mu\nu}$.

Now the coefficient functions are further expanded in terms of τ in the following manner such that the last power being the one which gives a non-zero contribution to the collision term,

$$A(x, \tau) = A_0(x) + A_1(x)\tau + A_2(x)\tau^2 = \sum_{s=0}^2 A_s(x)\tau^s, \quad (4.27)$$

$$B_\mu(x, \tau) = B_{0\mu}(x) + B_{1\tau}(x)\tau = \sum_{s=0}^1 (B_s)_\mu(x)\tau^s, \quad (4.28)$$

$$C_{\mu\nu}(x, \tau) = (C_0)_{\mu\nu}(x). \quad (4.29)$$

4.3.2 Determination of the coefficients A , B_μ and $C_{\mu\nu}$

Our next task is to put the expression of ϕ into (4.23) to obtain the respective equation of motions for the fluxes. For this purpose we first need to evaluate the unknown coefficient A , B and C . For our present purpose it is convenient to express them in terms of the thermodynamic fluxes. For this purpose we need to recall the definitions of bulk and shear viscous pressure as well as the heat flow from Chapter-3.

The bulk viscous pressure is defined as,

$$\Pi = \frac{1}{3} \int \frac{d^3p}{(2\pi)^3 p^0} \Delta_{\mu\nu} p^\mu p^\nu f^{(0)} (1 + f^{(0)}) \phi. \quad (4.30)$$

After substituting the expression of ϕ from (4.26) it takes the form,

$$\Pi = -A_2 \int \frac{d^3p}{(2\pi)^3 p^0} Q \tau^2 f^{(0)} (1 + f^{(0)}). \quad (4.31)$$

The terms consisting of A_0 and A_1 vanishes due to the properties of summation invariant. Now we define a quantity called α_n for our convenience in the following manner,

$$\alpha_n = -\frac{1}{nT} \int \frac{d^3p}{(2\pi)^3 p^0} f^{(0)} (1 + f^{(0)}) Q \tau^n. \quad (4.32)$$

From the definition of α_n , equation (4.31) can be expressed in terms of A_2 in the following way

$$\Pi = nT \alpha_2 A_2. \quad (4.33)$$

Similarly the energy 4-flow is defined as,

$$I_q^\mu = \int \frac{d^3p}{(2\pi)^3 p^0} p^\sigma \Delta_\sigma^\mu (p \cdot u - h) f^{(0)} (1 + f^{(0)}) \phi. \quad (4.34)$$

After substituting the expression of ϕ it takes the form,

$$I_q^\mu = -T^2 (B_{1\nu}) \int \frac{d^3p}{(2\pi)^3 p^0} \Pi^\sigma \Delta_\sigma^\mu (\tau - \hat{h}) \tau \langle \Pi^\nu \rangle f^{(0)} (1 + f^{(0)}). \quad (4.35)$$

Now from the definition of $\beta_n = -\frac{1}{Tn} \int \frac{d^3p}{(2\pi)^3 p^0} f^{(0)} (1 + f^{(0)}) \tau^n (\tau - \hat{h}) \Delta^{\mu\nu} p_\mu p_\nu$, we obtain the heat flow in terms of the vector $B_{1\mu}$ such as,

$$I_q^\mu = \frac{1}{3} n T B_{1\nu} \Delta^{\mu\nu} \beta_1. \quad (4.36)$$

Finally the traceless part of the viscous pressure tensor is defined as,

$$\langle \Pi^{\mu\nu} \rangle = \int \frac{d^3p}{(2\pi)^3 p^0} (\Delta_\sigma^\mu \Delta_\tau^\nu - \frac{1}{3} \Delta_{\sigma\tau} \Delta^{\mu\nu}) p^\sigma p^\tau f^{(0)} (1 + f^{(0)}) \phi. \quad (4.37)$$

After substituting the expression of ϕ it takes the form,

$$\langle \Pi^{\mu\nu} \rangle = -\frac{\rho \gamma_0}{5} \langle C^{\mu\nu} \rangle, \quad (4.38)$$

where we have introduced $\gamma_n = -\frac{1}{\rho T^2} \int \frac{d^3p}{(2\pi)^3 p^0} f^{(0)} (1 + f^{(0)}) \tau^n \langle p_\mu p_\nu \rangle \langle p^\mu p^\nu \rangle$.

Now from the fact that the number density of the particles, the corresponding energy density and the hydrodynamic 4-velocity can be completely determined by the equilibrium distribution function, we can set constraint equations between the coefficient functions A and B .

The zeroth order distribution function contains some arbitrary parameters which is identified with some macroscopic quantities such as number densities, energy densities and hydrodynamic 4-velocity of the system. This means the number density of particles, the corresponding energy density and the hydrodynamic velocity can be completely determined by the equilibrium distribution function in the following way,

$$n = g \int \frac{d^3p}{(2\pi)^3 p^0} p^\mu u_\mu f = g \int \frac{d^3p}{(2\pi)^3 p^0} p^\mu u_\mu f^{(0)}, \quad (4.39)$$

$$en = g \int \frac{d^3p}{(2\pi)^3 p^0} (p^\mu u_\mu)^2 f = g \int \frac{d^3p}{(2\pi)^3 p^0} (p^\mu u_\mu)^2 f^{(0)}, \quad (4.40)$$

where g is the degeneracy of the system. Furthermore from Eckart's definition of velocity we get,

$$\Delta^{\mu\nu} N_\nu = \int \frac{d^3p}{(2\pi)^3 p^0} \Delta^{\mu\nu} p_\nu f^{(0)} = 0 . \quad (4.41)$$

From the above three equations we obtain the following set of constraint equations on ϕ

$$\int \frac{d^3p}{(2\pi)^3 p^0} p^\mu u_\mu f^{(0)} (1 + f^{(0)}) \phi = 0, \quad (4.42)$$

$$\int \frac{d^3p}{(2\pi)^3 p^0} (p^\mu u_\mu)^2 f^{(0)} (1 + f^{(0)}) \phi = 0, \quad (4.43)$$

$$\int \frac{d^3p}{(2\pi)^3 p^0} \langle p^\mu \rangle f^{(0)} (1 + f^{(0)}) \phi = 0, \quad (4.44)$$

which on substituting the expression of ϕ gives the three following equations.

$$\int \frac{d^3p}{(2\pi)^3 p^0} \tau A(x, \tau) f^{(0)} (1 + f^{(0)}) = 0, \quad (4.45)$$

$$\int \frac{d^3p}{(2\pi)^3 p^0} \tau^2 A(x, \tau) f^{(0)} (1 + f^{(0)}) = 0, \quad (4.46)$$

$$\int \frac{d^3p}{(2\pi)^3 p^0} \langle \Pi^\mu \rangle B_\nu(x, \tau) \langle \Pi^\nu \rangle f^{(0)} (1 + f^{(0)}) = 0. \quad (4.47)$$

Here we have used the properties of the irreducible tensors that the inner product of any power of τ with an irreducible tensor or the inner product of two irreducible tensors with different ranks vanishes.

Expanding the coefficients A and B_μ according to equations (4.28) and (4.29), finally we obtain the following equations.

The coefficient A follow the equations,

$$a_1 A_0 + a_2 A_1 + a_3 A_2 = 0, \quad (4.48)$$

$$a_2 A_0 + a_3 A_1 + a_4 A_2 = 0, \quad (4.49)$$

with $a_n = \int \frac{d^3p}{(2\pi)^3 p^0} f^{(0)} (1 + f^{(0)}) \tau^n$. Similarly the equation of constrain between the coefficient B_μ is,

$$B_\nu^0 \Delta^{\mu\nu} b_0 + B_\nu^1 \Delta^{\mu\nu} b_1 = 0, \quad (4.50)$$

with $\Delta^{\mu\nu}b_n = \int \frac{d^3p}{(2\pi)^3p^0} f^{(0)}(1 + f^{(0)})\tau^n \langle \Pi_\mu \rangle \langle \Pi^\nu \rangle$.

Using equations (4.33,4.36,4.38,4.48,4.49,4.50) we obtain the complete set of coefficient functions in terms of the thermodynamic flows. These are given by

$$A_0 = \frac{(a_2a_4 - a_3^2)}{(a_1a_3 - a_2^2)} \frac{\Pi}{nT\alpha_2} \quad (4.51)$$

$$A_1 = \frac{(a_1a_4 - a_2a_3)}{(a_2^2 - a_1a_3)} \frac{\Pi}{nT\alpha_2} \quad (4.52)$$

$$A_2 = \frac{\Pi}{nT\alpha_2} \quad (4.53)$$

$$B_{0\nu} = \frac{I_q^\mu \Delta^{\mu\nu}}{nT\beta_1} \left(-\frac{b_1}{b_0}\right) \quad (4.54)$$

$$B_{1\nu} = \frac{I_q^\mu \Delta^{\mu\nu}}{nT\beta_1} \quad (4.55)$$

$$\langle (C_0)^{\mu\nu} \rangle = -\frac{5}{\rho\gamma_0} \langle \Pi^{\mu\nu} \rangle. \quad (4.56)$$

Defining all the space-time dependent coefficients of equation (4.26) in terms of the known functions it is now possible to specify the deviation function ϕ completely. Knowing ϕ , we now go back and use it in the Boltzmann equation (4.23) to evaluate the equations of motion for the dissipative fluxes.

4.3.3 Equation of motion of dissipative fluxes

Bulk viscous pressure equation

Taking inner product of both sides of equation (4.23) with τ^2 and applying the (inner product) properties of irreducible tensors [9] we obtain the equation of motion for bulk viscous pressure equation,

$$\begin{aligned} \Pi = \zeta [& \nabla_\mu u^\mu - \frac{1}{n^2\alpha_2^2} \left\{ \frac{a_3^3 - 2a_2a_3a_4 + a_1a_4^2}{a_2^2 - a_1a_3} + a_5 \right\} D\Pi \\ & - \frac{1}{n^2\alpha_2} \left\{ \frac{3}{\beta_1} \left(\frac{b_1b_2}{b_0} - b_3 \right) + (1 - \gamma') \delta \left(\frac{S_2^1}{S_2^2} \right) a_4 \right. \\ & \left. + \{ (\hat{h}(\gamma'' - 1) - \gamma''') \delta \left(\frac{S_2^1}{S_2^2} \right) - \delta' \} a_3 \right\} \nabla_\mu I_q^\mu] . \end{aligned} \quad (4.57)$$

Retaining only the first term on the right hand side of (4.57) the equation for the bulk viscous pressure reduces to the same in the first order theory of dissipative fluids. Following the usual convention we have defined the coefficient of this term as the bulk viscous coefficient ζ .

Note that the equation (4.57) is indeed hyperbolic and contains a time derivative of the bulk viscous pressure. This yields a relaxation time for bulk viscous pressure given by,

$$\tau_\zeta = \zeta \frac{1}{n^2 \alpha_2^2} \left[\frac{a_3^3 - 2a_2 a_3 a_4 + a_1 a_4^2}{a_2^2 - a_1 a_3} + a_5 \right], \quad (4.58)$$

with

$$\begin{aligned} a_1 &= \frac{n}{T} \left\{ \frac{S_2^0}{S_1^1} \right\}, \\ a_2 &= \frac{n}{T} \left\{ z \frac{S_3^0}{S_2^1} - 1 \right\}, \\ a_3 &= \frac{n}{T} z^2 \left\{ \frac{S_2^0}{S_1^1} + 3z^{-1} \frac{S_3^1}{S_2^1} \right\}, \\ a_4 &= \frac{n}{T} z^3 \left\{ 15z^{-2} \frac{S_3^2}{S_2^1} + 2z^{-1} + \frac{S_3^0}{S_2^1} \right\}, \\ a_5 &= \frac{n}{T} z^4 \left[6z^{-1} \left\{ \frac{S_3^1}{S_2^1} + 15z^{-2} \frac{S_3^3}{S_2^1} \right\} + \left\{ \frac{S_2^0}{S_1^1} + 15z^{-2} \frac{S_2^2}{S_1^1} \right\} \right]. \end{aligned} \quad (4.59)$$

$$\begin{aligned} \alpha_2 &= z^3 \left[\frac{1}{3} \left(\frac{S_3^0}{S_2^1} - z^{-1} \right) + \left(\frac{S_2^0}{S_2^1} + \frac{3}{z} \frac{S_3^1}{S_2^1} \right) \left\{ (1 - \gamma'') \frac{S_3^1}{S_2^1} + \gamma''' z^{-1} \right\} \right. \\ &\quad \left. - \left(\frac{4}{3} - \gamma' \right) \left\{ \frac{S_3^0}{S_2^1} + 15z^{-2} \frac{S_3^2}{S_2^1} + 2z^{-1} \right\} \right]. \end{aligned} \quad (4.60)$$

Heat flow equation

In this case we take the inner product of both sides of equation (4.23) with $\langle \Pi^\mu \rangle \tau$. Following similar techniques as above we get the equation for heat flow,

$$I_q^\mu = T \lambda \left[\left\{ \frac{\nabla^\mu T}{T} - \frac{\nabla^\mu P}{nh} \right\} - \frac{1}{nT} \left\{ \beta'' D I_q^\mu + \gamma'' \nabla_\nu \langle \Pi^{\mu\nu} \rangle + \alpha'' \nabla^\mu \Pi \right\} \right], \quad (4.61)$$

with

$$\beta'' = -\frac{1}{\beta_1} \left\{ \frac{9T}{n\beta_1} \left(b_3 - \frac{b_1 b_2}{b_0} \right) - \frac{3T b_2}{n \hat{h}} \right\}, \quad (4.62)$$

$$\gamma'' = \frac{1}{\beta_1} \left\{ \frac{\gamma_1}{\gamma_0} + \frac{3T b_2}{n \hat{h}} \right\}, \quad (4.63)$$

$$\alpha'' = \frac{3T}{n} \frac{1}{\beta_1} \left[\frac{1}{\alpha_2} \left\{ b_1 \frac{a_2 a_4 - a_3^2}{a_1 a_3 - a_2^2} + b_2 \frac{a_1 a_4 - a_2 a_3}{a_2^2 - a_1 a_3} + b_3 \right\} + \frac{b_2}{\hat{h}} \right]. \quad (4.64)$$

The thermal conductivity appears as the coefficient of the linear term on right hand side of (4.61).

So from the above equation the relaxation time for heat flow is given by,

$$\tau_\lambda = \lambda T \frac{1}{nT} \beta'', \quad (4.65)$$

with

$$\begin{aligned} b_0 &= - \frac{n}{T}, \\ b_1 &= - \frac{n}{T} z \frac{S_3^1}{S_2^1}, \\ b_2 &= - \frac{n}{T} \left\{ 5z \frac{S_3^2}{S_2^1} + z^2 \right\}, \\ b_3 &= - \frac{n}{T} \left\{ 30z \frac{S_3^3}{S_2^1} + 5z^2 \frac{S_2^2}{S_2^1} + z^3 \frac{S_3^1}{S_2^1} \right\}. \end{aligned} \quad (4.66)$$

$$\beta_1 = 3z^2 \left[1 + 5z^{-1} \frac{S_3^2}{S_2^1} - \left(\frac{S_3^1}{S_2^1} \right)^2 \right]. \quad (4.67)$$

Shear viscous pressure equation

Multiplying both sides of equation (4.23) with $\langle \Pi^\mu \Pi^\nu \rangle$ and using the similar technique as before produces the equation of motion for shear viscous pressure and it is given by,

$$\langle \Pi^{\mu\nu} \rangle = \eta \left[2 \langle \nabla^\mu u^\nu \rangle - \frac{1}{nT} \left\{ \gamma''' D \langle \Pi^{\mu\nu} \rangle - \beta''' \nabla^\mu I_q^\nu \right\} \right], \quad (4.68)$$

with

$$\gamma''' = \frac{z^2[\frac{S_2^2}{S_1^2} + 6z^{-1}\frac{S_3^3}{S_2^2}]}{[z\frac{S_3^2}{S_2^2}]^2}, \quad (4.69)$$

$$\beta''' = \frac{6}{\beta_1}[\hat{h} - (6\frac{S_3^3}{S_2^2} + z\frac{S_2^2}{S_3^2})]. \quad (4.70)$$

The coefficient of shear viscosity can be followed from the first term of the right hand side of equation (4.68).

From (4.68) the relaxation time for shear viscous pressure is obtained as,

$$\tau_\eta = \eta \frac{1}{nT} \gamma'''. \quad (4.71)$$

Bibliography

- [1] C. Eckart Phys. Rev. **58**, 919 (1940).
- [2] L.D. Landau and E.M. Lifshitz, Fluid Mechanics (Elsevier, Amsterdam,1987).
- [3] M. Luzum and P. Romatschke Phys. Rev. **C 78**, 034915 (2008).
- [4] A. Muronga Phys. Rev. **Lett 88**, 6 (2002).
- [5] P. Romatchke IJMPE**19**,1-53, (2010).
- [6] S. Gavin, Nucl. Phys. A **435** (1985) 826.
- [7] M. Prakash, M. Prakash, R. Venugopalan and G. Welke, Phys. Rept. **227** (1993) 321.
- [8] D. Davesne, Phys. Rev. C **53**, 3069 (1996).
- [9] S. R. De Groot, W. A. Van Leeuwen and C. G. Van Weert, *Relativistic Kinetic Theory, Principles And Applications: Amsterdam, Netherlands: North-holland (1980).*

Chapter 5

The $\pi\pi$ cross-section in the medium

In Chapter-3 and 4 it is shown that the evaluation of the transport coefficients consists of the differential scattering cross sections due to mutual interactions of the constituent particles of the system under consideration which appear explicitly in the denominator of their expressions. These cross sections serve as the dynamical inputs of the respective transport processes and hence bear significant consequences on the magnitude of transport coefficients. In this thesis we intend to evaluate the transport coefficients of a one component hot pion gas, so in this chapter we will proceed to obtain a realistic temperature dependent interaction cross section of a hot pion gas at finite temperature including all the medium effects into consideration. In the literature there are many estimations of transport coefficients in hadronic medium as well as in the pion gas. A substantial amount of calculations of the cross sections have been carried out in different approaches, a few of which are worth mentioning.

In most of the cases the lowest order (LO) chiral perturbation theory has been utilized to evaluate the pion cross section. The corresponding Lagrangian for LOChPT is given by,

$$\mathcal{L} = -\frac{1}{6f_\pi^2}[\partial_\mu \vec{\pi} \cdot \partial^\mu \vec{\pi} \vec{\pi} \cdot \vec{\pi} - \vec{\pi} \cdot \partial_\mu \vec{\pi} \vec{\pi} \cdot \partial^\mu \vec{\pi}] + \frac{m_\pi^2}{24f_\pi^2}(\vec{\pi} \cdot \vec{\pi})^2, \quad (5.1)$$

which results only in the contact diagrams for $\pi\pi$ elastic scattering. The isospin averaged $\pi\pi$ scattering amplitude is found to be [1],

$$\overline{|M|^2} = \frac{1}{9f_\pi^2} \{21m_\pi^4 + 9s^2 - 24m_\pi^2s + 3(t-u)^2\}, \quad (5.2)$$

with $f_\pi = 0.093\text{GeV}$ and $m_\pi = 0.14\text{GeV}$. In [2] the shear viscosity of pion gas has been estimated employing this scattering amplitude. In [3] the cross section is evaluated employing the hard core interaction model. In [4] the bulk viscosity of pion gas has been evaluated with the help of inelastic scatterings from chiral perturbation theory. The problem with the lowest order chiral perturbation theory is that it fails to reproduce the experimental $\pi\pi$ scattering data beyond $\sqrt{s} = 600$ MeV. Due to this reason the transport coefficients have been evaluated by many methods [5, 6, 7, 8] using a parameterized cross section for binary elastic collision which corresponds to a resonance saturation parameterization of isoscalar and isovector phase shifts obtained from various empirical data involving the $\pi\pi$ system [9]. The isospin averaged parameterized differential cross-section is given by

$$\frac{d\sigma(s)}{d\Omega} = \frac{4}{q_{cm}^2} \left[\frac{1}{9} \sin^2 \delta_0^0 + \frac{5}{9} \sin^2 \delta_0^2 + \frac{1}{3} \cdot 9 \sin^2 \delta_1^1 \cos^2 \theta \right], \quad (5.3)$$

where

$$\begin{aligned} \delta_0^0 &= \frac{\pi}{2} + \arctan \left(\frac{E - m_\sigma}{\Gamma_\sigma/2} \right) \\ \delta_1^1 &= \frac{\pi}{2} + \arctan \left(\frac{E - m_\rho}{\Gamma_\rho/2} \right) \\ \delta_0^2 &= -0.12p/m_\pi . \end{aligned} \quad (5.4)$$

The widths are given by $\Gamma_\sigma = 2.06p$ and $\Gamma_\rho = 0.095p \left(\frac{p/m_\pi}{1+(p/m_\rho)^2} \right)^2$ with $m_\sigma = 5.8m_\pi$ and $m_\rho = 5.53m_\pi$.

As seen in Fig. 5.1 these phase shifts agree quite well with those obtained from solutions of the Roy equations as given in [10]. The bands bordered by the dotted lines represent the uncertainties in the solution. The experimentally measured phase shifts (not shown) have error bars [10] which are not reflected in the parameterizations (5.4) plotted in Fig. 5.2.

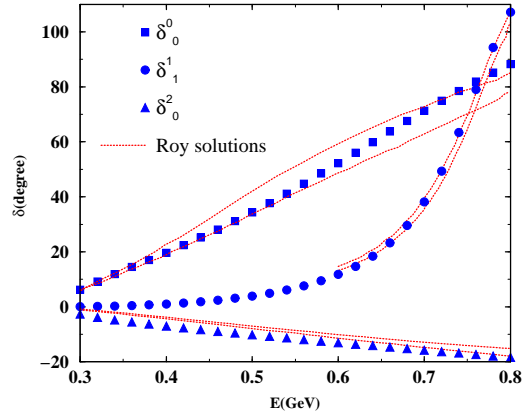


Figure 5.1: The $\pi\pi$ phaseshifts (5.4) as a function of energy compared to Roy equation solutions given in Ref. [10]

In Fig. (5.2) it is shown that the cross-section estimated from LOChPT fails to match the data beyond 600MeV of centre of mass energy. So far the parameterized data has served as a good approximation of pion cross section at vacuum. We proceed to evaluate the $\pi\pi$ cross section from field theoretic calculations keeping this experimental cross section as the benchmark. Our objective is now to set up a dynamical model which agrees reasonably with the parameterized vacuum cross section and at the same time is amenable to the incorporation of medium effects at finite temperature. We observe that the cross-section below 1GeV is dominated by a resonance peaked around 770MeV which is the mass of ρ meson. So it is appropriate to consider the $\pi\pi$ interaction in the medium using ρ meson exchange with the help of an effective Lagrangian. So in next few sections the cross section will be evaluated first in vacuum and compared to the 'data'. Therefore we will introduce the thermal effects in the propagation of the ρ and σ mesons.

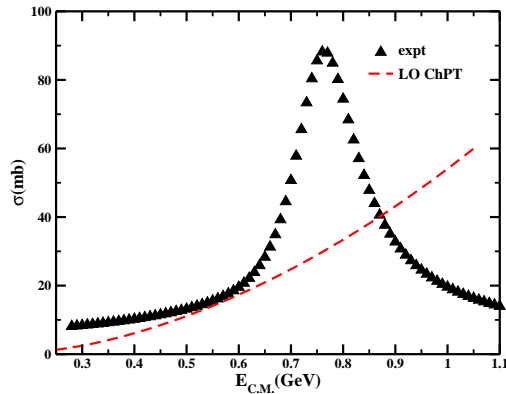


Figure 5.2: Cross-section as a function of C.M. energy from LOChPT which fails to represent the experimental data beyond 600MeV .

5.1 The $\pi\pi$ cross section in vacuum due to ρ meson exchange

5.1.1 Interaction Lagrangian

We evaluate the invariant amplitude for $\pi\pi$ scattering using an effective Lagrangian in which the coupling of the ρ meson to the pions is introduced through the gauge covariant derivative of the pion field operator to obtain [11]

$$\mathcal{L}_{\rho\pi\pi} = \frac{ig_{\rho\pi\pi}}{4} \text{Tr}[V^\mu, [\partial_\mu\Phi, \Phi]], \quad (5.5)$$

where Tr indicates trace in $\text{SU}(2)$ space. The matrix Φ collects the pion fields in the form $\begin{pmatrix} \pi^0 & \sqrt{2}\pi^+ \\ \sqrt{2}\pi^- & -\pi^0 \end{pmatrix}$ and V^μ collects the ρ meson fields analogously. So finally the interaction Lagrangian reduces to the form

$$\mathcal{L}_{\rho\pi\pi} = g_{\rho\pi\pi}[\rho_\mu, \{\vec{\pi} \times \partial^\mu \vec{\pi}\}], \quad (5.6)$$

which will now be used to evaluate the scattering amplitudes. After decomposing the Lagrangian with $\pi_1 = \frac{1}{\sqrt{2}}(\pi_+ + \pi_-)$ and $\pi_2 = \frac{i}{\sqrt{2}}(\pi_+ - \pi_-)$ the Lagrangian finally becomes,

$$\begin{aligned} \mathcal{L}_{\rho\pi\pi} = & \quad ig_{\rho\pi\pi}\{\rho_{+\mu}\pi_0\partial^\mu\pi_- + \rho_{-\mu}\pi_+\partial^\mu\pi_0 + \rho_{0\mu}\pi_-\partial^\mu\pi_+\} \\ & - \quad ig_{\rho\pi\pi}\{\rho_{+\mu}\pi_-\partial^\mu\pi_0 + \rho_{-\mu}\pi_0\partial^\mu\pi_+ + \rho_{0\mu}\pi_+\partial^\mu\pi_-\}. \end{aligned} \quad (5.7)$$

$g_{\rho\pi\pi}$ is the coupling constant and will be fixed from $\rho \rightarrow \pi\pi$ decay width. The Lagrangian gives rise to different Feynman diagrams that give the invariant amplitudes which finally contribute in the scattering cross section. In next section the evaluation of these amplitudes will be discussed in detail.

5.1.2 Setting the coupling constant $g_{\rho\pi\pi}$

The coupling constant $g_{\rho\pi\pi}$ is fixed from the decay width of ρ meson into two pions in vacuum. The expression of decay width is given by,

$$\Gamma = \frac{1}{2E_p} \int \frac{d^3p_1}{(2\pi)^3 2E_1} \frac{d^3p_2}{(2\pi)^3 2E_2} (2\pi)^4 \delta^4(p - p_1 - p_2) \overline{|M_{\rho \rightarrow \pi\pi}|^2}, \quad (5.8)$$

where p_1 and p_2 are momentum of the two pions into which the ρ with momentum p decays.

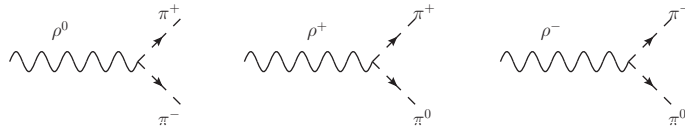


Figure 5.3: Different decay modes for the $\rho \rightarrow \pi\pi$ process.

The amplitudes for respective diagrams are given below,

$$\begin{aligned}
M_{\rho^0 \rightarrow \pi^+ \pi^-} &= g_{\rho\pi\pi}^2 (m_\rho^2 - 4m_\pi^2), \\
M_{\rho^+ \rightarrow \pi^+ \pi^0} &= g_{\rho\pi\pi}^2 (m_\rho^2 - 4m_\pi^2), \\
M_{\rho^- \rightarrow \pi^- \pi^0} &= g_{\rho\pi\pi}^2 (m_\rho^2 - 4m_\pi^2).
\end{aligned} \tag{5.9}$$

Employing those amplitudes for respective decay channels the decay width finally comes to be,

$$\begin{aligned}
\Gamma &= \frac{g_{\rho\pi\pi}^2}{8\pi m_\rho} (m_\rho^2 - 4m_\pi^2) \frac{\lambda^{1/2}(s, m_\pi^2, m_\pi^2)}{2s} \\
&= \frac{g_{\rho\pi\pi}^2 m_\rho}{48\pi} \left\{ 1 - \frac{4m_\pi^2}{m_\rho^2} \right\}^{3/2}.
\end{aligned} \tag{5.10}$$

In vacuum the value of Γ is 150 MeV [12], from which the value of the coupling constant is fixed at $g_{\rho\pi\pi} = 6.05$.

5.1.3 Amplitudes of $\pi\pi$ scattering by exchanging ρ meson

It is convenient to use an isospin averaged amplitude for the estimation of the pion cross section. The expression of the isospin averaged scattering amplitude is,

$$\overline{|M_{\pi\pi}|^2} = \frac{1}{\sum_I (2I + 1)} \left\{ \sum_{I=0}^2 (2I + 1) (M_{\pi\pi}^I)^2 \right\}, \tag{5.11}$$

where I is the isospin of the respective channel. Since the initial state pions each have isospin $\vec{1}$, so for binary elastic collision the total isospin of initial and final states have to be $\vec{2}$, $\vec{1}$ and $\vec{0}$ giving rise to,

$$\overline{|M_{\pi\pi}|^2} = \frac{1}{9} \{ |M_{\pi\pi}^0|^2 + 3|M_{\pi\pi}^1|^2 + 5|M_{\pi\pi}^2|^2 \}. \tag{5.12}$$

The amplitude corresponding to each isospin state involves the interactions among the following charge states. The amplitude for total isospin $\vec{I} = \vec{0}$ state is

$$M_{\pi\pi}^{I=0} = \frac{1}{3} \left\{ \langle \pi^+\pi^- | \mathcal{L} | \pi^+\pi^- \rangle + \langle \pi^+\pi^- | \mathcal{L} | \pi^-\pi^+ \rangle + \langle \pi^+\pi^- | \mathcal{L} | \pi^0\pi^0 \rangle \right. \\ \left. + \langle \pi^-\pi^+ | \mathcal{L} | \pi^+\pi^- \rangle + \langle \pi^-\pi^+ | \mathcal{L} | \pi^-\pi^+ \rangle + \langle \pi^-\pi^+ | \mathcal{L} | \pi^0\pi^0 \rangle \right. \\ \left. + \langle \pi^0\pi^0 | \mathcal{L} | \pi^+\pi^- \rangle + \langle \pi^0\pi^0 | \mathcal{L} | \pi^-\pi^+ \rangle + \langle \pi^0\pi^0 | \mathcal{L} | \pi^0\pi^0 \rangle \right\}. \quad (5.13)$$

The amplitude for total isospin $\vec{I} = \vec{1}$ and $I_z = +1$ state is

$$M_{\pi\pi}^{I=1} = \frac{1}{2} \left\{ \langle \pi^+\pi^0 | \mathcal{L} | \pi^+\pi^0 \rangle - \langle \pi^+\pi^0 | \mathcal{L} | \pi^0\pi^+ \rangle - \langle \pi^0\pi^+ | \mathcal{L} | \pi^+\pi^0 \rangle + \langle \pi^0\pi^+ | \mathcal{L} | \pi^0\pi^+ \rangle \right\}, \quad (5.14)$$

and finally the amplitude corresponding to total isospin $\vec{I} = \vec{2}$, $I_z = +2$ state is

$$M_{\pi\pi}^{I=2} = \langle \pi^+\pi^+ | \mathcal{L} | \pi^+\pi^+ \rangle. \quad (5.15)$$

Now the interaction amplitudes between each set of charged states can be obtained from the Feynman diagrams resulting from the Lagrangian (5.7). The Feynman diagrams for each set of interaction along with the value of amplitudes are described below.

1. $\pi^+\pi^+ \rightarrow \pi^+\pi^+$

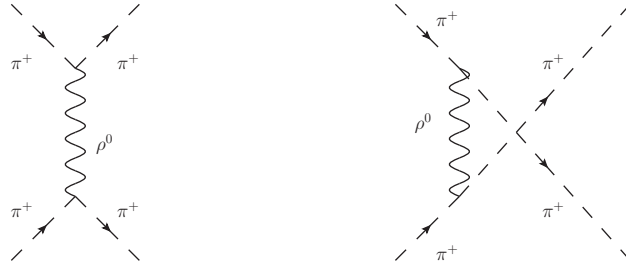


Figure 5.4: t and u-channel diagrams for $\pi^+\pi^+ \rightarrow \pi^+\pi^+$ scattering

The interaction amplitude for the interaction between above charge states of pion is,

$$\langle \pi^+\pi^+ | \mathcal{L} | \pi^+\pi^+ \rangle = g_{\rho\pi\pi}^2 \left[\frac{u-s}{t-m_\rho^2} + \frac{t-s}{u-m_\rho^2} \right]. \quad (5.16)$$

2. $\pi^+\pi^0 \rightarrow \pi^+\pi^0$

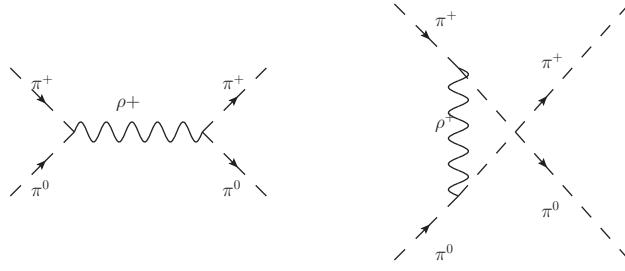


Figure 5.5: s and u-channel diagrams for $\pi^+\pi^0 \rightarrow \pi^+\pi^0$ scattering

The interaction amplitude for the interaction between above charge states of pion is,

$$\langle \pi^+\pi^0 | \mathcal{L} | \pi^+\pi^0 \rangle = g_{\rho\pi\pi}^2 \left[\frac{t-u}{s-m_\rho^2} + \frac{t-s}{u-m_\rho^2} \right]. \quad (5.17)$$

3. $\pi^+\pi^0 \rightarrow \pi^0\pi^+$

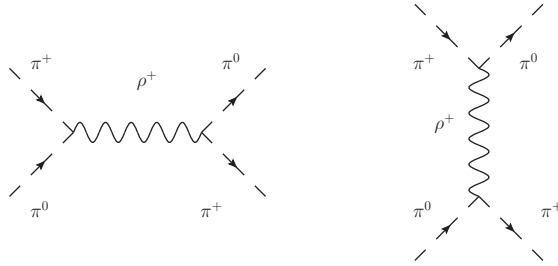


Figure 5.6: s and t-channel diagrams for $\pi^+\pi^0 \rightarrow \pi^0\pi^+$ scattering

The interaction amplitude for the interaction between above charge states of pion is,

$$\langle \pi^+\pi^0 | \mathcal{L} | \pi^0\pi^+ \rangle = g_{\rho\pi\pi}^2 \left[\frac{u-t}{s-m_\rho^2} + \frac{u-s}{t-m_\rho^2} \right]. \quad (5.18)$$

4. $\pi^0\pi^+ \rightarrow \pi^+\pi^0$

The interaction amplitude for the interaction between above charge states of pion is,

$$\langle \pi^0\pi^+ | \mathcal{L} | \pi^+\pi^0 \rangle = g_{\rho\pi\pi}^2 \left[\frac{u-t}{s-m_\rho^2} + \frac{u-s}{t-m_\rho^2} \right]. \quad (5.19)$$

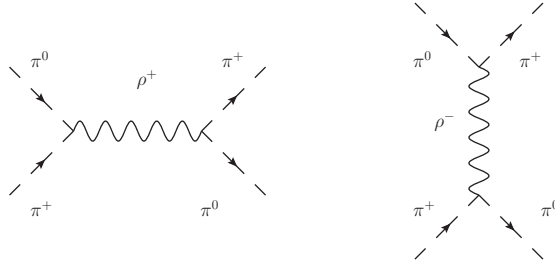


Figure 5.7: s and t-channel diagrams for $\pi^0\pi^+ \rightarrow \pi^+\pi^0$ scattering

5. $\pi^0\pi^+ \rightarrow \pi^0\pi^+$

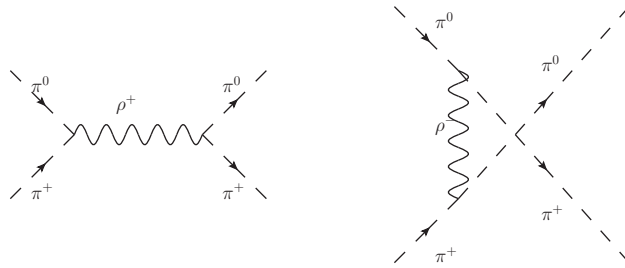


Figure 5.8: s and u-channel diagrams for $\pi^0\pi^+ \rightarrow \pi^0\pi^+$ scattering

The interaction amplitude for the interaction between above charge states of pion is,

$$\langle \pi^0\pi^+ | \mathcal{L} | \pi^0\pi^+ \rangle = g_{\rho\pi\pi}^2 \left[\frac{t-u}{s-m_\rho^2} + \frac{t-s}{u-m_\rho^2} \right]. \quad (5.20)$$

6. $\pi^+\pi^- \rightarrow \pi^+\pi^-$

The interaction amplitude for the interaction between above charge states of pion is,

$$\langle \pi^+\pi^- | \mathcal{L} | \pi^+\pi^- \rangle = g_{\rho\pi\pi}^2 \left[\frac{t-u}{s-m_\rho^2} + \frac{s-u}{t-m_\rho^2} \right]. \quad (5.21)$$

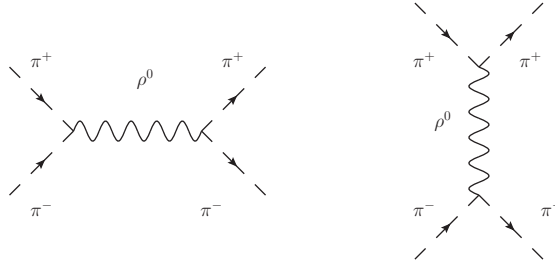


Figure 5.9: s and t-channel diagrams for $\pi^+\pi^- \rightarrow \pi^+\pi^-$ scattering

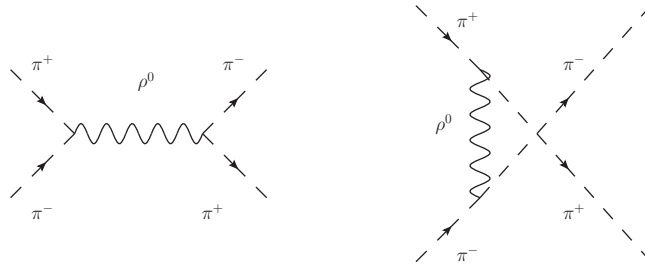


Figure 5.10: s and u-channel diagrams for $\pi^+\pi^- \rightarrow \pi^-\pi^+$ scattering

7. $\pi^+\pi^- \rightarrow \pi^-\pi^+$

The interaction amplitude for the interaction between above charge states of pion is,

$$\langle \pi^+\pi^- | \mathcal{L} | \pi^-\pi^+ \rangle = g_{\rho\pi\pi}^2 \left[\frac{u-t}{s-m_\rho^2} + \frac{s-t}{u-m_\rho^2} \right]. \quad (5.22)$$

8. $\pi^+\pi^- \rightarrow \pi^0\pi^0$

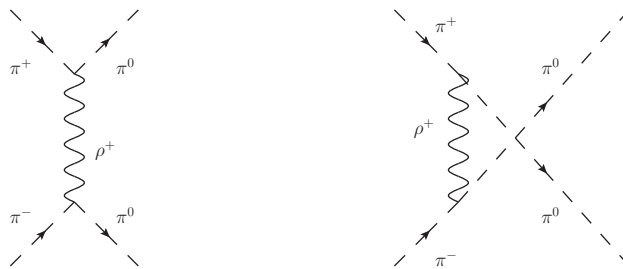


Figure 5.11: t and u-channel diagrams for $\pi^+\pi^- \rightarrow \pi^0\pi^0$ scattering

The interaction amplitude for the interaction between above charge states of pion is,

$$\langle \pi^+ \pi^- | \mathcal{L} | \pi^0 \pi^0 \rangle = g_{\rho\pi\pi}^2 \left[\frac{s-u}{t-m_\rho^2} + \frac{s-t}{u-m_\rho^2} \right]. \quad (5.23)$$

9. $\pi^- \pi^+ \rightarrow \pi^+ \pi^-$

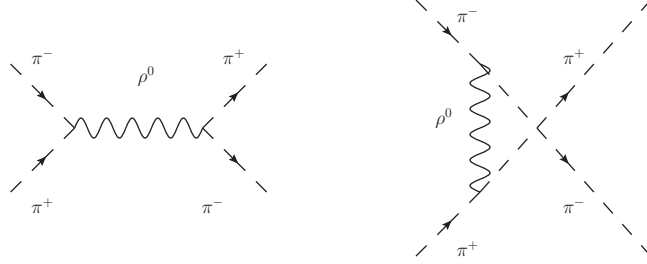


Figure 5.12: s and u-channel diagrams for $\pi^- \pi^+ \rightarrow \pi^+ \pi^-$ scattering

The interaction amplitude for the interaction between above charge states of pion is,

$$\langle \pi^- \pi^+ | \mathcal{L} | \pi^+ \pi^- \rangle = g_{\rho\pi\pi}^2 \left[\frac{u-t}{s-m_\rho^2} + \frac{s-t}{u-m_\rho^2} \right]. \quad (5.24)$$

10. $\pi^- \pi^+ \rightarrow \pi^- \pi^+$

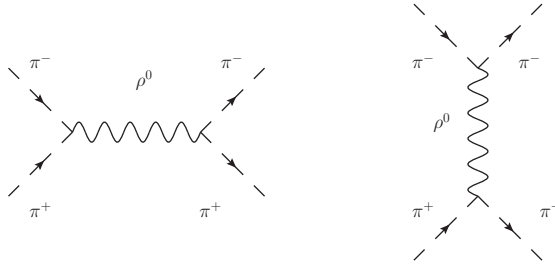


Figure 5.13: s and t-channel diagrams for $\pi^- \pi^+ \rightarrow \pi^- \pi^+$ scattering

The interaction amplitude for the interaction between above charge states of pion is,

$$\langle \pi^- \pi^+ | \mathcal{L} | \pi^- \pi^+ \rangle = g_{\rho\pi\pi}^2 \left[\frac{t-u}{s-m_\rho^2} + \frac{s-u}{t-m_\rho^2} \right]. \quad (5.25)$$

11. $\pi^- \pi^+ \rightarrow \pi^0 \pi^0$

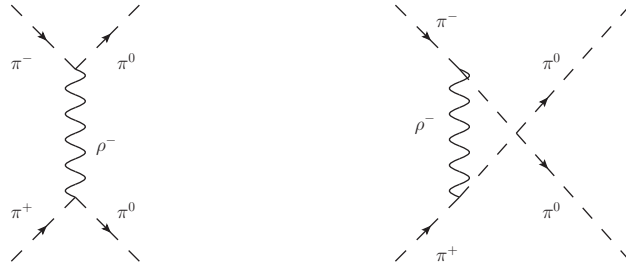


Figure 5.14: t and u-channel diagrams for $\pi^- \pi^+ \rightarrow \pi^0 \pi^0$ scattering

The interaction amplitude for the interaction between above charge states of pion is,

$$\langle \pi^- \pi^+ | \mathcal{L} | \pi^0 \pi^0 \rangle = g_{\rho\pi\pi}^2 \left[\frac{s-u}{t-m_\rho^2} + \frac{s-t}{u-m_\rho^2} \right]. \quad (5.26)$$

12. $\pi^0 \pi^0 \rightarrow \pi^+ \pi^-$

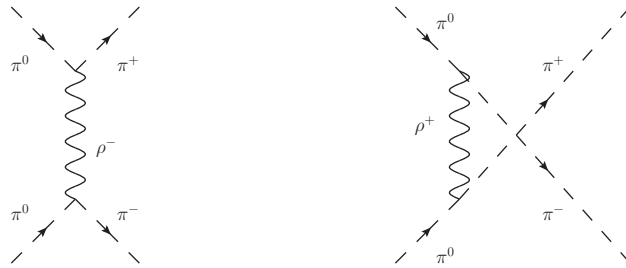


Figure 5.15: t and u-channel diagrams for $\pi^0 \pi^0 \rightarrow \pi^+ \pi^-$ scattering

The interaction amplitude for the interaction between above charge states of pion is,

$$\langle \pi^0 \pi^0 | \mathcal{L} | \pi^+ \pi^- \rangle = g_{\rho\pi\pi}^2 \left[\frac{s-u}{t-m_\rho^2} + \frac{s-t}{u-m_\rho^2} \right]. \quad (5.27)$$

13. $\pi^0 \pi^0 \rightarrow \pi^- \pi^+$

The interaction amplitude for the interaction between above charge states of pion is,

$$\langle \pi^0 \pi^0 | \mathcal{L} | \pi^- \pi^+ \rangle = g_{\rho\pi\pi}^2 \left[\frac{s-u}{t-m_\rho^2} + \frac{s-t}{u-m_\rho^2} \right]. \quad (5.28)$$

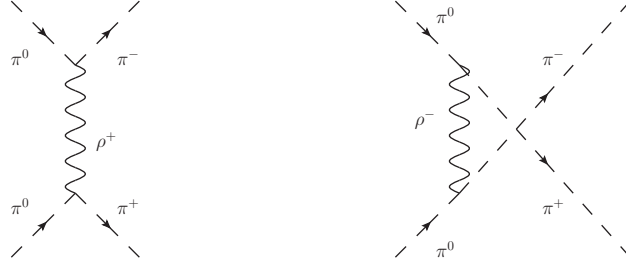


Figure 5.16: t and u-channel diagrams for $\pi^0\pi^0 \rightarrow \pi^-\pi^+$ scattering

The above charge state amplitudes finally give the interaction amplitude corresponding to different isospin states mentioned in equations (5.13), (5.14) and (5.15),

$$M_{\pi\pi}^{I=0} = 2g_{\rho\pi\pi}^2 \left[\frac{s-u}{t-m_\rho^2} + \frac{s-t}{u-m_\rho^2} \right], \quad (5.29)$$

$$M_{\pi\pi}^{I=1} = g_{\rho\pi\pi}^2 \left[2\frac{t-u}{s-m_\rho^2} + \frac{t-s}{u-m_\rho^2} - \frac{u-s}{t-m_\rho^2} \right], \quad (5.30)$$

$$M_{\pi\pi}^{I=2} = g_{\rho\pi\pi}^2 \left[\frac{u-s}{t-m_\rho^2} + \frac{t-s}{u-m_\rho^2} \right]. \quad (5.31)$$

The corresponding isospin averaged amplitude for $\pi\pi$ scattering via ρ meson exchange can now be given by (5.12). Now we can evaluate the cross section by the following equation,

$$\sigma = \frac{1}{16\pi} \int_{-s}^0 \frac{|M|^2}{(s^2 - 4m_\pi^2 s)} dt. \quad (5.32)$$

So we can see that the interaction leads to $\pi\pi$ scattering diagrams with ρ exchange in the s , t and u channels. In these calculations we modify the ρ propagator $D_{\mu\nu}^{(0)} = (-g_{\mu\nu} + q_\mu q_\nu / m_\rho^2) / (q^2 - m_\rho^2 + i\epsilon)$ replacing $i\epsilon$ with $im_\rho \Gamma_\rho(s)$ where the two-pion decay width $\Gamma_\rho(s)$ is taken from (5.10). This is done only for s -channel ρ -exchange diagrams, which contribute only in the case of total isospin $I = 1$, since only the s channel diagrams contribute in the resonance structure.

By ignoring the $I = 2$ contribution, then the integrated cross section (with an additional factor of 1/2 for identical particles) is plotted as a function of the center-of-mass energy in Fig. 5.17. It is seen that the evaluated cross section in vacuum is in quite good agreement with experimental data only except very low energy below 0.4GeV . In order to describe $\pi\pi$ scattering at low

energies it is essential to also include σ -exchange diagrams, details of which will be discussed in next section.

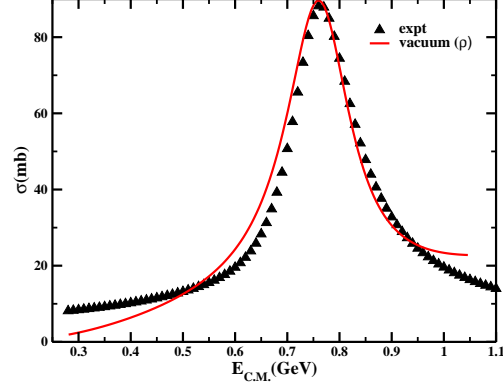


Figure 5.17: The $\pi\pi$ cross-section evaluated from ρ exchange diagrams shows good agreement with experimental data except at low energies.

5.1.4 Amplitudes of $\pi\pi$ scattering including both ρ and σ mesons exchange

For the σ exchanged $\pi\pi$ interaction the following Lagrangian has been used,

$$\mathcal{L}_{\sigma\pi\pi} = \frac{1}{2}g_{\sigma\pi\pi}m_{\sigma}\vec{\pi} \cdot \vec{\pi}\sigma, \quad (5.33)$$

with $g_{\sigma\pi\pi} = 2.5$. Following the same scheme as for the ρ , we obtain the amplitudes for respective isospin channels.

$$M_{\pi\pi}^{I=0} = g_{\sigma\pi\pi}^2 m_{\sigma}^2 \left[\frac{3}{s - m_{\sigma}^2} + \frac{1}{t - m_{\sigma}^2} + \frac{1}{u - m_{\sigma}^2} \right], \quad (5.34)$$

$$M_{\pi\pi}^{I=1} = g_{\sigma\pi\pi}^2 m_{\sigma}^2 \left[\frac{1}{t - m_{\sigma}^2} - \frac{1}{u - m_{\sigma}^2} \right], \quad (5.35)$$

$$M_{\pi\pi}^{I=2} = g_{\sigma\pi\pi}^2 m_{\sigma}^2 \left[\frac{1}{t - m_{\sigma}^2} + \frac{1}{u - m_{\sigma}^2} \right]. \quad (5.36)$$

We have introduced as before the σ width in the s -channel diagram which now appear only for $I = 0$. The values $m_\sigma = 450$ MeV and $\Gamma_\sigma = 550$ MeV that we use are in conformity with estimates in [13]. So finally we obtain the total amplitude for binary elastic scattering for pion involving both ρ and σ meson exchange diagrams and their respective decay widths as the following,

$$\begin{aligned}
\mathcal{M}_{I=0} &= 2g_\rho^2 \left[\frac{s-u}{t-m_\rho^2} + \frac{s-t}{u-m_\rho^2} \right] + g_\sigma^2 m_\sigma^2 \left[\frac{3}{s-m_\sigma^2 + im_\sigma \Gamma_\sigma} + \frac{1}{t-m_\sigma^2} + \frac{1}{u-m_\sigma^2} \right] \\
\mathcal{M}_{I=1} &= g_\rho^2 \left[\frac{2(t-u)}{s-m_\rho^2 + im_\rho \Gamma_\rho(s)} + \frac{t-s}{u-m_\rho^2} - \frac{u-s}{t-m_\rho^2} \right] + g_\sigma^2 m_\sigma^2 \left[\frac{1}{t-m_\sigma^2} - \frac{1}{u-m_\sigma^2} \right] \\
\mathcal{M}_{I=2} &= g_\rho^2 \left[\frac{u-s}{t-m_\rho^2} + \frac{t-s}{u-m_\rho^2} \right] + g_\sigma^2 m_\sigma^2 \left[\frac{1}{t-m_\sigma^2} + \frac{1}{u-m_\sigma^2} \right]. \quad (5.37)
\end{aligned}$$

In Fig. 5.18 it is shown that now the estimated cross section agrees really well with the parameterized experimental data for c.m. energy upto 1GeV . So now we can say that in vacuum we have modeled a cross section phenomenologically which is in good agreement with the experimental one into which now the effects of a thermal medium can be introduced by extending the field theoretic calculations to finite temperature.

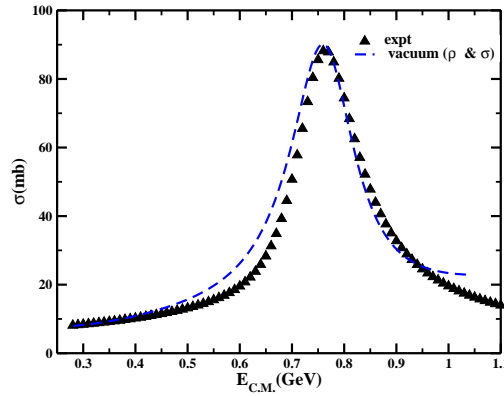


Figure 5.18: The $\pi\pi$ cross-section evaluated from both ρ and σ exchange diagrams agrees with the experimental data quite nicely.

5.2 The $\pi\pi$ cross section at finite temperature

The effect of the medium on ρ propagation is quantified through its self-energy. The standard procedure is to evaluate this quantity by perturbative methods using effective interactions and then obtain the exact propagator using the Dyson equation, depicted pictorially in Fig. 5.19. In the real time formulation of thermal field theory, all two-point functions assume a 2×2 matrix form [16] which can be diagonalized. The diagonal components also obey the Dyson equation [17] by means of which the full propagator $D_{\mu\nu}$ is obtained as

$$D_{\mu\nu} = D_{\mu\nu}^{(0)} + D_{\mu\sigma}^{(0)} \Pi^{\sigma\lambda} D_{\lambda\nu}, \quad (5.38)$$

where $D_{\mu\nu}^{(0)}$ is the vacuum propagator for the ρ meson and $\Pi^{\sigma\lambda}$ is the self energy function obtained from one-loop diagrams shown in Fig. 5.19. Following [16, 14] we write the in-medium self-energy in terms of longitudinal and transverse parts

$$\Pi_{\mu\nu} = P_{\mu\nu} \Pi^T + Q_{\mu\nu} \Pi^L \quad (5.39)$$

where $P_{\mu\nu}$ and $Q_{\mu\nu}$ are the transverse and longitudinal projection tensors respectively. These are defined as [14]

$$P_{\mu\nu} = -g_{\mu\nu} + \frac{q_\mu q_\nu}{q^2} - \frac{q^2}{\bar{q}^2} \tilde{u}_\mu \tilde{u}_\nu, \quad \tilde{u}_\mu = u_\mu - (u \cdot q) q_\mu / q^2 \quad (5.40)$$

and

$$Q_{\mu\nu} = \frac{(q^2)^2}{\bar{q}} \tilde{u}_\mu \tilde{u}_\nu, \quad \bar{q}^2 = (u \cdot q)^2 - q^2. \quad (5.41)$$

where u_μ is four velocity of the thermal bath. It is easy to see that

$$P_{\mu\nu} + Q_{\mu\nu}/q^2 = -g_{\mu\nu} + q_\mu q_\nu / q^2. \quad (5.42)$$

Note that while P and Q are four-dimensionally transverse, P is also three-dimensionally transverse while Q is longitudinal. Solving (5.38), the exact ρ propagator is obtained as

$$D_{\mu\nu}(q_0, \vec{q}) = -\frac{P_{\mu\nu}}{q^2 - m_\rho^2 - \Pi^T} - \frac{Q_{\mu\nu}/q^2}{q^2 - m_\rho^2 - q^2 \Pi^L} + \frac{q_\mu q_\nu}{m_\rho^2 q^2} \quad (5.43)$$

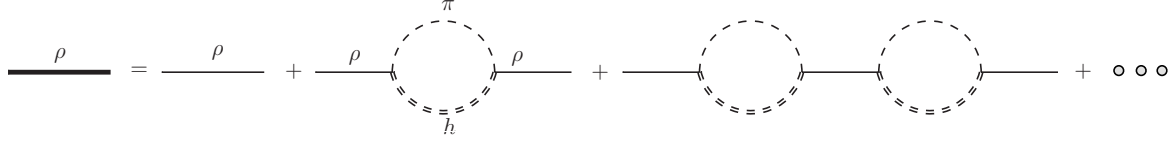


Figure 5.19: The exact ρ propagator with $\pi - h$ loop diagrams for $h = \pi, \omega, h_1, a_1$ mesons.

where Π^T and Π^L can be obtained from the relations

$$\Pi^T = -\frac{1}{2}(\Pi_\mu^\mu + \frac{q^2}{\bar{q}^2}\Pi_{00}), \quad \Pi^L = \frac{1}{\bar{q}^2}\Pi_{00}, \quad \Pi_{00} \equiv u^\mu u^\nu \Pi_{\mu\nu}. \quad (5.44)$$

As shown in [14], the three-momentum dependence of the ρ self-energy is not substantial for the present case and we can replace Π^T and $q^2\Pi^L$ in the above expression by a self-energy function which is averaged over polarization. Defining this as

$$\Pi = \frac{1}{3}(2\Pi^T + q^2\Pi^L) \quad (5.45)$$

and neglecting the non-pole piece in (5.43), the in-medium propagator can be written as

$$D_{\mu\nu}(q_0, \vec{q}) = \frac{-g_{\mu\nu} + q_\mu q_\nu / q^2}{q^2 - m_\rho^2 - \text{Re}\Pi(q_0, \vec{q}) + i\text{Im}\Pi(q_0, \vec{q})}. \quad (5.46)$$

In the real-time formulation of thermal field theory the self-energy which has been used in (5.46) assumes a 2×2 matrix structure of which the 11-component is given by

$$\Pi_{\mu\nu}^{11}(q) = i \int \frac{d^4k}{(2\pi)^4} N_{\mu\nu}(q, k) D_\pi^{11}(k) D_h^{11}(q - k) \quad (5.47)$$

where D^{11} is the 11-component of the scalar propagator which constitute the internal line of the loop, given by $D^{11}(k) = \Delta(k) + 2\pi i f^{(0)}(k) \delta(k^2 - m^2)$, where $\Delta(k)$ is its vacuum part. It turns out that the real and imaginary parts of the self-energy function which appear in eq. (5.46) can be obtained in terms of the 11-component through the relations [16, 17]

$$\begin{aligned} \text{Re}\Pi_{\mu\nu} &= \text{Re}\Pi_{\mu\nu}^{11} \\ \text{Im}\Pi_{\mu\nu} &= \epsilon(q_0) \tanh(\beta q_0/2) \text{Im}\Pi_{\mu\nu}^{11}. \end{aligned} \quad (5.48)$$

Tensor structures associated with the two vertices and the vector propagator are included in $N_{\mu\nu}$ and are available in [14] where the interactions were taken from chiral perturbation theory.

It is easy to perform the integral over k_0 using suitable contours to obtain

$$\begin{aligned} \Pi^{\mu\nu}(q_0, \vec{q}) = & \int \frac{d^3k}{(2\pi)^3} \frac{1}{4\omega_\pi\omega_h} \left[\frac{(1 + f^{(0)}(\omega_\pi))N_1^{\mu\nu} + f^{(0)}(\omega_h)N_3^{\mu\nu}}{q_0 - \omega_\pi - \omega_h + i\eta\epsilon(q_0)} + \frac{-f^{(0)}(\omega_\pi)N_1^{\mu\nu} + f^{(0)}(\omega_h)N_4^{\mu\nu}}{q_0 - \omega_\pi + \omega_h + i\eta\epsilon(q_0)} \right. \\ & \left. + \frac{f^{(0)}(\omega_\pi)N_2^{\mu\nu} - f^{(0)}(\omega_h)N_3^{\mu\nu}}{q_0 + \omega_\pi - \omega_h + i\eta\epsilon(q_0)} + \frac{-f^{(0)}(\omega_\pi)N_2^{\mu\nu} - (1 + f^{(0)}(\omega_h))N_4^{\mu\nu}}{q_0 + \omega_\pi + \omega_h + i\eta\epsilon(q_0)} \right] \end{aligned} \quad (5.49)$$

where $f^{(0)}(\omega) = \frac{1}{e^{(\omega - \mu_\pi)/T} - 1}$ is the Bose distribution function with arguments $\omega_\pi = \sqrt{\vec{k}^2 + m_\pi^2}$ and $\omega_h = \sqrt{(\vec{q} - \vec{k})^2 + m_h^2}$. The subscript $i (= 1, \dots, 4)$ on $N^{\mu\nu}$ in (5.49) correspond to its values for $k_0 = \omega_\pi, -\omega_\pi, q_0 - \omega_h, q_0 + \omega_h$ respectively. It is easy to read off the real and imaginary parts from (5.49). The angular integration can be carried out using the δ -functions in each of the four terms in the imaginary part which define the kinematically allowed regions in q_0 and \vec{q} where scattering, decay and regeneration processes occur in the medium leading to the loss or gain of ρ mesons [14].

The real part of the self-energy modifies the pole position and the imaginary part embodies the effect of collisions and decay processes by means of which the ρ is lost or gained in the medium. Using interactions from chiral perturbation theory, the one-loop self energy is calculated [14]. The imaginary parts for $\pi\pi, \pi\omega, \pi h_1$ and πa_1 loops were obtained from the discontinuities of the self-energy in the complex energy plane. While for the $\pi\pi$ loop, the contribution at the nominal ρ pole comes from the unitary cut, the Landau type discontinuity is responsible for contributions from loops with heavier particles. The mesons ω, h_1 and a_1 all have negative G-parity and have substantial 3π and $\rho\pi$ decay widths [12]. The self-energies containing these unstable particles in the loop graphs have thus been folded with their spectral functions as shown in [15]. The contributions from the loops with heavy mesons may then be considered as a multi-pion contribution to the ρ self-energy.

The (polarization averaged) self-energies containing these unstable particles in the loop graphs have thus been folded with their spectral functions,

$$\Pi(q, m_h) = \frac{1}{N_h} \int_{(m_h - 2\Gamma_h)^2}^{(m_h + 2\Gamma_h)^2} dM^2 \frac{1}{\pi} \text{Im} \left[\frac{1}{M^2 - m_h^2 + iM\Gamma_h(M)} \right] \Pi(q, M) \quad (5.50)$$

with $N_h = \int_{(m_h - 2\Gamma_h)^2}^{(m_h + 2\Gamma_h)^2} dM^2 \frac{1}{\pi} \text{Im} \left[\frac{1}{M^2 - m_h^2 + iM\Gamma_h(M)} \right]$. The contributions from the loops with heavy mesons (the πh loops) may then be considered as a multi-pion contribution to the

ρ self-energy.

The medium effect on propagation of the σ meson is estimated analogously as above. The effective propagator in this case is given by

$$D(q_0, \vec{q}) = \frac{-1}{q^2 - m_\sigma^2 - \text{Re}\Pi(q_0, \vec{q}) + i\text{Im}\Pi(q_0, \vec{q})}. \quad (5.51)$$

Following the steps outlined above the expression for the self-energy of the σ is given by

$$\begin{aligned} \Pi(q_0, \vec{q}) = & N \int \frac{d^3k}{(2\pi)^3} \frac{1}{4\omega_\pi\omega'_\pi} \left[\frac{1 + f^{(0)}(\omega_\pi) + f^{(0)}(\omega'_\pi)}{q_0 - \omega_\pi - \omega'_\pi + i\eta\epsilon(q_0)} + \frac{f^{(0)}(\omega'_\pi) - f^{(0)}(\omega_\pi)}{q_0 - \omega_\pi + \omega'_\pi + i\eta\epsilon(q_0)} \right. \\ & \left. + \frac{f^{(0)}(\omega_\pi) - f^{(0)}(\omega'_\pi)}{q_0 + \omega_\pi - \omega'_\pi + i\eta\epsilon(q_0)} - \frac{1 + f^{(0)}(\omega_\pi) + f^{(0)}(\omega'_\pi)}{q_0 + \omega_\pi + \omega'_\pi + i\eta\epsilon(q_0)} \right] \end{aligned} \quad (5.52)$$

where $\omega'_\pi = \sqrt{(\vec{q} - \vec{k})^2 + m_\pi^2}$. The imaginary part for the kinematic region of our interest in this case receives contribution only from the first term which essentially describes the decay of the σ into two pions minus the reverse process of formation.

The cross-section obtained by using the in-medium ρ -propagator (5.46) in place of the vacuum propagator $D_{\mu\nu}^{(0)}$ along with the in medium σ propagator (5.51) in the evaluation of the amplitudes is shown in Fig. 5.20. We observe a small suppression of the peak for the $\pi\pi$ loop and a larger effect when all the loops (indicated by multi-pion) are considered accompanied by a small shift in its position. This is due to the temperature dependence of the real and imaginary parts of the self-energy and is manifested as the modified spectral function of the ρ and σ meson. The widths occurring in the denominator of the propagator increase with increasing temperature, reducing the cross-section peak when plotted with centre of mass energy.

5.3 Inclusion of temperature dependent pion chemical potential

In heavy ion collisions pions are known to get out of chemical equilibrium early, at about a temperature of $T \sim 170$ MeV. Chemical freeze out indicates the stopping of the number

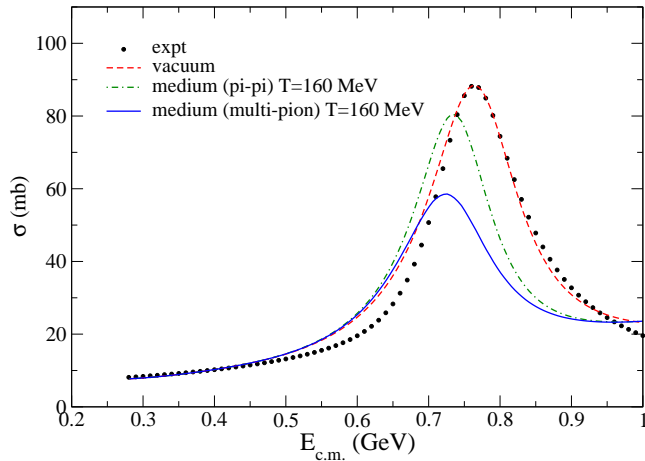


Figure 5.20: The $\pi\pi$ cross-section as a function of centre of mass energy. The dashed line indicates the cross-section obtained using eq. (5.37) which agrees well with the experimental values shown by filled circles. The dash-dotted and solid lines depict the in-medium cross-section for $\pi\pi$ and multi-pion loops respectively in the ρ self-energy evaluated at $T=160$ MeV.

changing inelastic processes so that only the elastic processes (including the resonances), that only involve momentum transfer dominate the kinetics of the gas, as a result of which the chemical equilibrium of the gas is lost. At a still lower temperature $T \sim 100$ MeV, momentum transfer stops indicating the kinetic freeze out of the system. This scenario is quite compatible with the treatment of medium modification of the $\pi\pi$ cross-section being employed in this work where the $\pi\pi$ interaction is mediated by ρ and σ exchange and the subsequent propagation of these mesons are modified by two-pion and effective multi-pion fluctuations. From chemical to kinetic freeze out the temperature drops from 170MeV to 100MeV but particle number does not change since the inelastic collisions cease to occur in this temperature range. In order to keep the particle number fixed a temperature dependent pion chemical potential is introduced which starts building up with decrease in temperature. We take the temperature dependent pion chemical potential from Ref. [18] which implements the formalism described in [19] and reproduces the slope of the transverse momentum spectra of identified hadrons observed in experiments. Here, by fixing the ratio s/n where s is the entropy density and n the number density, to the value at chemical freeze-out where $\mu_\pi = 0$, one can go down in temperature up to

the kinetic freeze-out by increasing the pion chemical potential. This provides the temperature dependence leading to $\mu_\pi(T)$ which is shown in Fig. (5.21). In this partial chemical equilibrium scenario of [19] the chemical potentials of the heavy mesons are determined from elementary processes. The ω chemical potential e.g. is given by $\mu_\omega = 3 \times 0.88\mu_\pi$, as a consequence of the processes $\omega \leftrightarrow \pi\pi\pi$ occurring in the medium. The branching ratios are taken from [12].

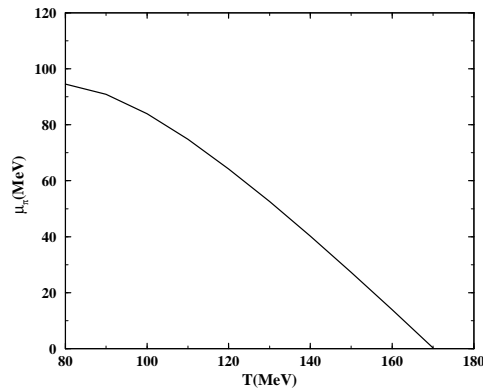


Figure 5.21: The pion chemical potential as a function of temperature [18].

This temperature dependent pion chemical potential then has been incorporated into the $\pi\pi$ cross section to consider the effect of early chemical freeze out of pion gas in heavy ion collisions in the estimation of the transport coefficients. The integrated cross section as a function of centre of mass energy is depicted in Fig. (5.22) where the temperature dependent $\mu_\pi(T)$ has been used for all three cases mentioned earlier.

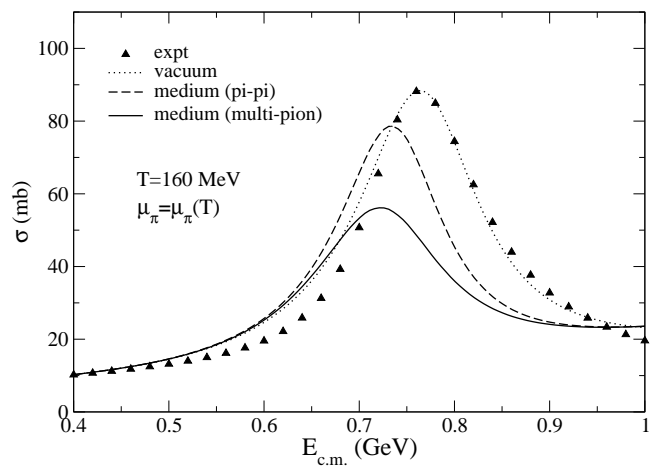


Figure 5.22: The $\pi\pi$ cross-section as a function of centre of mass energy at $T=160 \text{ MeV}$ and $\mu_\pi = \mu_\pi(T)$.

Bibliography

- [1] S. Weinberg, *Physica A* **96**, 327 (1979).
- [2] E. Nakano, arXiv:hep-ph/0612255.
- [3] Oleg N. Moroz, arXiv:hep-ph/1112.0277v6.
- [4] Egang Lu and Guy D. Moore, *Phys. Rev. C* **83** (2011) 044901.
- [5] K. Itakura, O. Morimatsu and H. Otomo, *Phys. Rev. D* **77**, 014014 (2008).
- [6] M. Prakash, M. Prakash, R. Venugopalan and G. Welke, *Phys. Rept.* **227** (1993) 321.
- [7] A. Wiranata and M. Prakash, *Phys.Rev. C* **85** (2012) 054908 arXiv:1203.0281 [nucl-th].
- [8] D. Davesne, *Phys. Rev. C* **53**, 3069 (1996).
- [9] G. Bertsch, M. Gong, L. D. McLerran, P. V. Ruuskanen and E. Sarkkinen, *Phys. Rev. D* **37** (1988) 1202.
- [10] B. Ananthanarayan, G. Colangelo, J. Gasser and H. Leutwyler, *Phys. Rept.* **353** (2001) 207.
- [11] F. Klingl, N. Kaiser and W. Weise, *Z. Phys. A* **356** (1996) 193 .
- [12] K. Nakamura *et al.* [Particle Data Group], *J. Phys. G* **37** (2010) 075021.
- [13] J. Nieves and E. Ruiz Arriola, *Phys. Rev. D* **80** (2009) 045023.
- [14] S. Ghosh, S. Sarkar and S. Mallik, *Eur. Phys. J. C* **70**, 251 (2010).

- [15] S. Ghosh and S. Sarkar, Nucl. Phys. A **870-871**, 94 (2011).
- [16] M. Le Bellac, *Thermal Field Theory* (Cambridge University Press, Cambridge, 1996).
- [17] S. Mallik and S. Sarkar, Eur. Phys. J. C **61**, 489 (2009).
- [18] T. Hirano and K. Tsuda, Phys. Rev. C **66** (2002) 054905
- [19] H. Bebie, P. Gerber, J. L. Goity and H. Leutwyler, Nucl. Phys. B **378** (1992) 95.

Chapter 6

The effect of medium on the transport coefficients and relaxation of flows in an interacting pion gas

We have seen that the temperature dependence of the transport coefficients evaluated in Chapter-3 and 4 originates from the phase space factors and through the interaction cross section providing the dynamics for the respective processes. As discussed earlier in most of the literatures the temperature dependence of the transport coefficients comes from only the phase space factors, while the finite temperature contribution from the dynamics part is neglected. In this chapter the effect of the medium modified cross section estimated in Chapter-5, on the transport coefficients and relaxation times of the corresponding dissipative flows will be discussed in detail.

We also observed that in a thermal medium a number of decay and scattering processes occur in addition to the decay of ρ and σ mesons into two pions, which alter the abundance of the ρ and σ mesons within the system compared to vacuum. So at finite temperature the contributions from a thermal medium have to be taken into consideration in order to incorporate all these additional processes. In this Chapter the in medium cross section estimated at finite temperature has been

introduced in the expressions of the transport coefficients and then the medium modified first order transport coefficients have been used to evaluate the relaxation times for the viscous and thermal flows. The temperature dependence of these quantities has been depicted with and without the medium dependent cross section to quantify the effect of the thermal medium on the dissipative quantities. Further the effect of the temperature dependent pion chemical potential on these quantities has been demonstrated.

6.1 Shear Viscosity

6.1.1 Effect of medium on shear viscosity

The temperature dependence of shear viscosity η obtained in the Chapman-Enskog approximation has been depicted in the η versus T plot in fig. 6.1, showing the effect of the in-medium ρ and σ propagation in the pion gas. Shear viscosity shows an increasing trend with temperature indicating larger momentum transfer at higher temperature. The temperature dependence of shear viscosity is enhanced when the medium effects are taken into consideration. This is quite evident since the interaction cross section which appears in the denominator of transport coefficients gets suppressed due to the inclusion of the medium effects. This enhancement is larger for multipion loops in the ρ propagator than only the $\pi\pi$ loop. Here one can observe $\sim 10\%$ change at $T = 150$ MeV due to medium effects compared to the vacuum when all the loops in the ρ self-energy are considered. The effect reduces with temperature and reaches to less than 5% at 100 MeV. In Fig. 6.1 we have presented only the case of zero pion chemical potential, in which a noticeable medium effect is observed as indicated by the dashed and dot-dashed lines [1].

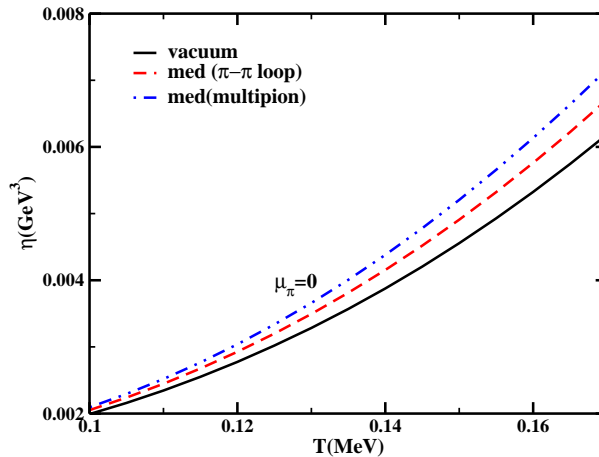


Figure 6.1: The shear viscosity as a function of temperature in the Chapman-Enskog approximation. The dashed and dot-dashed lines correspond to the use of in-medium cross-sections for $\pi\pi$ and multi-pion loops respectively. The solid line represents the vacuum case.

6.1.2 Effect of temperature dependent chemical potential on shear viscosity

In this section the effect of chemical potential will be discussed on the temperature dependence of shear viscosity. First we have plotted η versus T at three different values of chemical potential for vacuum cross section only. The three values of chemical potentials are $\mu_\pi = 0$ that corresponds to chemical freeze out, $\mu_\pi = 85\text{MeV}$ that corresponds to kinetic freeze out, and finally the temperature dependent pion chemical potential, $\mu_\pi = \mu_\pi(T)$ that has been discussed in Chapter-5. We recall that this temperature dependent pion chemical potential has been introduced in order to keep the particle number fixed in the temperature range between chemical and kinetic freeze out. In Fig. 6.2, the curve with $\mu_\pi = \mu_\pi(T)$ depicts the situation when μ_π increases as the temperature decreases as mentioned in Chapter-5. This resembles the situation encountered in the later stages of heavy ion collisions and interpolates between the results with the constant values of the pion chemical potential mentioned above at $T = 100\text{MeV}$ and $T = 170\text{MeV}$.

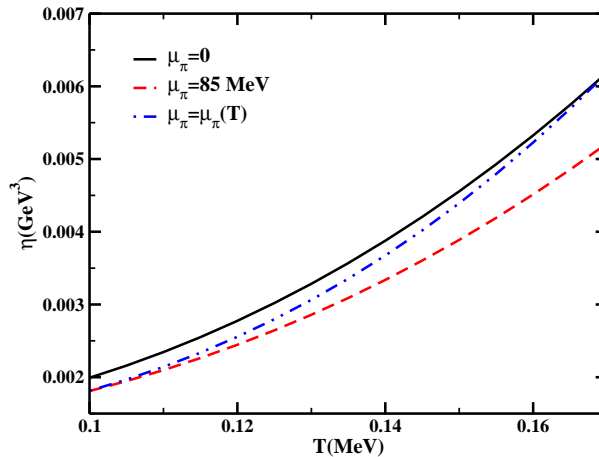


Figure 6.2: The shear viscosity as a function of temperature for different values of pion chemical potentials using vacuum cross section.

In Fig. 6.3, the shear viscosity η has been plotted against T for both $\mu_\pi = 0$ and $\mu_\pi = \mu_\pi(T)$ case where the in medium cross section has been used along with the vacuum case. In a thermal medium the effect of chemical potential enters into the expression of η in two ways, one in the phase space, i.e, through the distribution functions of the interacting pions and the other in interaction dynamics, i.e, through the distribution function of the loop particles contributing to the in medium ρ and σ propagators. In both sets of graphs the effect of a thermal medium is clearly visible. The three curves in each set show the effect of medium on the $\pi\pi$ cross-section. The dashed lines in each of the sets depict medium effects for pion loops in the ρ propagator and the dash-dotted lines correspond to the situation when the heavy mesons are included i.e. for πh loops where $h = \pi, \omega, h_1, a_1$. The clear separation between the curves in each set displays a significant effect brought about by the medium dependence of the cross-section even for temperature dependent pion chemical potential [2].

6.1.3 Effect of medium on shear viscosity to entropy density ratio

Viscosities for relativistic fluids are generally expressed in terms of a dimensionless ratio obtained by dividing it with the entropy density of the system. The latter is obtained from the

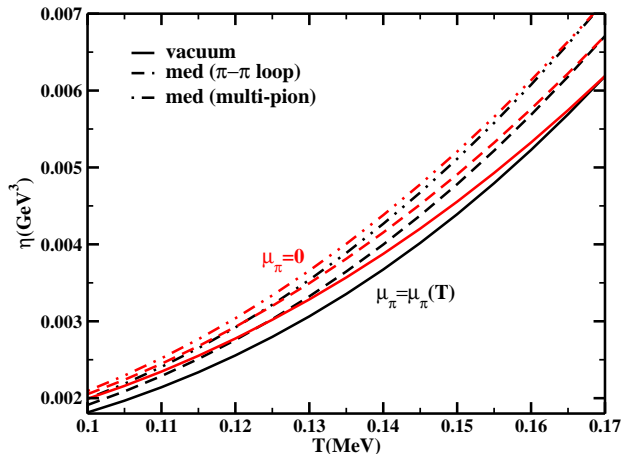


Figure 6.3: The shear viscosity in various scenarios as a function of T . The red (upper) and the black (lower) sets of curves correspond to $\mu_\pi = 0$ MeV and $\mu_\pi = \mu_\pi(T)$ respectively. In each set the solid line represents the vacuum cross-section, the dashed line represents the in-medium modification due to pion loop and the dash-dotted line for loops with heavy particles in addition.

thermodynamic relation

$$Ts = \epsilon + P - n\mu_\pi . \quad (6.1)$$

For a free pion gas, the expressions of the energy density ϵ , pressure P and number density n are derived in Chapter-2. With the help of these quantities the expression for the entropy density comes out to be,

$$s = \frac{g_\pi}{2\pi^2} m_\pi^2 [m_\pi S_3^1(z) - \mu_\pi S_2^1(z)] \quad g_\pi = 3. \quad (6.2)$$

Interactions between pions lead to corrections to this formula. To $O(T^6)$ this has been calculated for finite pion chemical potential in [4] using chiral perturbation theory to give

$$\Delta s = -\frac{3m_\pi^4}{16\pi^4 f_\pi^2} S_1^1(z) [m_\pi S_2^0(z) - \mu_\pi S_1^0(z)] \quad (6.3)$$

where $f_\pi = 93$ MeV. It is easily verified that this expression reduces for $\mu_\pi = 0$ to those given in [5, 6]. This correction is $\sim 1 - 2\%$ for values of μ_π and T considered here. In Fig. 6.4 the entropy density of an interacting pion gas as a function of temperature is shown for three values of the pion chemical potential mentioned earlier.

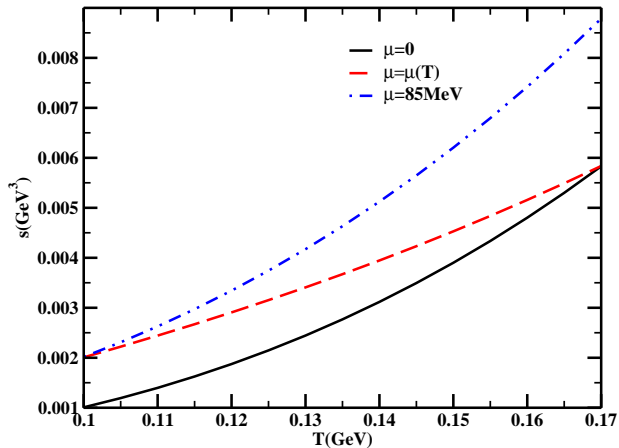


Figure 6.4: The entropy density of an interacting pion gas as a function of T for different values of the pion chemical potential.

In Fig. 6.5 η/s is plotted as a function of T using different pion chemical potentials. The red and the blue set of curves corresponding to $\mu_\pi = 0$ and $\mu_\pi = 85$ representing the values of μ_π at chemical and kinetic freeze out show the usual decreasing trend as seen, for example in [8, 9] while the black set of curves with $\mu_\pi = \mu_\pi(T)$ increases with T in contrast with the other two sets. The values in all cases remain well above $1/4\pi$ which is the lower bound of the η/s value conjectured by Kovtun, Starinets and Sonnenschein [7] from their AdS/CFT calculations. The effect of medium is still clearly visible in each set of curves portraying the effect of finite temperature on the shear viscosity to entropy density ratio for each value of pion chemical potential. For each value of μ_π the temperature dependence of η/s ratio appears to be enhanced which turns out to be larger for the multipion loop contribution in the in-medium thermal ρ propagator compared to only the pion loop effect.

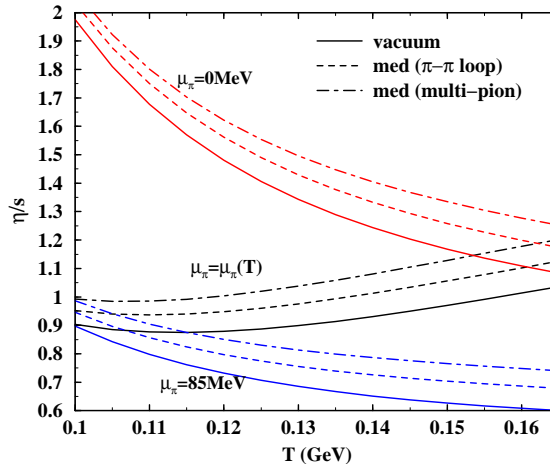


Figure 6.5: η/s as a function of T for different values of μ_π .

6.2 Bulk Viscosity

6.2.1 Effect of medium and temperature dependent chemical potential on bulk viscosity

In this section we present the results for bulk viscosity ζ as a function of temperature T . In Fig. 6.6 the three sets of curves correspond to different values of the pion chemical potential. The uppermost set of curves (with circles) show the bulk viscosity calculated with a pion chemical potential $\mu_\pi \sim 85$ MeV. The corresponding curves in the lowermost set are evaluated with $\mu_\pi = 0$. These values are representative of the kinetic and chemical freeze-out in heavy ion collisions respectively. The solid line in the lowermost set represents the case where the vacuum cross-section has been used and agrees with the estimate in [10]. The set of curves with triangles depicts the situation when μ is a (decreasing) function of temperature as given in [11]. This resembles the situation encountered in the later stages of heavy ion collisions and the curves interpolate between the sets with the constant values of the pion chemical potential discussed above. The three curves in each set show the effect of medium on the $\pi\pi$ cross-section. The short-dashed lines in each of the sets depict medium effects for pion loops in the ρ propagator and the long dashed lines correspond to the situation when the heavy mesons are included

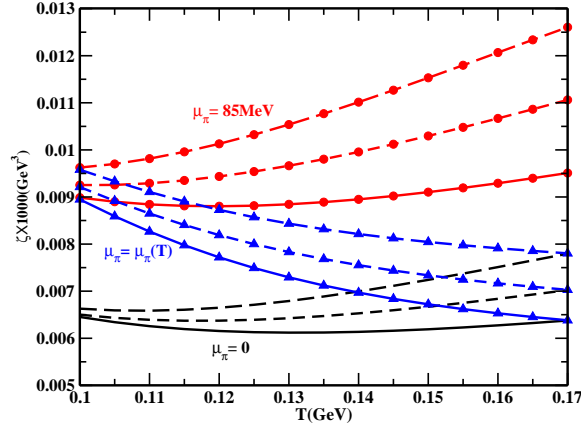


Figure 6.6: The bulk viscosity in various scenarios as a function of T . The upper (with circles), middle (with triangles) and lower sets of curves correspond to $\mu_\pi = 85$ MeV, $\mu_\pi = \mu_\pi(T)$ and $\mu_\pi = 0$ respectively. In each set the solid lines represents use of vacuum cross-section, the small dashed lines for in-medium modification due to pion loop and the long dashed lines for loops with heavy particles in addition.

i.e. for πh loops where $h = \pi, \omega, h_1, a_1$. The clear separation between the curves in each set displays a significant effect brought about by the medium dependence of the cross-section. A large dependence on the pion chemical potential is also inferred since the three sets of curves appear nicely separated [2].

6.2.2 Effect of medium and temperature dependent chemical potential on bulk viscosity to entropy density ratio

In Fig. 6.7 we show ζ/s as a function of T using the temperature dependent pion chemical potential. The medium dependence is clearly observed when we compare the results obtained using the vacuum cross-section with the ones where the σ and ρ propagation is modified due to $\pi\pi$ and πh (multi-pion) loops [2]. The decreasing trend with increasing temperature was observed also in [12] and [13].

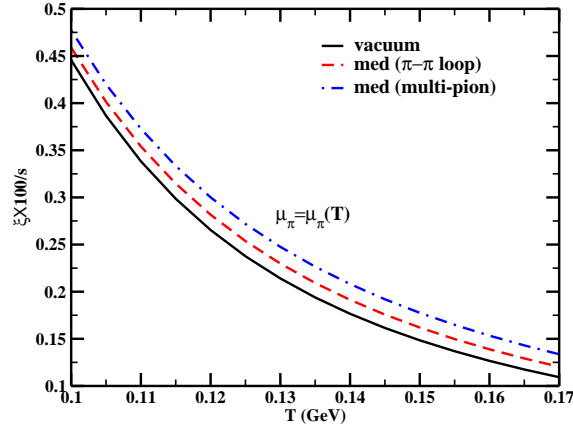


Figure 6.7: ζ/s as a function of T for different $\pi\pi$ cross-section. The temperature dependent pion chemical potential has been used in all cases.

6.3 Thermal conductivity

6.3.1 Effect of medium on thermal conductivity

The results of the temperature dependent thermal conductivity have been shown introducing the vacuum as well as medium widths in the dynamical cross section. In fig. 6.8 the thermal conductivity times the temperature T is plotted against the temperature for zero chemical potential of the pion gas. The three different curves explicitly show the effect of a finite temperature medium on the $\pi\pi$ cross-section, which in turn reflects on the temperature dependence of λ . The lowermost solid-lined curve indicate the vacuum cross-section without medium effect. The other two curves have been plotted introducing the medium dependent cross-section using ρ and σ self-energy. The dashed line depict the medium effect when only $\pi\pi$ loop is taken in the ρ self-energy. Lastly the dot-dashed line corresponds to the case when also the heavy mesons are introduced in the ρ self-energy, i.e. $\pi\pi$, $\pi\omega$, πa_1 , πh_1 loops are considered.

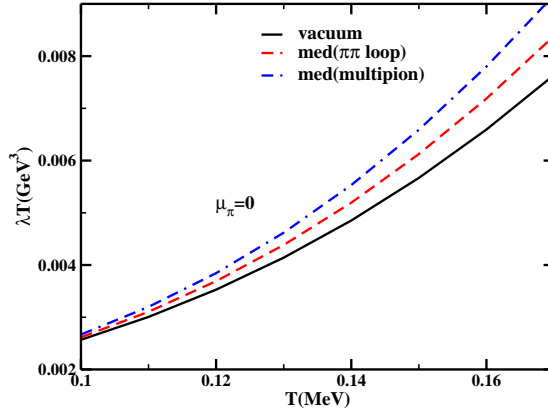


Figure 6.8: λT as a function of T for different $\pi\pi$ cross-sections with zero pion chemical potential.

6.3.2 Effect of temperature dependent chemical potential on thermal conductivity

In Fig. 6.9 again λT is plotted as a function of temperature, but this time we have used a temperature dependent pion chemical potential. In this plot also the effect of medium dependent cross-section is clearly visible when compared with the vacuum cross-section. The effect of temperature dependent pion chemical potential shows noticeable differences on the temperature dependence of thermal conductivity of pion gas with respect to the $\mu_\pi = 0$ case [3].

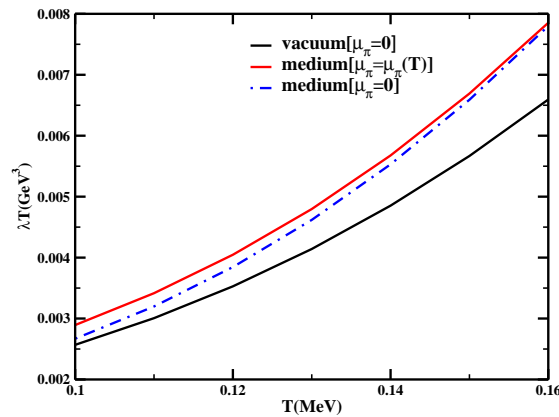


Figure 6.9: λT as a function of T for different $\pi\pi$ cross-sections and chemical potentials.

6.4 Effect of medium and temperature dependent chemical potential on relaxation times of dissipative flows

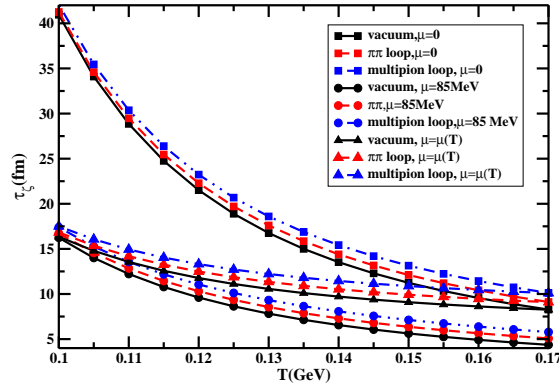


Figure 6.10: Relaxation time of bulk viscous pressure as a function of T for different $\pi\pi$ cross-sections with different pion chemical potentials.

In this section we present the effect of the thermal medium on the temperature dependence of the relaxation times of the dissipative flows [14]. We start with the results for the relaxation time of the bulk viscous flow τ_ζ , as a function of temperature. In Fig. 6.10 the three different set of curves correspond to different values of the pion chemical potentials. The uppermost set of curves (with squares) show the temperature dependence of τ_ζ calculated with a pion chemical potential $\mu_\pi = 0$. The corresponding curves in the lowermost set (with circles) are evaluated with $\mu_\pi \sim 85 \text{ MeV}$. These values are representative of the chemical and kinetic freeze-outs in heavy ion collisions, respectively. The set in between consists of curves with triangles use the temperature dependent pion chemical potential $\mu_\pi = \mu_\pi(T)$ and interpolates between the points representing chemical and kinetic freeze-outs. In each set the τ_ζ shows a decreasing trend with temperature which is in accordance with [15]. The three different curves in each set show the effect of the medium on the $\pi\pi$ cross section. The lowermost solid curve in each set of Fig. 6.10 represents vacuum cross section with no medium effect which agrees with [10] for zero chemical potential case. The dashed curves depict medium effects for pion loops in the ρ propagator. These curves appear to be enhanced with respect to the vacuum ones indicating the effect of a thermal medium on τ_ζ . Finally the dot-dashed curves correspond

to the situation when the heavy mesons are included in the ρ propagator loop, i.e., for πh loops where $h = \pi, \omega, h_1, a_1$. These curves appear to be further enhanced showing the larger effect of the multipion loop propagator on τ_ζ . The clear separation between the curves in each set displays a significant effect brought about by the medium dependence of the $\pi\pi$ cross section.

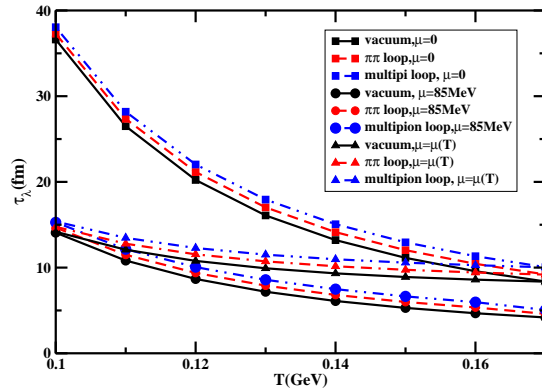


Figure 6.11: Relaxation time of heat flow as a function of T for different $\pi\pi$ cross-sections with different pion chemical potentials.

Next we plot the relaxation time for the irreversible heat flow, τ_λ against temperature for three different values of pion chemical potentials mentioned above. In each set the curves are plotted for different $\pi\pi$ cross sections. Alike the earlier case here also we notice that the medium modified cross sections evaluated at finite temperature influence the temperature dependence of τ_λ which appear to be enhanced for the in medium cases with respect to the vacuum ones. The multipion loop contribution due to heavier mesons in the ρ propagator turns out to be more significant than the $\pi\pi$ loop in the same. In Fig. 6.11 the nicely separated three curves in each set plotted as a function of temperature reveal the effects of medium on the temperature dependence of τ_λ .

Finally we present our result of τ_η , i.e, the relaxation time of the shear viscous flow for a medium induced $\pi\pi$ cross section. In Fig. 6.12 the three set of curves indicate three different values of chemical potential demonstrating the effect of μ_π on the values of τ_η . In each set the temperature dependence of τ_η is shown for vacuum cross section (solid curves), medium

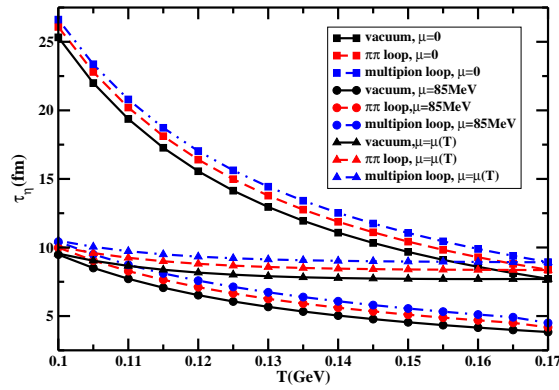


Figure 6.12: Relaxation time of shear viscous pressure as a function of T for different $\pi\pi$ cross-sections with different pion chemical potentials.

dependent cross section with $\pi\pi$ loop in the thermal ρ propagator (dashed curves) and with multipion loops in ρ propagator (dot-dashed curves) respectively. The effect of medium is shown by the enhancement of the curves which appears to be more significant for multipion case than $\pi\pi$ loop. In all the three cases (τ_ζ , τ_λ and τ_η) the effect of medium on relaxation times increases with increasing temperature.

6.5 Discussions

We end this Chapter by stating that the main focus in this work has been to emphasize the role of medium modifications of the cross-section in the evaluation of the transport coefficients. The transport coefficients and their temperature dependence could affect the quantitative estimates of signals of heavy ion collisions particularly where hydrodynamic simulations are involved. For example, it has been argued in [16] that corrections to the freeze-out distribution due to bulk viscosity can be significant. As a result the hydrodynamic description of the p_T spectra and elliptic flow of hadrons could be improved by including a realistic temperature dependence of the transport coefficients. So a realistic evaluation of these quantities is essential to obtain the proper temperature profile and consequently the cooling laws of the evolving system. In addition it is found that the relaxation times of the bulk viscous flow and the heat flow to be

of similar magnitude to that of the shear viscous flow which suggests that they should all be taken into consideration in dissipative hydrodynamic simulations.

Bibliography

- [1] S. Mitra, S. Ghosh and S. Sarkar, Phys. Rev. C **85** (2012) 064917 [arXiv:1204.2388 [nucl-th]].
- [2] S. Mitra and S. Sarkar, Phys. Rev. D **87** (2013) 9, 094026 [arXiv:1303.6408 [hep-ph]].
- [3] S. Mitra and S. Sarkar, Phys. Rev. D **89** (2014) 5, 054013 [arXiv:1403.3554 [nucl-th]].
- [4] D. Fernandez-Fraile and A. Gomez Nicola, Phys. Rev. D **80** (2009) 056003.
- [5] P. Gerber and H. Leutwyler, Nucl. Phys. B **321** (1989) 387.
- [6] R. Lang, N. Kaiser and W. Weise, Eur. Phys. J. A **48** (2012) 109.
- [7] P. Kovtun, D. T. Son and A. O. Starinets, Phys. Rev. Lett. **94**, 111601 (2005).
- [8] K. Itakura, O. Morimatsu and H. Otomo, Phys. Rev. D **77** (2008) 014014 [arXiv:0711.1034 [hep-ph]].
- [9] E. Nakano, hep-ph/0612255.
- [10] D. Davesne, Phys. Rev. C **53**, 3069 (1996).
- [11] T. Hirano and K. Tsuda, Phys. Rev. C **66** (2002) 054905
- [12] E. Lu and G. D. Moore, Phys. Rev. C **83** (2011) 044901.
- [13] A. Dobado, F. J. Llanes-Estrada and J. M. Torres-Rincon, Phys. Lett. B **702** (2011) 43.
- [14] S. Mitra, U. Gangopadhyaya and S. Sarkar, submitted to PRD.

- [15] M. Prakash, M. Prakash, R. Venugopalan and G. Welke, Phys. Rept. **227** (1993) 321.
- [16] K. Dusling and T. Schafer, Phys. Rev. C **85** (2012) 044909.

Chapter 7

Drag and Diffusion of hidden charm mesons in hadronic medium

7.1 Introduction

The experimental evidence of J/ψ suppression by NA50 [1], NA60 [2] as well as by the PHENIX [3] collaboration has long been suggested as a signal of quark-gluon plasma formation in heavy ion collisions [4, 5]. However, other mechanisms based on J/ψ absorption by comoving hadrons have also been proposed as an alternative suppression mechanism to explain the phenomenon [6]. In this connection the inelastic scattering rates of J/ψ in the hadronic phase have been investigated with the help of different effective hadronic models [7, 8, 9]. In addition, the opening of $J/\psi \rightarrow D\bar{D}$ decay in the medium due to in-medium modification of D mesons [10, 11] may also play a significant role in J/ψ suppression in a hadronic environment.

Heavy quark transport in hadronic matter is a topic of high contemporary interest [12, 13, 14, 15, 16, 17]. The drag and diffusion of open charm [14] and bottom [16] mesons and the role of hadronic matter in their suppression in heavy ion collisions [18] have been investigated using effective hadronic interactions based on heavy quark effective theory. The suppression of heavy flavour in the hadronic phase was found to be more significant at RHIC than at LHC suggesting

that the characterization of QGP at LHC could be less complicated than at RHIC. Recently the drag and diffusion of the Λ_c baryon are also obtained in hadronic matter [19] and found to be significant. In fact, the drag of the Λ_c being lower than that of the D mesons was seen to non-trivially affect the p_T dependence of the Λ_c/D ratio and thus the R_{AA} of single electrons originating from the decay of Λ_c . Motivated by these interesting results we evaluate in this work the drag and diffusion of hidden charm mesons J/ψ and η_c and study their dependence with temperature.

In the next few section the formulae for the drag and diffusion coefficients will be provided followed by a discussion on the matrix elements of elastic scattering of the J/ψ with the light vector mesons. Finally in the result section the drag and diffusion coefficients will be given for J/ψ and η_c .

7.2 Formalism

The drag (γ) and diffusion (D) coefficients of J/ψ are obtained from the elastic scattering of J/ψ with the light thermal hadrons (H) which constitute the equilibrated thermal medium. For the process $J/\psi(p_1) + H(p_2) \rightarrow J/\psi(p_3) + H(p_4)$, the drag γ can be expressed as [20]:

$$\gamma = p_i A_i / p^2 \quad (7.1)$$

where A_i is given by

$$A_i = \frac{1}{2E_{p_1}} \int \frac{d^3 p_2}{(2\pi)^3 E_{p_2}} \int \frac{d^3 p_3}{(2\pi)^3 E_{p_3}} \int \frac{d^3 p_4}{(2\pi)^3 E_{p_4}} \frac{1}{g_{J/\psi}} \sum |\overline{M}|^2 (2\pi)^4 \delta^4(p_1 + p_2 - p_3 - p_4) f(p_2) \{1 \pm f(p_4)\} [(p_1 - p_3)_i] \equiv \langle\langle (p_1 - p_3)_i \rangle\rangle, \quad (7.2)$$

$g_{J/\psi}$ is the statistical degeneracy of the probe particle, J/ψ . The thermal distribution function $f(p_2)$ of the hadron H in the incident channel takes the form of Bose-Einstein or Fermi-Dirac distribution depending on its spin and the terms $1 \pm f(p_4)$ are their corresponding Bose enhanced

or Pauli blocked phase space factor in their final states. The drag coefficient of Eq.(8.1) is just a measure of the thermal average of the momentum transfer, $p_1 - p_3$ weighted by the square of the invariant amplitude $\overline{|M|^2}$.

In a similar way, the diffusion coefficient D can be defined as:

$$D = \frac{1}{4} \left[\langle \langle p_3^2 \rangle \rangle - \frac{\langle \langle (p_1 \cdot p_3)^2 \rangle \rangle}{p_1^2} \right]. \quad (7.3)$$

With an appropriate choice of $T(p_3)$ both the γ and D can be obtained from a single expression, which is given by

$$\begin{aligned} \langle \langle T(p_1) \rangle \rangle = & \frac{1}{512\pi^4} \frac{1}{E_{p_1}} \int_0^\infty \frac{p_2^2 dp_2 d(\cos\chi)}{E_{p_2}} \\ & \hat{f}(p_2) \{1 \pm f(p_4)\} \frac{\lambda^{\frac{1}{2}}(s, m_{p_1}^2, m_{p_2}^2)}{\sqrt{s}} \int_1^{-1} d(\cos\theta_{c.m.}) \\ & \frac{1}{g} \sum \overline{|M|^2} \int_0^{2\pi} d\phi_{c.m.} T(p_3) \end{aligned} \quad (7.4)$$

where $\lambda(s, m_{p_1}^2, m_{p_2}^2) = (s - m_{p_1}^2 - m_{p_2}^2)^2 - 4m_{p_1}^2 m_{p_2}^2$ is the triangular function.

7.3 Dynamics

The hot hadronic matter produced in the later stages of relativistic heavy ion collisions is populated by light pseudoscalars and vector mesons like $\pi, K, \eta, \rho, \omega$ and ϕ . The magnitude of such scatterings are estimated either by introducing different perturbative or non-perturbative approach at quark level [21, 22] or by using an effective Lagrangian to calculate Feynman diagrams. Concerning the latter approach, SU(4) is the smallest possible symmetry group which includes the charmonium state explicitly along with the light and heavy pseudoscalar and vector mesons.

The corresponding pseudoscalar and vector meson matrices and as well as the chiral Lagrangian is explicitly given in works like [23, 24]. However since SU(4) symmetry is badly broken by the large mass of the charmed meson, terms involving hadron masses are included to the chiral Lagrangian using the experimentally determined values.

Since pions are identified with the Nambu-Goldstone bosons of QCD their interaction strength with other particles should abruptly decrease in the chiral limit. We recall the standard relation [25, 26] for the s-wave scattering length of pion with a heavy meson like say J/ψ ,

$$a_{l=0}^{\pi J/\psi} = -\left(1 + \frac{m_\pi}{m_{J/\psi}}\right)^{-1} \frac{m_\pi}{4\pi F_\pi^2} \vec{I}_\pi \cdot \vec{I}_{J/\psi} + \mathcal{O}(m_\pi^2), \quad (7.5)$$

with the dot product defined as,

$$\vec{I}_\pi \cdot \vec{I}_{J/\psi} = \frac{1}{2}[I(I+1) - I_{J/\psi}(I_{J/\psi}+1) - I_\pi(I_\pi+1)]. \quad (7.6)$$

$I_\pi, I_{J/\psi}$ are respectively the isospin quantum numbers of the pion and J/Ψ and I represents their total isospin quantum number. In the chiral limit ($m_\pi \rightarrow 0$), the first term of eq.(7.5) exactly vanishes. When the other hadron is much heavier like J/ψ or η_c , this term in (7.5) vanishes exactly, not only in the chiral limit but also for finite pion mass (because $\vec{I}_\pi \cdot \vec{I}_{J/\psi} = 0$). Hence the contribution of the pion in the charmonium scattering length starts from $\mathcal{O}(m_\pi^2)$, which shows that at least at low energy the pion-charmonium interaction should be very weak. To support this argument we refer to the calculations of the meson exchange model of Haglin et.al [23]. From their calculations we can see that the elastic channels of J/Ψ interaction involving the light pseudoscalars are significantly smaller in comparison with the vector mesons. They suggest that π, η , and K elastic cross sections with J/Ψ are of order 100 fb, 1 nb and 100 nb respectively. On the other hand the contributions for elastic scattering with ρ, ω and ϕ mesons are quantitatively much larger, up to about a few mb. We hence consider the elastic scattering of the heavy charmonium states like J/Ψ and η_c with vector mesons only. These processes involve vector-vector-pseudoscalar interactions which are not present in the chiral Lagrangian. The relevant effective interaction describing $J + V \rightarrow \eta_c \rightarrow J/\Psi + V$ processes [23] is

$$\mathcal{L}_{JV\eta_c} = g_{JV\eta_c} \epsilon_{\alpha\beta\sigma\delta} \{\partial^\alpha J/\Psi^\beta\} \{\partial^\sigma V^\delta\} \eta_c \quad (7.7)$$

where $g_{JV\eta_c} = 2.44 \text{ GeV}^{-1}$, 7.03 GeV^{-1} and 4.51 GeV^{-1} for $V = \rho, \omega$ and ϕ respectively [23].

The s and u channel diagrams for the process $J/\Psi + V \rightarrow \eta_c \rightarrow J/\Psi + V$ are shown in the panels (A) and (B) of Fig.7.1. The matrix elements for the two channels are respectively given

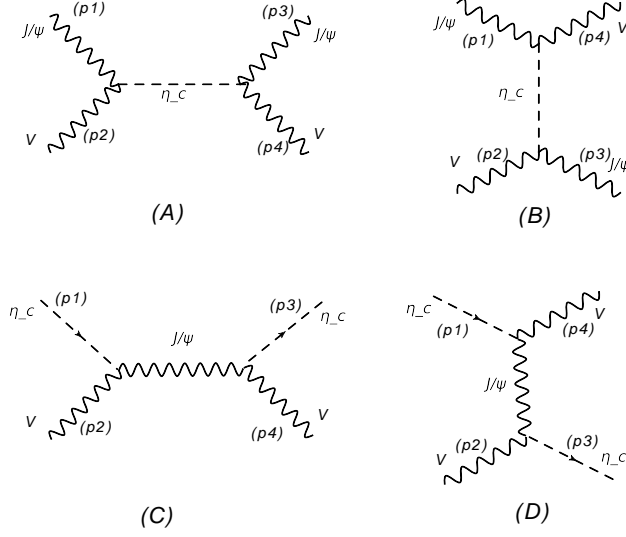


Figure 7.1: The s and u channel of J/ψ - V scattering via η_c exchange are respectively depicted in diagrams (A) and (B). Diagrams (C) and (D) are the same for the η_c - V scattering via J/ψ .

by,

$$M_s = -g_{JV\eta_c}^2 [\varepsilon^\beta(p_1) \varepsilon^\delta(p_2) \varepsilon^{*\beta_1}(p_3) \varepsilon^{*\delta_1}(p_4) \epsilon_{\alpha\beta\sigma\delta} p_1^\alpha p_2^\sigma \epsilon_{\alpha_1\beta_1\sigma_1\delta_1} p_3^{\alpha_1} p_4^{\sigma_1}] / (s - m_{\eta_c}^2) \quad (7.8)$$

and

$$M_u = -g_{JV\eta_c}^2 [\varepsilon^\beta(p_1) \varepsilon^{*\delta}(p_4) \varepsilon^{\delta_1}(p_2) \varepsilon^{*\beta_1}(p_3) \epsilon_{\alpha\beta\sigma\delta} p_1^\alpha p_4^\sigma \epsilon_{\alpha_1\beta_1\sigma_1\delta_1} p_2^{\sigma_1} p_3^{\alpha_1}] / (u - m_{\eta_c}^2). \quad (7.9)$$

The modulus square of the spin averaged total amplitude for the processes of $J/\Psi + V \rightarrow \eta_c \rightarrow J/\Psi + V$ is given by the following expression,

$$\overline{|M|^2} = \overline{|M_s|^2} + \overline{|M_u|^2} + 2\overline{M_s M_u^*} \quad (7.10)$$

where the respective terms in the expression are given by

$$\begin{aligned} \overline{|M_s|^2} &= \frac{g_{JV\eta_c}^4}{36(s - m_{\eta_c}^2)^2} \lambda^2(s, m_{J/\psi}^2, m_V^2) \\ \overline{|M_u|^2} &= \frac{g_{JV\eta_c}^4}{36(u - m_{\eta_c}^2)^2} \lambda^2(u, m_{J/\psi}^2, m_V^2) \\ \overline{M_s M_u^*} &= \frac{g_{JV\eta_c}^4}{9(s - m_{\eta_c}^2)(u - m_{\eta_c}^2)} I. \end{aligned}$$

where,

$$\begin{aligned} I = & \frac{1}{8} [m_J^8 + s^4 + 2s^3(t - 2m_V^2) + 2sm_V^4(t - 2m_V^2) \\ & - 4m_J^6(s + m_V^2) + m_V^4(t^2 + m_V^4) \\ & + s^2(t^2 - 4tm_V^2 + 6m_V^4) \\ & + m_J^4(6s^2 + t^2 + 6m_V^4 + 2s(t + 2m_V^2)) \\ & - 2m_J^2\{2s^3 + 2s(t - m_V^2)(s + m_V^2) \\ & + m_V^2(t^2 + 2m_V^4)\}]. \end{aligned}$$

and $\lambda(x, y, z) = x^2 + y^2 + z^2 - 2xy - 2yz - 2zx$ is the triangular function.

Next the s and u channel diagrams of the η_c meson scattering with the thermalized vector mesons by exchanging J/Ψ are shown in the panels (C) and (D) of Fig. 7.1. The respective matrix elements are given by

$$\begin{aligned} M_s = & -g_{JV\eta_c}^2 [\varepsilon^\delta(p_2) \varepsilon^{*\delta_1}(p_4) \epsilon_{\alpha\beta\sigma\delta} (p_1 + p_2)^\alpha p_2^\sigma \\ & \epsilon_{\alpha_1\beta_1\sigma_1\delta_1} (p_1 + p_2)^{\alpha_1} p_4^{\sigma_1}] \{ -g^{\beta\beta_1} + \\ & \frac{(p_1 + p_2)^\beta (p_1 + p_2)^{\beta_1}}{m_J^2} \} / (s - m_J^2) \end{aligned} \quad (7.11)$$

and

$$\begin{aligned} M_u = & -g_{JV\eta_c}^2 [\varepsilon^{*\delta}(p_4) \varepsilon^{\delta_1}(p_2) \epsilon_{\alpha\beta\sigma\delta} (p_1 - p_4)^\alpha p_4^\sigma \\ & \epsilon_{\alpha_1\beta_1\sigma_1\delta_1} (p_1 - p_4)^{\alpha_1} p_2^{\sigma_1}] \{ -g^{\beta\beta_1} + \\ & \frac{(p_1 - p_4)^\beta (p_1 - p_4)^{\beta_1}}{m_J^2} \} / (u - m_J^2) \end{aligned} \quad (7.12)$$

The spin averaged modulus square of total amplitude for the processes $\eta_c + V \rightarrow J/\psi \rightarrow \eta_c + V$ are given by

$$\overline{|M|^2} = \overline{|M_s|^2} + \overline{|M_u|^2} + 2\overline{M_s M_u^*} \quad (7.13)$$

where

$$\begin{aligned} \overline{|M_s|^2} = & (g_{JV\eta_c}^4/3) \left\{ \frac{s}{4} (t - 4m_V^2)(s + m_V^2 - m_{\eta_c}^2)^2 \right. \\ & + \frac{1}{8} (s + m_V^2 - m_{\eta_c}^2)^4 \\ & \left. + \frac{s^2}{4} (t^2 - 4tm_V^2 + 8m_V^4) \right\} / (s - m_J^2)^2. \end{aligned}$$

$$\begin{aligned} \overline{|M_u|^2} = & (g_{JV\eta_c}^4/3) \left\{ \frac{u}{4} (t - 4m_V^2)(u + m_V^2 - m_{\eta_c}^2)^2 \right. \\ & + \frac{1}{8} (u + m_V^2 - m_{\eta_c}^2)^4 \\ & \left. + \frac{u^2}{4} (t^2 - 4tm_V^2 + 8m_V^4) \right\} / (u - m_J^2)^2. \end{aligned}$$

and

$$\begin{aligned} \overline{M_s M_u^*} = & (g_{JV\eta_c}^4/3) \frac{1}{8} [m_{\eta_c}^8 + m_V^8 + s^4 - 4m_{\eta_c}^6(m_V^2 + s) \\ & + 2m_V^4 s(3s - t) + 2s^3 t - st^3 + m_V^6(-4s + 2t) \\ & - 2m_V^2 s(2s^2 + st - 2t^2) \\ & + 2m_{\eta_c}^4 \{3m_V^4 + m_V^2(2s + t) + s(3s + t)\} \\ & - 2m_{\eta_c}^2 \{2m_V^6 - 2m_V^2 s(s - 2t) - 2m_V^4(s - t) \\ & + s(2s^2 + 2st - t^2)\}] / (s - m_J^2)(u - m_J^2). \end{aligned}$$

Using these scattering amplitudes in eq. (7.4) we obtain the drag and diffusion coefficients of the J/Ψ and η_c mesons in hadronic matter.

The low-energy interactions of J/Ψ (as well as η_c) with π , ρ or N have been investigated by Yokokawa et. al [?] in the quenched lattice framework. From the scattering lengths, a (say) of J/Ψ interacting with light hadrons H (where $H = \pi, \rho$ and N) we can extract the dimensionless threshold, the T -matrix element by using the relation

$$T = 4\pi(m_J + m_H)a. \quad (7.14)$$

Using these $\overline{|T|^2}$ in place of $\overline{|M|^2}$ in Eq. (7.4), we can get an alternative estimation of the diffusion (and drag) coefficients of J/Ψ as well as η_c mesons in hadronic matter. The extracted values of T from a (in fm) are given in Table I.

	$J/\Psi\pi$	$J/\Psi\rho$	$J/\Psi N$
$a(fm)$	0.01 ± 0.003	0.23 ± 0.04	0.71 ± 0.4
T	2 ± 0.4	50 ± 15	180 ± 120
	$\eta_c\pi$	$\eta_c\rho$	$\eta_c N$
$a(fm)$	0.01 ± 0.003	0.21 ± 0.1	0.5 ± 0.6
T	2.2 ± 0.6	50.20 ± 25	174.85 ± 150

Table 7.1: Table showing the extracted values of T-matrix from the spin averaged values of scattering length, a , which are obtained in the framework of quenched lattice calculation by Yokokawa et. al [?].

7.4 Results

We begin this section by plotting in Fig. 7.2 the drag coefficients of the J/ψ (solid line) and η_c mesons (dashed line) as a function of temperature.

In Fig. 7.3 the corresponding results for the case where the amplitudes are extracted from scattering lengths are shown. Not much difference is seen between the J/Ψ and η_c in this case. As mentioned before the drag is a measure of the momentum transfer between the J/Ψ and the thermal hadrons weighted by the interactions implemented through $|M|^2$. The average momentum of the bath particles increase with temperature. Therefore, the thermal hadrons gain the ability to transfer larger momentum through interactions as the temperature of the bath increases. This causes the rise of drag at high temperatures both for J/Ψ and η_c .

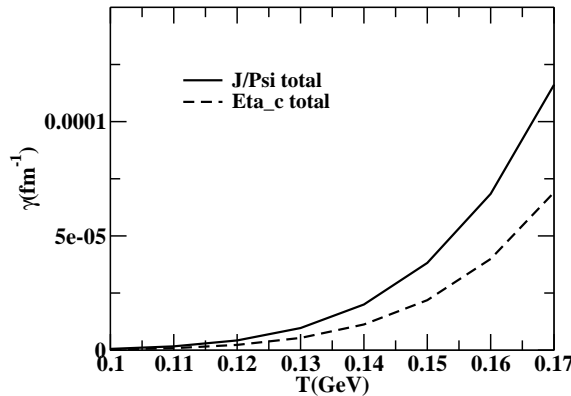


Figure 7.2: The drag coefficient (γ) as a function of temperature calculated in the effective Lagrangian approach.

Let us now show results for the diffusion coefficient D . This is plotted against T in Figs. 7.4 and 7.5 respectively corresponding to the effective Lagrangian and scattering length approaches. In addition to the results of direct calculation using eq. (7.4), also shown are the results using the fluctuation-dissipation theorem (in red). As for the earlier case of the drag coefficient, the diffusion in the scattering length approach is similar for the J/Ψ and η_c mesons. The rise of diffusion coefficients with increasing temperature has the same origin as that of drag coefficients as explained above.

7.5 Discussions

The momentum suppression of J/Ψ at high momenta in nuclear collisions compared to proton-proton collision may be approximately estimated as, $R_{AA} \sim e^{-\Delta\tau\gamma}$ [13], where $\Delta\tau$ is typically the life time of the hadronic phase. Taking $\Delta\tau \sim 5$ fm/c and $\gamma \sim 10^{-4}$ one finds that R_{AA} is close to unity. Thus the hadronic phase appears to play no significant role in the suppression of J/ψ at high p_T . Therefore, if a significant suppression is observed that will indicate the presence of QGP in the evolving fireball produced in heavy ion collisions at relativistic energies.

So the drag and diffusion coefficients of J/ψ and η_c in a hot hadronic medium using effective field theory and T matrices have been estimated. The values of these transport coefficients

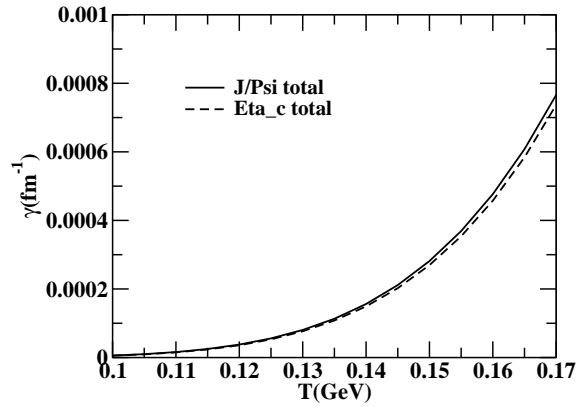


Figure 7.3: The drag coefficient (γ) as a function of temperature obtained using scattering lengths.

turn out to be small compared to the values obtained for open charmed hadrons for the temperature range relevant for the hadronic phase expected to be formed in the later stages of the evolving matter produced in nuclear collisions at RHIC and LHC energies. It is found that the momentum suppression of J/Ψ and η_c are not significant in the hadronic phase. Therefore, such a suppression if observed experimentally will possibly indicate creation of QGP in heavy ion collisions at relativistic energies.

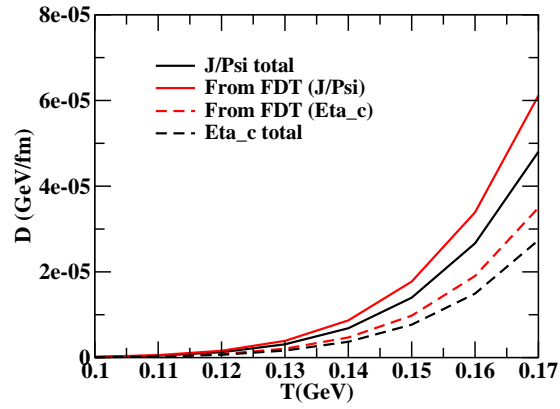


Figure 7.4: The diffusion coefficient (D) as a function of temperature calculated in the effective Lagrangian approach.

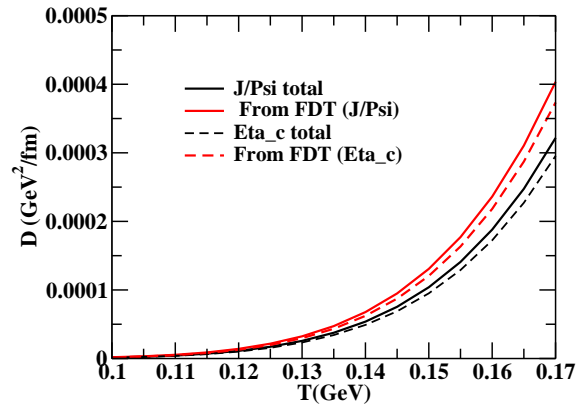


Figure 7.5: The diffusion coefficient (D) as a function of temperature obtained using scattering lengths.

Bibliography

- [1] M. Gonin et al. [NA50 Collaboration], Nucl. Phys. **A 610**, 404C (1996); M. C. Abreu et al. [NA50 Collaboration], Phys. Lett. **B 410**, 337 (1997); B. Alessandro et al. [NA50 Collaboration], Eur. Phys. J. **C 39**, 335 (2005).
- [2] R. Arnaldi et al. [NA60 Collaboration], Nucl. Phys. **A 774**, 711 (2006), Phys. Rev. Lett. **99**, 132302 (2007).
- [3] A. Adare et al. [PHENIX Collaboration], Phys. Rev. Lett. **98**, 172301 (2007).
- [4] T. Matsui and H. Satz, Phys. Lett. **B 178**, 416 (1986).
- [5] J. P. Blaizot and J. Y. Ollitrault, Phys. Rev. Lett. **77**, 1703 (1996).
- [6] R. Vogt, Phys. Rep. **310**, 197 (1999).
- [7] K.L. Haglin, Phys. Rev. **C 61** (2000) 031902; K.L. Haglin, C. Gale, Phys. Rev. **C 63**, 065201 (2001).
- [8] Z. Lin and C. M. Ko Phys. Rev. **C 62**, 034903 (2000).
- [9] R. Molina, C. W. Xiao, and E. Oset, Phys. Rev. **C 86**, 014604 (2012).
- [10] B. Friman, S. H. Lee, T. Song, Phys. Lett. **B 548** (2002) 153.
- [11] S. Ghosh, S. Mitra, S. Sarkar, Nucl. Phys. **A 917** (2013) 71
- [12] M. Laine, JHEP 1104 (2011) 124; D. Bodeker, M. Laine, JHEP 1207 (2012) 130.

- [13] M. He, R. J. Fries, R. Rapp, Phys. Lett. **B 701** (2011) 445.
- [14] S. Ghosh, S. K. Das, S. Sarkar, J. Alam, Phys. Rev. **D 84** (2011) 011503.
- [15] L. M. Abreu, D. Cabrera, F. J. Llanes-Estrada, J. M. Torres-Rincon, Annals Phys. 326 (2011) 2737; L. Tolos, J. M. Torres-Rincon, Phys. Rev. **D 88**, 074019 (2013).
- [16] S. K. Das, S. Ghosh, S. Sarkar, J. Alam, Phys. Rev. **D 85** (2012) 074017.
- [17] L. M. Abreu, D. Cabrera, J. M. Torres-Rincon, Phys. Rev. **D 87** (2013) 3, 034019; J. M. Torres-Rincon, arXiv:1205.0782 [hep-ph].
- [18] S. K. Das, S. Ghosh, S. Sarkar, J. Alam, Phys. Rev. **D 88** (2013) 017501.
- [19] S. Ghosh, S. K. Das, V. Greco, S. Sarkar and J. Alam, Phys. Rev. **D** (in press).
- [20] B. Svetitsky, Phys. Rev. **D 37**, 2484(1988).
- [21] M. E. Peskin, Nucl. Phys. **B156**, 365 (1979).
- [22] K.Martins, D.Blaschke, and E. Quack, Phys. Rev. **C 51**, 2723 (1995).
- [23] K.L. Haglin and C. Gale, Phys. Rev. **C 63**, 065201 (2001).
- [24] Z. Lin and C.M. Ko, Phys. Rev. **C 62**, 034903 (2000).
- [25] S. Weinberg, Phys. Rev Lett. **17**, 616 (1966)
- [26] K. Yokokawa, S. Sasaki, T. Hatsuda and A. Hayashigaki Phys. Rev. **D 74**, 034504 (2006)

Chapter 8

Effect of viscosity on the photon spectra

8.1 Introduction

Nuclear collisions at Relativistic Heavy Ion Collider (RHIC) and Large Hadron Collider (LHC) energies are aimed at creating a thermalized state of quarks and gluons called quark gluon plasma (QGP). The weakly interacting picture of the QGP stems from the perception of asymptotic freedom of QCD at high temperatures and densities. However, the experimental data from RHIC [1, 2, 3, 4] especially the measured elliptic flow of hadrons indicate that the matter produced in Au+Au collisions exhibit properties which are more like a strongly interacting liquid than a weakly interacting gas. The magnitude of the transport coefficients can be used to understand the strength of the interaction within the QGP. Therefore, the study of the transport properties of QGP and hot hadrons is of paramount importance in characterizing the matter formed in heavy ion collisions (HIC) at relativistic energies. For example, the shear viscosity or the internal friction of the fluid symbolizes the ability to transfer momentum over a distance of about one mean free path. In a system where the constituents interact strongly the transfer of momentum is performed easily - resulting in lower values of η . Consequently such a system may

be characterized by a small value of η/s where s is the entropy density. On the other hand, for a weakly interacting system the momentum transfer between the constituents becomes strenuous which gives rise to large η . The importance of viscosity also lies in the fact that it damps out the variation in the velocity and makes the fluid flow laminar. A very small viscosity (large Reynold number) may make the flow turbulent. A lower bound on the value of η/s has been found using AdS/CFT [5] (see also [6]).

Collisions between nuclei at ultra-relativistic energies produce charged particles - either in the hadronic or in the partonic state, depending on the collision energy. Interactions among these charged particles produce photons, both real and virtual. Because of their nature of interaction, the mean free path of photons in the medium (hadronic or partonic) is large compared to the size of the system formed in HIC. Therefore, photons emanating from such a system brings out the information of the source point very efficiently [7, 8, 9] (see [10, 11, 12] for review) and hence electromagnetic probes (photons and lepton pairs) may play crucial role in extracting the transport coefficients.

The effects of viscosity on the photon spectra resulting from HIC enter through two main factors: (a) the modification of the phase space factors of the constituents of the medium due to the deviation of the system from equilibrium and (b) the space time evolution of the matter governed by dissipative hydrodynamics. One more important issue deserves to be mentioned here. Normally, the initial temperature (T_i) and the thermalization time (τ_i) are constrained by the measured (final) hadron multiplicity (dN/dy). This approach is valid for a system where there is no viscous loss and the time reversal symmetry is valid. However, for a viscous system the entropy at the freeze-out point (which is proportional to the multiplicity) contains the initially produced entropy as well as the entropy produced during the space time evolution due to non-zero shear and bulk viscosities. Therefore, the amount of entropy generated during the evolution has to be subtracted from the total entropy at the freeze-out point and the remaining part which is produced initially should be used to estimate the initial temperature. As a result for a given dN/dy (which is associated with the freeze-out point) and τ_i the value of T_i will be lower in case of viscous dynamics compared to ideal flow.

Effects of viscosity on the transverse momentum distribution of photons was earlier considered in [13, 14] and recently the interest in this field is renewed [15, 16, 17]. Beyond a certain threshold in collision energy the system is expected to be formed in the QGP phase which eventually makes a transition to the hadronic matter. The measured spectra contain contributions from both QGP and hadronic phases. Therefore, it becomes imperative to estimate photon emission with viscous effects from QGP as well as hadronic matter and identify a kinematic window where photons from QGP dominate. While in some of the earlier works [15, 16, 17] contributions from hadrons were ignored, in others [13, 14] the effects of dissipation on the phase space factors were omitted. In the present work we show that if the effects of viscosity are taken into account both on the phase space factor as well as in the space-time evolution self consistently then the photon spectra alter from the ideal scenario by a quantitatively small but finite amount.

8.2 Production of thermal photons

The transverse momentum (p_T) distribution of photons from a reaction of the type: $1+2 \rightarrow 3+\gamma$ taking place in a thermal bath at a temperature, T is given by [18]:

$$E \frac{dR}{d^3p} = \frac{\mathcal{N}}{2(2\pi)^8} \int \frac{d^3p_1}{2E_1} \frac{d^3p_2}{2E_2} \frac{d^3p_3}{2E_3} f_1 f_2 (1 \pm f_3) \delta^{(4)}(p_1 + p_2 - p_3 - p) \overline{|\mathcal{M}|^2} \quad (8.1)$$

where R is the number of photon produced per unit four-volume, \mathcal{N} is the overall degeneracy for the reaction under consideration and p_i , E_i and $f_i(E_i)$ are the three-momentum, energy and thermal phase space factors of the particle i (either parton or hadron). $\overline{|\mathcal{M}|^2}$ is the square of the invariant amplitude for the process under consideration. After some straight forward algebra Eq. 8.1 can be simplified to (see Appendix A):

$$\frac{dR}{d^2p_T dy} = \frac{\mathcal{N}}{16(2\pi)^8} \int p_{1T} dp_{1T} dp_{2T} d\phi_1 dy_1 dy_2 f_1 f_2 (1 \pm f_3) \times \frac{\overline{|\mathcal{M}|^2}}{|p_{1T} \sin(\phi_1 - \phi_2) + p_T \sin \phi_2|_{\phi_2=\phi_2^0}} \quad (8.2)$$

The collision of nuclei at RHIC and LHC energies is expected to produce QGP. Once created the QGP, with high internal pressure will undergo rapid expansion. Consequently it will cool down

and make a transition to hadrons at a temperature, T_c . Thermal equilibrium is maintained in the hot hadronic phase till the freeze-out point (achieved at a temperature, T_F) where the mean free path of the hadrons is too large for collisions to take place.

The measured photon spectra ($dN/d^2p_T dy$) is the yield obtained after performing a space-time integration over the entire evolution history - from the initial state to the freeze-out point. Therefore, Eq. 8.2 needs to be integrated over the four volume to connect the theoretical results with experiments:

$$\frac{dN}{d^2p_T dy} \Big|_{y=0} = \sum_{i=Q,H} \int d^4x \left[\frac{dR}{d^2p_T dy} \Big|_{y=0} \right]_i \quad (8.3)$$

where $i \equiv Q$ and H represents QGP and hadronic phases respectively. The effects of viscosity enter the photon spectra through the space time evolution governed by the dissipative hydrodynamics and the phase space factors, f_i in Eq. 8.2.

8.2.1 Thermal photons from QGP

The contribution from QGP to the spectrum of thermal photons due to annihilation ($q\bar{q} \rightarrow g\gamma$) and Compton ($q(\bar{q})g \rightarrow q(\bar{q})\gamma$) processes have been calculated in [19, 20] using hard thermal loop (HTL) approximation [21]. Later, it was shown that photons from the processes [22]: $gq \rightarrow gq\gamma$, $qq \rightarrow qq\gamma$, $qq\bar{q} \rightarrow q\gamma$ and $gq\bar{q} \rightarrow g\gamma$ contribute in the same order $O(\alpha\alpha_s)$ as the Compton and annihilation processes. The complete calculation of emission rate from QGP to $O(\alpha\alpha_s)$ has been performed by resumming ladder diagrams in the effective theory [23, 24, 25]. However, in the present work we consider only the Compton and annihilation processes for photon production. We expect that the shift in the photon spectra from the ideal to the viscous scenario will not alter drastically due to the replacement of the Compton + annihilation rates by the rate obtained in Ref. [23, 24, 25].

8.2.2 Thermal photons from hadronic matter

In heavy ion collisions at relativistic energies the production of charged hadrons and hence photons from hadronic matter is inevitable. Therefore, the inclusion of hadrons is mandatory to study the viscous effects on photon production in HIC. This has been neglected in some of the recent works [15, 16, 17]. Here, we have considered a set of hadronic reactions with all possible iso-spin combinations to evaluate production of photons [26, 27, 28, 29] from hadronic matter. These are (i) $\pi\pi \rightarrow \rho\gamma$, (ii) $\pi\rho \rightarrow \pi\gamma$ (with π, ρ, ω, ϕ and a_1 in the intermediate state [28]), (iii) $\pi\pi \rightarrow \eta\gamma$ and (iv) $\pi\eta \rightarrow \pi\gamma, \rho \rightarrow \pi\pi\gamma$ and $\omega \rightarrow \pi\gamma$. The corresponding vertices are obtained from various phenomenological Lagrangians described in detail in Ref. [26, 27, 28]. We have also included dipole form factors as in [29] to take into account the finite size of the hadrons.

8.3 Viscous correction to the distribution function

We assume that the system is slightly away from equilibrium which relaxes back to equilibrium through dissipative processes. Here we briefly recall the main considerations leading to the commonly used form for the first viscous correction, δf to the phase space factor, f defined as follows [30]:

$$\begin{aligned} f(p) &= f_0(1 + \delta f) \\ &= f_0 \left(1 + \frac{p^\alpha p^\beta}{2T^3} [C \langle \nabla_\alpha u_\beta \rangle + A \Delta_{\alpha\beta} \nabla \cdot u] \right) \end{aligned} \quad (8.4)$$

where f_0 is the equilibrium distribution function, $\langle \nabla_\alpha u_\beta \rangle \equiv \nabla_\alpha u_\beta + \nabla_\beta u_\alpha - \frac{2}{3} \Delta_{\alpha\beta} \nabla_\gamma u^\gamma$, $\Delta_{\alpha\beta} = g_{\alpha\beta} - u_\alpha u_\beta$, $\nabla_\alpha = (g_{\alpha\beta} - u_\alpha u_\beta) \partial^\beta$, u_μ being the four-velocity of the fluid. The coefficients C and A can be determined in the following way. Substituting f in the expression for stress-energy tensor, $T^{\mu\nu}$ we get,

$$\begin{aligned} T^{\mu\nu} &= \int \frac{d^3p}{(2\pi)^3 E} p^\mu p^\nu f_0(1 + \delta f) \\ &= T_0^{\mu\nu} + \Delta T^{\mu\nu} \end{aligned} \quad (8.5)$$

where $T_0^{\mu\nu} = (\epsilon + P)u^\mu u^\nu - g^{\mu\nu}P$ is the energy momentum tensor for ideal fluid. From general considerations [31] the dissipative part can be written as

$$\Delta T^{\mu\nu} = \eta \langle \nabla^\mu u^\nu \rangle + \zeta \Delta^{\mu\nu} \nabla \cdot u \quad (8.6)$$

Equating the part containing δf from (8.4) with (8.6), C and A can be expressed in terms of the coefficients of shear (η) and bulk (ζ) viscosities respectively in terms of which the phase space distribution for the system can be written as:

$$f = f_0 \left(1 + \frac{\eta/s}{2T^3} p^\alpha p^\beta \langle \nabla_\alpha u_\beta \rangle - \frac{\zeta/s}{5T^3} p^\alpha p^\beta \Delta_{\alpha\beta} \nabla \cdot u \right) \quad (8.7)$$

For a boost invariant expansion this can be simplified to get,

$$f = f_0 [1 + \delta f_\eta - \delta f_\zeta] \quad (8.8)$$

where

$$\delta f_\eta = \frac{\eta/s}{3T^3 \tau} (p_T^2 - 2p_z'^2) \quad (8.9)$$

and

$$\delta f_\zeta = \frac{\zeta/s}{5T^3 \tau} (p_T^2 + p_z'^2) \quad (8.10)$$

where $p_z' = m_T \sinh(y - \eta)$ is the z -component of the momentum in the fluid co-moving frame. The phase space distribution with viscous corrections (8.8) thus enters the production rate of photons through Eq. 8.2.

8.4 Expansion dynamics

As mentioned before the p_T distribution of thermal photons is obtained by integrating the emission rate over the evolution history of the expanding fluid. Second order relativistic viscous hydrodynamics has been used here as a tool for the space-time dynamics of the fluid. The evolution equation within the framework of second order relativistic fluid dynamics [32, 33] for a boost invariant expansion [34] can be written as [35]

$$\frac{dT}{d\tau} = -\frac{T}{3\tau} + \frac{\Phi}{12aT^3\tau} \quad (8.11)$$

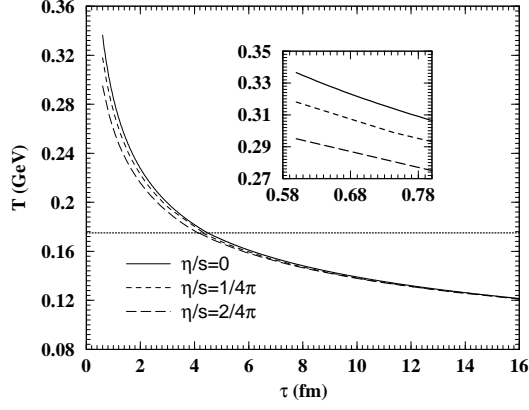


Figure 8.1: Variation of temperature with proper time for different phases for various values of the shear viscosities. Inset shows the effect of viscosity on the cooling of the QGP phase (in an amplified scale) for different values of η/s .

and

$$\frac{d\Phi}{d\tau} = -\frac{2aT\Phi}{3b} - \Phi \left(\frac{1}{2\tau} - \frac{5}{2T} \frac{dT}{d\tau} \right) + \frac{8aT^4}{9\tau} \quad (8.12)$$

where T is the temperature, τ is the proper time, Φ is the traceless part of the viscous stress tensor, a is a constant related to the statistical degeneracy g as $a = \pi^2 g/30$ and $b = \eta/T^3$. We assume that the system is formed in QGP phase after HIC at time τ_i with initial temperature, T_i . The value of $\Phi(\tau_i)$ is taken as $(4/3)(\eta/s_i)(s_i/\tau_i)$ where s_i is the initial entropy density. Eqs. 8.11 and 8.12 have simultaneously been solved numerically with lattice QCD Equation of State (EoS) [36] to get the variation of temperature with proper time required to evaluate the photon spectra originating from the evolving matter.

In a realistic scenario, the value of η may be different for QGP [37, 38, 39, 40, 41] and hadronic [42, 43, 44, 45] phases. However, in the present work we take the same value of η/s both for QGP and hadronic matter.

8.5 Results

In case of an ideal fluid, the conservation of entropy implies that the rapidity density dN/dy is a constant of motion for the isentropic expansion [34]. In such circumstances, the experimentally observed (final) multiplicity, dN/dy may be related to a combination of the initial temperature T_i and the initial time τ_i as $T_i^3\tau_i$. Assuming an appropriate value of τ_i (taken to be ~ 0.6 fm/c in the present case), one can estimate T_i .

For dissipative systems, such an estimate is obviously inapplicable. Generation of entropy during the evolution invalidates the role of dN/dy as a constant of motion. Moreover, the irreversibility arising out of dissipative effects implies that estimation of the initial temperature from the final rapidity density is no longer a trivial task. We can, nevertheless, relate the experimental dN/dy to the freeze-out temperature, T_F and the freeze-out time, τ_f by the relation,

$$\frac{dN}{dy} = \pi R_A^2 4a_H T_F^3 \tau_f / \kappa \quad (8.13)$$

where R_A is the radius of the colliding nuclei (we consider AA collision for simplicity) and κ is a constant ~ 3.6 for massless bosons.

To estimate the initial temperature for the dissipative fluid we adopt the following algorithm. We treat T_i as a parameter; for each T_i , we let the system evolve forward in time under the condition of dissipative fluid dynamics (Eqs. 8.11 and 8.12) till a given freeze-out temperature T_F is reached. Thus τ_f is determined. We then compute dN/dy at this instant of time from eq. 8.13 and compare it with the experimental dN/dy . The value of T_i for which the calculated dN/dy matches the experimental number is taken to be the value of the initial temperature. Once T_i is determined the evolution of the system from the initial to the freeze-out stage is determined by the simultaneous solution of Eqs. 8.11 and 8.12. We found that the amount of entropy generated during the evolution - from initial state to the freeze-out state is about 30% of the initial entropy for $\eta/s = 1/4\pi$, which will have crucial consequences on the photon spectra.

In Fig. 8.1 we display the variation of temperature with proper time. It is clear from the results shown in the inset (Fig. 8.1) that initial temperature for system which evolves with non-zero viscous effects is lower compared to the ideal case for a fixed dN/dy . This is because for a non-viscous isentropic evolution scenario the multiplicity (measured at the freeze-out point) is fixed by the initial entropy. However, for a viscous evolution scenario the generation of entropy due to dissipative effects contributes to the entropy (proportional to multiplicity). Therefore, for a given multiplicity at the freeze-out point one requires lower initial entropy and hence a lower initial temperature. It is also seen (Fig. 8.1) that the cooling of the system is slower for viscous dynamics due to the extra heat generated during the evolution.

8.5.1 Photon spectra

In this section we present the shift in the p_T distribution of the photons due to viscous effects. The integrand in Eq. 8.3 is a Lorentz scalar, consequently the Lorentz transformation of the integrand from the laboratory to the co-moving frame of the fluid can be effected by just transforming the argument, *i.e.* the energy of the photon ($E = p_T \cosh y$) in the laboratory frame should be replaced by $u_\mu p^\mu$ in the co-moving frame of the fluid, where p^μ is the four momentum of the photon and u_μ is fluid four velocity.

The results presented here are obtained with vanishing bulk viscosity. The effects of viscosity enters into the photon spectra through the phase space factor as well as through the space time evolution. We would like to examine these two effects separately. For convenience we define two scenarios: (i) where the effects of viscosity on the phase space factor is included (δf_η is non-zero in Eq. 8.8), but the viscous effects on the evolution are neglected (ideal Bjorken hydrodynamics [34]) and (ii) the effects of $\eta \neq 0$ are taken into account in the phase space factors as well as in the evolution dynamics.

Before presenting the results we estimate the value of p_T beyond which the viscous corrections become comparable (or more) to the equilibrium emission. In Fig. 8.2 the ratio of the transverse momentum distribution of thermal photons with the equilibrium distribution to that with the

viscous corrections is plotted against p_T . The results indicate that the viscous corrections become close to the equilibrium production for $p_T \sim 3.5$ GeV. Therefore, we set the maximum value of $p_T = 3$ GeV in presenting the p_T spectra of photon.

The space time integrated photon yield originating from the QGP in scenario (i) is displayed in Fig. 8.3. Note that the value of the initial temperatures for the results displayed in Fig. 8.3 is same for all η/s because the viscous effects on the evolution is ignored in scenario (i). The viscous effects on the p_T distribution of the photons is distinctly visible. The higher values of η/s make the spectra flatter through the p_T dependence of the correction, δf_η . Next we assess the effects of viscosity on photon spectra for scenario (ii). In Fig. 8.4 we depict the photon spectra for various values of η/s . In this scenario the value of T_i is lower for higher η/s for reasons described above. As a result the enhancement in the photon production due to change in phase space factor, δf_η is partially compensated by the reduction in T_i for non-zero η , which can be clearly seen by comparing the results displayed in Figs. 8.3 and 8.4.

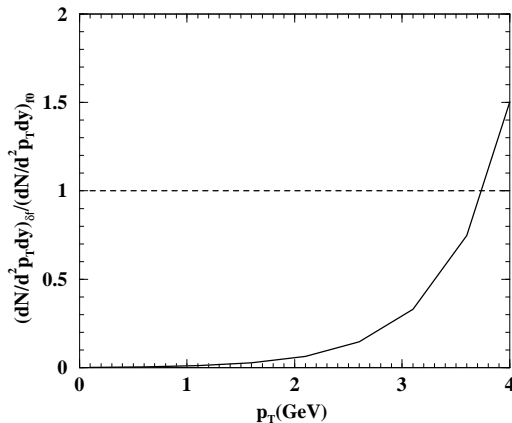


Figure 8.2: The p_T dependence of the ratio of the transverse momentum distribution of thermal photons with the equilibrium distribution to the viscous correction.

In Figs. 8.5 and 8.6 we exhibit results for the hadronic phase for scenarios (i) and (ii) respectively. The effects of dissipation on the p_T distribution of photons from hadronic phase is qualitatively similar to the QGP phase but quantitatively small. The (small) change in the spectra due to the change in the phase space factor (in scenario (i)) can not be compensated

by taking into account the viscous effects in the evolution (scenario (ii)) for fixed T_c and T_F for all values of η/s considered. Therefore, as indicated in Figs. 8.5 and 8.6, we observe similar effects for scenario (i) and (ii).

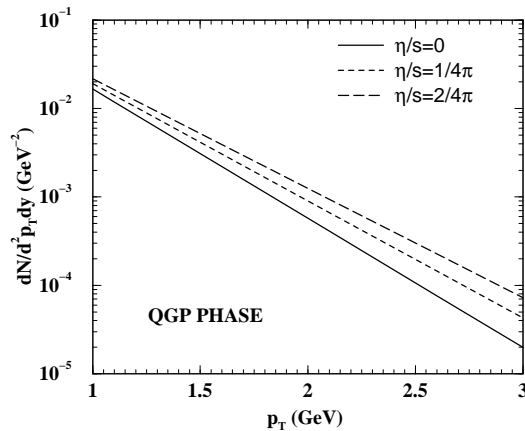


Figure 8.3: Transverse momentum distribution of thermal photons from QGP for various values of η/s in the scenario (i).

Finally in Figs. 8.7 and 8.8 we plot the p_T spectra of photons for the entire life time of the thermal system obtained by summing up contributions from QGP and hadronic phases for different values of η/s for scenarios (i) and (ii) respectively. The enhancement in the spectra due to dissipative effects in the phase space factors (Fig. 8.7) are compensated by the reduction in T_i and viscous evolution (Fig. 8.8). The results depicted in Fig. 8.8 indicate that the shift in the photon spectra due to viscous effects is small. The change in the spectra for $\eta/s = 0$ and $\eta/s = 1/4\pi$ is within the error-bars in the photon spectra measured by PHENIX collaborations [46].

In Fig. 8.9 we display the experimental data measured by PHENIX collaboration in Au+Au collision (0 – 20% centrality) at $\sqrt{s_{NN}} = 200$ GeV. The data contains contributions from the (i) photons produced in the hard collision processes of the energetic partons from colliding nuclei and (ii) contributions from the thermal system formed after the Au+Au collisions. The contributions from the decays, *e.g.* $\pi^0 \rightarrow \gamma\gamma$, $\eta \rightarrow \gamma\gamma$ etc have been subtracted out from the data. The contributions from pp collisions at a given collision energy can be used as a bench-

mark to estimate the hard contributions. To estimate the thermal contributions we adopt the following procedure. *Thermal contributions = experimental data from heavy ion collision provided by PHENIX collaboration minus $N_{coll} \times$ contributions from pp collisions*, where N_{coll} is the number of nucleon-nucleon interactions in the heavy ion collisions for 0 – 20% centrality. The data is well described by the contributions from (i) (solid line) for p_T above 2 GeV. Therefore, the scope of reproducing the data by photons from thermal processes is limited to $p_T \lesssim 2$ GeV. Thermal contributions, (ii) has been evaluated (see [48] for details) with the transverse expansion of the system described by ideal hydrodynamical model [47] with cylindrical symmetry and boost invariance along longitudinal direction. Here the value of $T_F = 140$ MeV is constrained to reproduce the charged pion and kaon spectra. The result is shown by dot-dashed line in Fig. 8.9 which contains contributions from both (i) and (ii). The radial flow of the matter provides transverse kick to the photons [49]. It is shown in [51] that the difference in radial kick for scenarios with and without viscosity is small for low p_T ($\lesssim 2$ GeV) domain [51]. Therefore, we expect that the *shift* in the transverse momentum spectra of thermal photons obtained with longitudinal expansion will not change much by the introduction of the radial flow. In this spirit we multiply the spectra obtained with radial flow (within the ambit of ideal hydrodynamics, shown in Fig. 8.9 by dot-dashed line) by the shift due to viscous effects obtained within the framework of longitudinal hydrodynamics. The result obtain in this scenario is added with hard contributions and displayed in Fig. 8.9(dotted line). The plot clearly shows that the relative *shift* in the spectra with viscous effect is much smaller than the error bar of the PHENIX data. This indicates that the *shift* due to viscous effects can not be observed through photon spectra with present experimental statistics.

The formalism discussed above has been applied to estimate the shift in the transverse momentum distribution [52] of pions due to the presence of shear viscosity. The results have been depicted in Fig. 8.10. The spectra has been normalized to unity at $p_T = 0$, which dose not affect the conclusion as we are interested in the shift in the spectra due to viscous effects. The effects seem to be more prominent in the hadron spectra than in the transverse momentum distribution of photons.

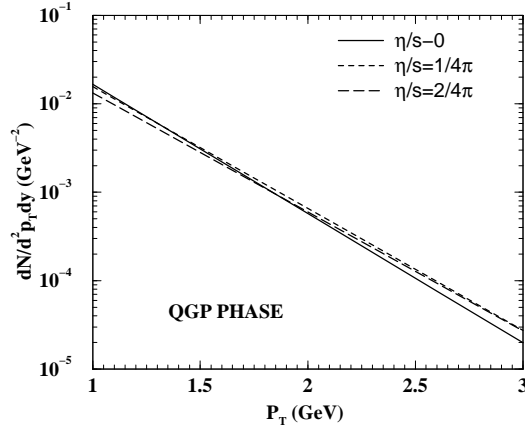


Figure 8.4: Transverse momentum distribution of thermal photons from QGP for various values of η/s in the scenario (ii).

8.6 Summary and Discussions

We have studied the effects of viscosity on the evolving QGP produced in nuclear collisions at RHIC energies. The generation of entropy due to dissipation on the final (experimentally measured) multiplicity has been taken into account. The initial temperature has been constrained by the multiplicity (entropy) at the freeze-out point. The viscous effects on the photon spectra has been introduced consistently through the evolution dynamics and phase space factors of all the particles participating in the production processes. The role of hadrons in studying the viscous effects on the photon production has been considered in contrast to some recent works. We observe that the effects of the shear viscosity on the photon spectra originating from QGP is small in contrast to the results obtained earlier. This is because the enhancement due to the dissipative effects entering the production rate through the phase space factors are partially balanced by the reduction in the emission rate due to smaller initial temperature. We have evaluated the photon spectra with transverse expansion within the framework of ideal relativistic hydrodynamics with cylindrical symmetry and boost invariance along longitudinal direction. The spectra so obtained is multiplied by the shift realized due to viscous effects on the photon spectra calculated for a longitudinally expanding system to retrieve the yield with viscous radial expansion. Recently it is shown that (using (2+1)D hydrodynamics) the effects

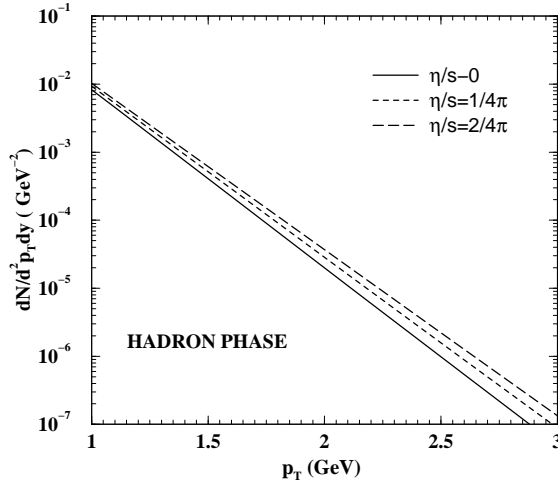


Figure 8.5: Transverse momentum distribution of photons from thermal hadrons for various values of η/s in the scenario (i).

of shear viscosity on hadron spectra is small for low p_T . In the light of this result, the procedure followed here to estimate the photon spectra with viscous effects for a radially expanding system may be considered as a good approximation. The small shift we obtained here is also in agreement with the results obtained in Ref [50] with (3+1)D relativistic viscous evolution.

Before closing this section some comments are in order here. First, as mentioned before, for the photon production rate from QGP we have used the Compton and annihilation processes. We have checked that the contribution from these two processes is down by a factor of 3-4 compared to the production rate obtained from the complete calculation of order α_s done in Ref. [23, 24, 25]. Taking these higher order processes into consideration in the present scenario involves a reevaluation of the photon production rates with thermal distribution factors containing viscous corrections. Secondly, we have confined only to the longitudinal flow of the matter in the present work ignoring the transverse kick (blue shift) received by the photons from radial flow [49]. However, both these factors will affect the photon spectra from ideal as well as dissipative scenarios in a similar fashion. Therefore, we expect the shift in the transverse momentum spectra of thermal photons in the presence of dissipative effects which is the main

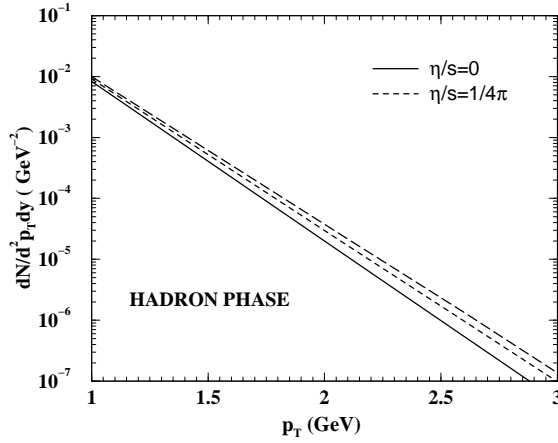


Figure 8.6: Transverse momentum distribution of photons from thermal hadrons for various values of η/s in the scenario (ii).

focus of the present work, will be similar even when a more rigorous photon production rate along with transverse expansion is employed [53].

Appendix A: Phase Space

In this appendix we derive Eq. 2 from 1. The photon production rate from the process, $1 + 2 \rightarrow 3 + \gamma$ is given by,

$$E \frac{dR}{d^3p} = \frac{1}{2} \frac{\mathcal{N}}{(2\pi)^8} \int \frac{d^3p_1}{2E_1} \int \frac{d^3p_2}{2E_2} \int \frac{d^3p_3}{2E_3} f_1(E_1) f_2(E_2) [1 \pm f_3(E_3)] |\overline{M}|^2 \delta(p_1 + p_2 - p_3 - p) \quad (8.14)$$

Performing the d^3p_3 integration using the delta function and using $d^3p/E = p_T dp_T dy d\phi$ we get,

$$E \frac{dR}{d^3p} = \frac{1}{16} \frac{\mathcal{N}}{(2\pi)^8} \int p_{1T} dp_{1T} dy_1 d\phi_1 p_{2T} dp_{2T} dy_2 d\phi_2 \frac{1}{E_3} f_1(E_1) f_2(E_2) [1 \pm f_3(E_3)] |\overline{M}|^2 \delta(E_1 + E_2 - E_3 - E) \quad (8.15)$$

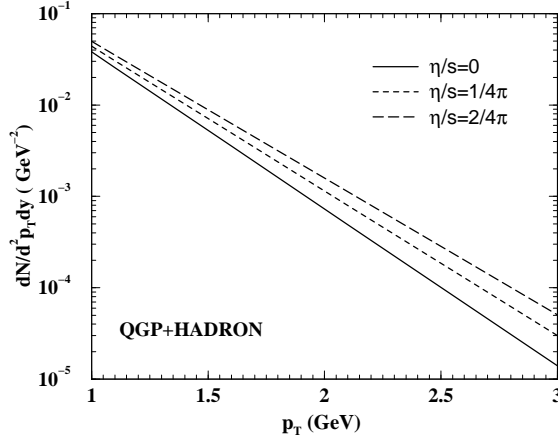


Figure 8.7: Transverse momentum distribution of thermal photons from the entire evolution history of the system for various values of η/s in the scenario (i).

where ϕ_1 and ϕ_2 are the angles made by the transverse momenta of first and second particles with the transverse momentum of the emitted photon. The momentum conservation along the z -direction: $p_{3z} = p_{1z} + p_{2z} - p_z$ can be written in terms of rapidity as:

$$m_{3T} \sinh y_3 = m_{1T} \sinh y_1 + m_{2T} \sinh y_2 - p_T \sinh y \quad (8.16)$$

Now the energy, E_3 can be written as:

$$E_3 = m_{3T} \cosh y_3 = \sqrt{m_{3T}^2 + m_{3T}^2 \sinh^2 y_3} \quad (8.17)$$

Substituting Eq. 8.16 in Eq. 8.17 we get,

$$E_3 = \sqrt{[(m_{1T} \sinh y_1 + m_{2T} \sinh y_2 - p_T \sinh y)^2 + m_{3T}^2]} \quad (8.18)$$

Considering the energy conservation ($E_3 = E_1 + E_2 - E$) and writing the energies in terms of rapidity ($E_i = m_{iT} \cosh y_i$) we get,

$$E_3 = m_{1T} \cosh y_1 + m_{2T} \cosh y_2 - p_T \cosh y \quad (8.19)$$

Equating Eqs. 8.18 and 8.19 we have,

$$\begin{aligned} m_{3T} = & [m_{1T}^2 + m_{2T}^2 + p_T^2 + 2m_{1T}m_{2T} \cosh(y_1 - y_2) \\ & - 2m_{1T}p_T \cosh(y_1 - y) - 2m_{2T}p_T \cosh(y_2 - y)]^{\frac{1}{2}} \end{aligned} \quad (8.20)$$

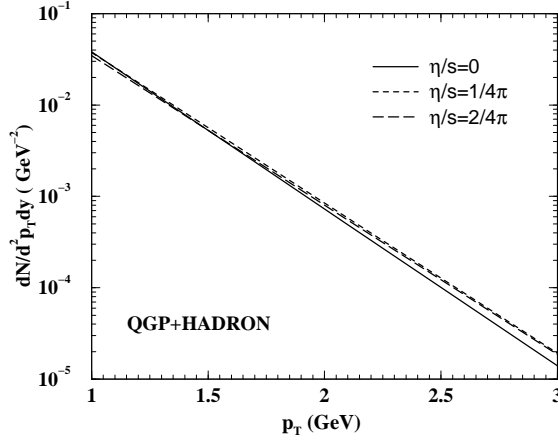


Figure 8.8: Transverse momentum distribution of thermal photons from the entire evolution history of the system for various values of η/s in the scenario (ii).

However, we also have,

$$\begin{aligned}
m_{3T} &= (p_{3T}^2 + m_3^2)^{\frac{1}{2}} \\
&= [(p_{1T} + p_{2T} - p_T)^2 + m_3^2]^{\frac{1}{2}} \\
&= [p_{1T}^2 + p_{2T}^2 + p_T^2 + 2p_{1T}p_{2T} \cos(\phi_{12}) \\
&\quad - 2p_T p_{1T} \cos(\phi_1) - 2p_T p_{2T} \cos(\phi_2) \\
&\quad + m_3^2]^{\frac{1}{2}}
\end{aligned} \tag{8.21}$$

where,

$$\cos(\phi_{12}) = \cos(\phi_1) \cos(\phi_2) + \sin(\phi_1) \sin(\phi_2) \tag{8.22}$$

Equating Eq. 8.20 with Eq. 8.21 leads to the expression,

$$\begin{aligned}
&[(p_{1T} \cos \phi_1 - p_T) \cos \phi_2 + p_{1T} \sin \phi_1 \sin \phi_2] = \\
&\frac{1}{2p_{2T}} [(m_1^2 + m_2^2 - m_3^2) + 2m_{1T}m_{2T} \cosh(y_1 - y_2) \\
&\quad - 2m_{1T}p_T \cosh(y_1 - y) - 2m_{2T}p_T \cosh(y_2 - y) \\
&\quad + 2p_T p_{1T} \cos \phi_1]
\end{aligned} \tag{8.23}$$

Solving Eq. 8.23 for ϕ_2 one gets,

$$\phi_2^0 = \tan^{-1} \left(\frac{p_{1T} \sin \phi_1}{p_{1T} \cos \phi_1 - p_T} \right) - \cos^{-1} \frac{H}{2Rp_{2T}} \tag{8.24}$$

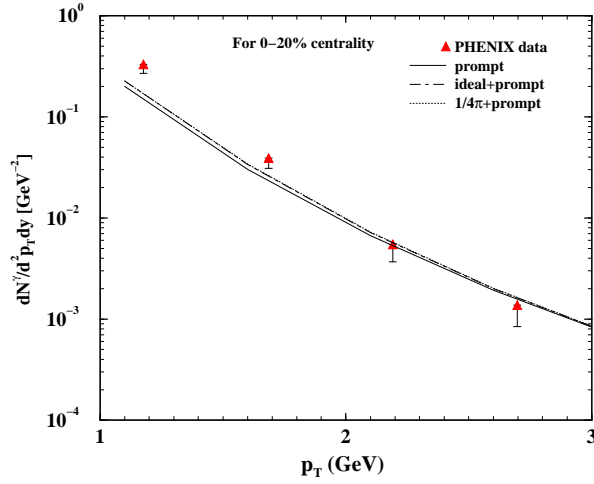


Figure 8.9: Transverse momentum distribution of thermal photons scaled with the effect of radial flow and compared with the direct photon data from PHENIX for 0-20% centrality.

where,

$$R = \sqrt{p_{1T}^2 + p_T^2 - 2p_{1T}p_T \cos \phi_1} \quad (8.25)$$

and,

$$\begin{aligned} H = & (m_1^2 + m_2^2 - m_3^2) + 2m_{1T}m_{2T} \cosh(y_1 - y_2) \\ & - 2m_{1T}p_T \cosh(y_1 - y) - 2m_{2T}p_T \cosh(y_2 - y) \\ & + 2p_T p_{1T} \cos \phi_1 \end{aligned} \quad (8.26)$$

Now we express the argument of the delta function in Eq. 8.15 as function of ϕ_2 as

$$\begin{aligned} f(\phi_2) = & E_1 + E_2 - E_3 - E \\ = & m_{1T} \cosh y_1 + m_{2T} \cosh y_2 - p_T \cosh y \\ & - [m_{3T}^2 + (m_{1T} \sinh y_1 + m_{2T} \sinh y_2 \\ & - p_T \sinh y)^2]^{\frac{1}{2}} \end{aligned} \quad (8.27)$$

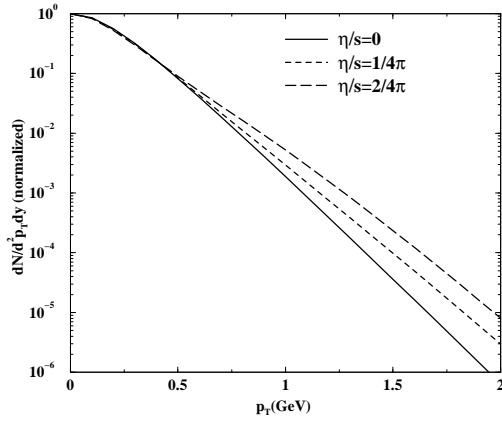


Figure 8.10: Transverse mass distribution of pions with and without viscous effects.

and performing the ϕ_2 integration in Eq. 8.15 we get,

$$\begin{aligned}
 E \frac{dR}{d^3p} = & \frac{1}{16} \frac{\mathcal{N}}{(2\pi)^8} \int_0^\infty p_{1T} dp_{1T} \int_0^\infty dp_{2T} \\
 & \int_{-\infty}^\infty dy_1 \int_{-\infty}^\infty dy_2 \int_0^{2\pi} d\phi_1 \\
 & f_1(E_1) f_2(E_2) [1 \pm f_3(E_3)] \\
 & \frac{|M|^2}{|p_{1T} \sin(\phi_1 - \phi_2) + p_T \sin \phi_2|_{\phi_2^0}} \quad (8.28)
 \end{aligned}$$

with the constraint

$$\left| \frac{H}{2R p_{2T}} \right| \leq 1 \quad (8.29)$$

originating from $|\cos(\phi)| \leq 1$.

Bibliography

- [1] I. Arsene *et al.* (BRAHMS Collaboration), Nucl. Phys. A **757**, 1 (2005).
- [2] B. B. Back *et al.* (PHOBOS Collaboration), Nucl. Phys. A **757**, 28 (2005).
- [3] J. Adams *et al.* (STAR Collaboration), Nucl. Phys. A **757**, 102 (2005).
- [4] K. Adcox *et al.* (PHENIX Collaboration), Nucl. Phys. A **757**, 184,(2005).
- [5] P. Kovtun, D. T. Son and O. A. Starinets, Phys. Rev. Lett. **94**, 111601 (2005).
- [6] A. Sinha and R. C. Myers, J. High Ener. Phys. **0903**, 084 (2009).
- [7] L. D. McLerran and T. Toimela, Phys. Rev. D **31** (1985) 545.
- [8] C. Gale and J.I. Kapusta, Nucl. Phys. B **357** (1991) 65.
- [9] H.A. Weldon, Phys. Rev. D **42** (1990) 2384.
- [10] J. Alam, S. Raha and B. Sinha, Phys. Rep. **273** (1996) 243.
- [11] J. Alam, S. Sarkar, P. Roy, T. Hatsuda and B. Sinha, Ann. Phys. **286** (2001) 159.
- [12] R. Rapp and J. Wambach, Adv. Nucl. Phys. **25** (2000) 1.
- [13] S. Sarkar, P. Roy, J. Alam, S. Raha and B. Sinha, J. Phys. G: Nucl. Part. Phys. **23**, 469 (1997).
- [14] A. K. Chaudhuri, Phys. Scripta **61**, 311 (2000).
- [15] A. K. Chaudhuri and B. Sinha, Phys. Rev. C **83**, 034905 (2010).

- [16] J. R. Bhatt, H. Mishra and V. Sreekanth, J. High Ener. Phys. **1011**, 106 (2010).
- [17] K. Dusling, Nucl. Phys. A **839**, 70 (2010).
- [18] C. Gale and J. Kapusta, Phys. Rev. C **35**, 2107 (1983).
- [19] J. Kapusta, P. Lichard, and D. Seibert, Phys. Rev. D **44**,2774 (1991).
- [20] R. Bair, H. Nakkagawa, A. Niegawa, and K. Redlich, Z. Phys. C **53**, 433(1992).
- [21] E. Braaten and R. D. Pisarski, Nucl. Phys. B **337**, 569 (1990); *ibid* **339**, 310 (1990).
- [22] P. Aurenche, F. Gelis, R. Kobes, and H. Zaraket, Phys. Rev. D **58**, 085003 (1998).
- [23] P. Arnold, G.D. Moore, and L.G. Yaffe, J. High Energy Phys. **11**, 057 (2001) .
- [24] P. Arnold, G.D. Moore, and L.G. Yaffe, J. High Energy Phys. **12**, 009 (2001) .
- [25] P. Arnold, G.D. Moore, and L.G. Yaffe, J. High Energy Phys. **06**, 030 (2001).
- [26] S. Sarkar, J. Alam, P. Roy, A. K. Dutt-Mazumder, B. Dutta-Roy and B. Sinha, Nucl. Phys. A **634** 206 (1998).
- [27] P. Roy, S. Sarkar, J. Alam and B. Sinha Nucl. Phys. A **653** 277 (1999).
- [28] J. Alam, P. Roy and S. Sarkar Phys. Rev. C **71** 059802 (2005).
- [29] S. Turbide, R. Rapp and C. Gale, Phys. ReV. C **69**, 014903(2004).
- [30] D. Teaney, Phys. Rev. C **68**, 034913 (2003).
- [31] S. Weinberg, The Astrophys. J. **168**, 175 (1971).
- [32] W. Israel and J. M. Stewart, Ann. Phys. **118**, 341 (1979).
- [33] W. Israel, Ann. Phys. **100**, 310 (1976).
- [34] J. D. Bjorken, Phys. Rev. D **27** (1983) 140.

- [35] A. Muronga, Phys. Rev. Lett. **88**, 062302 (2002); Erratum, Phys. Rev. Lett. **89**, 159901 (2002).
- [36] S. Borsányi *et al.*, J. High. Ener. Phys **1011**, 077 (2010).
- [37] H. B. Meyer, Phys. Rev. D **76**, 101701 (2007).
- [38] P. Arnold, G. D. Moore and L. G. Yaffe, J. High. Ener. Phys. **0305**, 051 (2003).
- [39] J. W. Chen, H. Dong, K. Ohnishi and Q. Wang, Phys. Lett. B **685**, 277 (2010)
- [40] S. K. Das and J. Alam, Phys. Rev. D **83**, 114011 (2011).
- [41] Z. Xu and C. Greiner, Phys. Rev. Lett. **100**, 172301 (2008)
- [42] K. Itakura, O. Morimatsu and H. Otomo, Phys. Rev. D **77**, 014014 (2008).
- [43] A. Dobado and I. J. Llanes-Estrada, Phys. Rev. D **69**, 116004 (2004).
- [44] P. Chakraborty and J. I. Kapusta, Phys. Rev. C **83**, 014906 (2011).
- [45] A. S. Khvorostukhin, V. D. Toneev and D. N. Voskresensky, Nucl. Phys. A **845**, 106 (2010).
- [46] A. Adare *et al.* (PHENIX Collaboration, Phys. Rev. Lett. **104**, 132301 (2010).
- [47] H. von Gersdorff, M. Kataja, L. D. McLerran and P. V. Ruskanen, Phys. Rev. D **34** (1986) 794.
- [48] P. Mohanty, J. K. Nayak, J. Alam and S. K. Das, Phys. Rev. C **82**, 034901 (2010).
- [49] J. Alam, D. K. Srivastava, B. Sinha and D. N. Basu, Phys. Rev. D **48**, 1117(1993).
- [50] M. Dion, J.F. Paquet, B. Schenke, C. Young, S. Jeon and C. Gale, Phys. Rev. C **84**, 064901 (2011).
- [51] V. Roy and A. K. Chaudhuri, Phys. Lett. B **703**, 313 (2011).
- [52] P.V. Ruuskanen, Acta Phys. Polon. B **18** (1987), 551.
- [53] S. Mitra *et al* work in progress

Chapter 9

Summary and Outlook

In this Chapter we will briefly summarize the work reported in this thesis and then provide an outlook that follow from the work.

In this thesis we have investigated the transport properties of the matter created in heavy ion collisions and the effect of a thermal medium on the temperature dependence of this quantities. Motivated from the recent results of heavy ion collision experiments indicating that the produced matter behaves as a strongly interacting liquid having small but finite values of shear viscosity to entropy density ratio, different transport coefficients have been evaluated with an aim to obtain a realistic temperature dependence of these quantities in hot hadronic medium. We have studied the temperature dependence of different transport coefficients of both first and second order in dissipative fluid dynamics for an interacting pion gas. The shear and the bulk viscous coefficients as well as the thermal conductivity from the first order theory have been estimated using Chapman-Enskog method and the relaxation times of dissipative flows from the second order theory have been evaluated using Grad's 14 moment method of the kinetic theory of fluids.

The novelty of our work is that we have used a temperature dependent interaction cross section instead of a constant or parameterized one as usually done in the literature. This temperature dependence has been introduced in the cross section from first principle calculations without

taking any effective temperature dependent mass or decay width. Instead of estimating the scattering amplitude from the lowest order Lagrangian of chiral perturbation theory used in most of the literature, we have estimated the pion-pion interaction cross section by introducing rho and sigma meson exchange, which agrees well with the experimental values and then inserted the medium effects in the interaction cross section by modifying the propagators in the medium accordingly. The effect of a thermal medium on ρ and σ propagation is quantified through its self-energy, which at finite temperature is evaluated using the real time formalism of thermal field theory. We consider the self energy loop of the ρ meson to consist of two pions or a pion and another heavy meson like ω, h_1, a_1 and for σ meson two pions only. The mesons ω, h_1 and a_1 all having substantial 3π and $\rho\pi$ decay widths, can be considered as a multi-pion contribution to the ρ self-energy. The cross section so obtained in a thermal medium gets suppressed compared to the vacuum one due to the larger decay width at finite temperature. Actually at finite temperature different scattering and decay processes occur in addition to the two-pion decay altering the abundance of ρ and σ mesons in the medium with respect to the vacuum. Since this cross section goes as the dynamical input for the transport processes we have evaluated, a significant enhancement is observed in the temperature dependence of both the first and second order transport coefficients. Moreover we have used a temperature dependent pion chemical potential in our estimations which is required for particle number conservation from chemical to kinetic freeze out instead of constant ones which also produce significant effects on the temperature dependence of transport quantities.

We have also investigated other transport quantities like the drag and diffusion coefficients for heavy mesons with charm degrees of freedom, like J/ψ and η_c in a mesonic medium of lighter particles consisting of $\pi, k, \eta, \rho, \omega$ and ϕ . The drag and diffusion coefficients are obtained as a function of temperature and the J/ψ absorption by the comoving hadrons has been investigated.

We have also shown the effects of viscosities on the photon spectra with some representative values of η/s at RHIC energies. The effects of viscosity on the space-time evolution of quark gluon plasma as well as hadronic matter produced in nuclear collisions at relativistic heavy ion

collider energies have been studied, where a small change in the transverse momentum (p_T) distribution of photons is observed due to viscous effects.

The mathematical schemes we have developed so far with the tools from kinetic theory of fluid dynamics and thermal field theory, have enabled us to furnish a hydrodynamical description of the system created out of the heavy ion collisions. From the kinetic theory approach we have obtained the hyperbolic equations of motion of dissipative fluxes of second order fluid dynamics which are the Israel-Stewart equations. Though the equations can be derived from the positive entropy change associated with irreversible processes, however the coefficients of each term in the equations can only be explicitly estimated from kinetic theory calculations. In this way we have obtained all the 14 equations of motion of the thermodynamic variables including the macroscopic temperature, number density and hydrodynamic velocity of the fluid system along its dissipative fluxes namely the shear and bulk viscous flows and heat flow, with the explicit expressions of the coefficients which are the relaxation times and the heat-viscous coupling lengths. Moreover within these second order transport coefficients the first order ones such as the shear and bulk viscous coefficients and the thermal conductivity go as inputs, which have been also evaluated explicitly. All those coefficients are evaluated at finite temperature incorporating the effects of a thermal medium in it. In this way we have developed a scheme of producing the hydrodynamic equations of motion of a system for a massive Bose-Einstein gas at finite temperature. In most of the available literature the Israel-Stewart hydro equations are provided with the coefficients that are estimated for either simple massless gases or low mass Boltzmann gases with constant representative values of the viscous coefficients (η/s as multiples of $1/4\pi$). Even the temperature dependent values of viscosities and thermal conductivity available in literature do not include the effects of a thermal medium at finite temperature in their dynamical interactions. Hence we are trying to provide the realistic hydro equations from first principles for an evolving system which undergoes dissipative processes.

It now remains to solve the hydro equations in order to obtain the temperature profile of the expanding system which sets its cooling laws. Since the transport coefficients which appear in the hydro equations play a very crucial role in their solutions we can expect that the medium

modifications performed here have significant implication on the system's cooling profile. Further with these cooling laws we can construct the transverse momentum spectra of the final state hadrons and of the electromagnetic probes as well as their collective flows. In this way we can quantify the effects of dissipation on the bulk properties of the system created out of the heavy ion collisions.

An exact solution of the Boltzmann equation can be obtained once the hydrodynamic equations are solved for an evolving medium. Since in kinetic theory the out of equilibrium distribution function is expanded in the basis of particle four-momenta with the coefficients depending on the thermodynamic dissipative fluxes, the solution of the flux equations can give the entire out of equilibrium distribution function. With the help of this distribution function the macroscopic thermodynamic quantities such as energy densities and the transverse and longitudinal pressures of the out of equilibrium system can be exactly estimated.

Again one could extend the above calculational scheme to a multi particle system consisting of both mesons and nucleons. The problem then turns into solving coupled transport equations simultaneously for each component instead of just one. Moreover each equation contains as many collision terms as contributed from the interactions between each component. For this purpose we need to extend the single component Chapman-Enskog and Grad's method discussed above to a multi component one. Finally it leads to a set of coupled equations which involves a $(N \times N)$ matrix whose elements are the interaction cross sections among respective species of constituent particles (N being the number of components present in the fluid). Then we need to estimate the cross section for interactions among different hadrons using effective interactions and incorporate the effect of medium by introducing the thermal propagator at finite temperature in each scattering channel. After obtaining the temperature dependent first and second order transport coefficients they can be employed in the evolution equations as before. On solving such a system of equations for a multi-component system we can obtain the particle spectra and collective flows for a mixture of bosonic and fermionic gas which will give us the opportunity to understand the properties of the matter created in heavy ion collisions at a more quantitative level.